EFFECTS OF FLOW DYNAMICS, SALINITY, AND WATER QUALITY ON THE ATLANTIC STURGEON, THE SHORTNOSE STURGEON AND THE EASTERN OYSTER IN THE OLIGOHALINE ZONE OF THE DELAWARE ESTUARY

Final Report Project Year 2008-2009
Submitted to the U.S. Army Corps of Engineers, Philadelphia District

By

Lisa Calvo, Principal Investigator
Seaboard Fisheries Institute

Harold M. Brundage III
Environmental Research and Consulting, Inc.

Dale Haidvogel
Rutgers University

Danielle Kreeger and Roger Thomas
Academy of Natural Sciences

John C. O'Herron, II
Amitrone O'Herron, Inc

Eric N. Powell
Haskin Shellfish Research Laboratory
Rutgers University

With
Sponsoring Agency

Joseph A. Balzano, CEO, South Jersey Port Corporation

Contract No. W912BU=08-P-0338 Award Date September 30, 2008 Project No: 151265
USACE Technical POC: Barbara Conlin

September 2010

Seaboard Fisheries Institute
31 W. Commerce Street, Bridgeton, New Jersey 08302

ACKNOWLEDGEMENTS

We would like to thank Marlin Peterson (South Jersey Port Corporation), Barbara Conlin (U.S. Army Corps of Engineers, Philadelphia District) and Steve Carnahan (Seaboard Fisheries Insitute) for their critical assistance and input in administering and guiding this effort; Jason Morson (Haskin Shellfish Research Laboratory) for coordinating water sample collections and for his overall contributions to the project; Bob Chant, Maria Aristizabal, Joseph Wang, Diego Narvaez (Rutgers University) for their contributions to developing the hydrodynamic-larval model; Captain Scott Bailey (Bailley's Oysters, Crabs, and Softcrabs); and David McQuaide, Wesley Gerardi, George Harrington, and Justin Lontz (Delaware Department of Natural Resources and Environmental Control, Division of Water Resources) for assisting with water sample collections. We also thank Matt Fisher (Delaware Division of Fish and Wildlife) for assistance with sturgeon sampling and tagging, and Dewayne Fox, Lori Brown, Matt Breece, and Johnny Moore (Delaware State University) for their cooperation in maintaining acoustic receiver network. We are especially thankful to the DuPont Clear into the Future initiative for fellowship support for participating Rutgers University graduate students.

TABLE OF CONTENTS

List of Tables……..…….4

List of Figures…….....5

Project Summary…… 8

Chapter 1. Acoustic Telemetry Studies of the Distribution and Movement of Juvenile Atlantic Sturgeons in the Delaware Estuary.....……10

Chapter 2. Spatial and Temporal Variability in Water and Oyster Food Quality in the Delaware Estuary……..……22

Chapter 3. Implementation and Validation of a Coupled Hydrodynamic-Larval Transport Model for the Delaware Estuary…….....46

Appendices

Chapter 1 Appendix……...67
Chapter 2 Appendix……...……99

LIST OF TABLES

Chapter 1

Table 1. Specifications of VEMCO acoustic tags used in the study…….12

Table 2. Monthly sampling effort and catch of Atlantic and shortnose sturgeons……13

Table 3. Summary of captures of presumed young-of-the-year Atlantic sturgeon in the Delaware River……. 19

Chapter 2

Table 1. Summary of sample analysis success……..24

Chapter 1 Appendix

Table 1. Juvenile Atlantic sturgeon collected in the lower tidal Delaware River, July-November 2009……68

Table 2. Occurrence of acoustically tagged Atlantic sturgeon in the Delaware Estuary and nearshore ocean…….....69

Table 3. Shortnose sturgeon collected in the tidal Delaware River, June 2008-October 2009……80

Table 4. Occurrence of acoustically tagged shortnose sturgeon at telemetry receivers in the Delaware Estuary……...……...81

Chapter 2 Appendix

Table 1. GPS coordinates for all 18 sites……100

Table 2. Collection dates and water parameters…….101

LIST OF FIGURES

Chapter 1

Figure 1. Acoustic telemetry receiver network in the Delaware-River, Bay and nearshore ocean. ……12

Figure 2. Length-frequency distribution of Atlantic sturgeon collected in the lower tidal Delaware River, July-November 2009..……... 14

Figure 3. Length-weight relationship of Atlantic sturgeon collected in the lower tidal Delaware River, July-November 2009..……... 14

Figure 4. Length-weight relationship of young-of-the-year Atlantic sturgeon collected in the lower tidal Delaware River, September-November 2009..……..15

Figure 5. Lengths of young-of-the-year Atlantic sturgeon plotted against collection date ……15

Figure 6. Length-frequency distribution of shortnose sturgeon collected in the lower tidal Delaware River, June 2008-October 2009…….17

Figure 7. Length-weight relationship of shortnose sturgeon collected in the lower tidal Delaware River, June 2008-November 2009……17

Chapter 2

Figure 1. Mean concentration particulate matter averaged across sampling stations…... 28

Figure 2. Mean pooled seston organic proportion and proportion of organic fraction averaged across sampling stations…… 29

Figure 3. Seston protein concentration and percentage protein content averaged across sampling stations……... 29

Figure 4. Seston carbohydrate concentration and percentage protein content averaged across sampling stations…….29

Figure 5. Seston lipid concentration averaged across sampling stations……. .30

Figure 6. Seston particulate matter concentration averaged across sampling stations…. 31

Figure 7. Percentage organic content averaged across sampling stations. ……...31

Figure 8. Percentage protein content (box and whisker plot) for stations averaged among months sampled…… 32

Figure 9. Percentage carbohydrate content (box and whisker plot) for stations averaged among months sampled……..32

Figure 10. Concentration of seston particulate material averaged across months for stations along downbay to upbay gradient…… 33

Figure 11. Percentage organic content particulate material averaged across months for stations along downbay to upbay gradient of Delaware bay sampling stations……... 34

Figure 12. Ratio of protein concentration to sum of protein, lipid,and carbohydrate concentrstions for seston collected along along downbay to upbay gradient of Delaware Bay sampling stations……... 34

Figure 13. Concentration of seston particulate material (box and whisker plot) averaged across months for paired stations located inshore versus offshore within Delaware Bay ……35

Figure 14. Salinity versus decimal latitude within Delaware Bay…… 36

Figure 15. Percentage organic content of seston versus decimal latitude within Delaware Bay……... 36

Figure 16. Least squares linear regression of percentage organic content of seston as a function of salinity within Delaware Bay……. 37

Figure 17. Concentration of seston particulate material (box and whisker plots) averaged across stations within Delaware Bay that were sampled on different tide stages…… 37

Figure 18. Annual average oyster condition index baywide…….....39

Figure 19. Annual average oyster condition index by bay group……40

Chapter 3

Figure 1. Water level, temperature salinity, and atmospheric forcing data station locations and bathymetry……..51

Figure 2. Comparison of time series for incoming solar short wave radiation as given by the North American Regional Reanalysis and by the Delaware Environmental Observation System……. 52

Figure 3. Schematic of the Taylor diagram……. 53

Figure 4. Taylor diagram for model-data comparisons at the 12 water level stations…...53

Figure 5. Taylor diagram for model-data comparisons at the 9 temperature stations….. 54

Figure 6. Taylor diagram for model-data comparisons at the 9 salinity stations…….. 54

Figure 7. Comparison between tidally averaged along channel flow from 2005 mooring deployment and model…….. 55

Figure 8. Vertical salinity stratification from model and observed from 2005 deployment Red line indicates peak of April 2005 Delaware River discharge…… 56

Figure 9. Comparison between observed along-channel tidally mean flow from observations and model (right). Negative velocity is landward, positive (yellow/red) is seaward……. 56

Figure 10. Particle release locations for the Lagrangian particle tracking simulations… 57

Figure 11. Comparison of larval transport without and with behavior……...58

Figure 12. Final settling location of particles released between June and August……....59

Figure 13. The percent of simulated particles (oyster larvae) released from a particular reef that settle at various locations in Delaware Bay…… 60

Figure 14. Spat-to-adult oyster ratio for each Bay region. ……..…….61

Figure 15. Time series of oyster abundance by bay region…….… .62

Chapter 1 Appendix

Figures A1-A25. Movements of Atlantic sturgeon in the Delaware Estuary…….…….83

Figures B1-B6. Movements of shortnose sturgeon in the Delaware Estuary……..... 96

Chapter 2 Appendix

Map of Delaware Bay and River……105

PROJECT SUMMARY

A regional concern of global warming is the acceleration of sea-level rise in the Delaware Estuary. Associated increases in salinity could have a major impact on critical estuarine processes and species. Three species of particular concern are the Atlantic sturgeon *Acipenser oxyrinchus*, the shortnose sturgeon, *Acipenser brevirostrum*, and the eastern oyster, *Crassostrea virginca.*

The Atlantic and shortnose sturgeon belong to a prehistoric group of fish that have existed for more than 70 million years. Atlantic sturgeon are anadromous, migrating between freshwater and marine environments, and returning to their natal estuaries to spawn. Shortnose sturgeon, generally, remain in their natal estuary, occurring primarily in fresh and brackish waters. Atlantic sturgeon supported a principal fishery in the Delaware Estuary in the late 1800s and early1900s; their roe being heavily sought for the international caviar trade. The abundance of both sturgeon species declined in the Delaware River and throughout their ranges in the late 19th and early 20th centuries as a result of over exploitation, water pollution, and habitat modification. The shortnose sturgeon is presently listed as Federally endangered and the Atlantic sturgeon is a candidate for listing as a threatened or endangered species. Considerable research on the biology of sturgeon in the Delaware River and Bay has been performed. However, little is known regarding the occurrence, distribution, and movements of juveniles. Knowledge of the seasonal utilization of different parts of the estuary by juvenile sturgeon and their habitat requirements is critical to the species' protection, management, and recovery. The lack of informed knowledge of their essential habitats precludes the implementation of appropriate protection and enhancement management strategies.

The eastern oyster is an important keystone species of the Delaware Estuary; providing several vital ecological services. The oyster has also served as a principal Delaware Bay fishery, holding particular economic, social, and cultural-historical significance to communities along the Delaware Bay shore. For over 50 years extensive research on oyster biology and ecology has been conducted. Population models, a product of these research efforts, have been essential to the management and sustainability of the Delaware Bay oyster resource. Additionally, there has been a highly successful oyster restoration program in recent years that has demonstrated an effective means to preserve this critical resource.

Though very different in their functional significance to the estuary, oysters, and sturgeon both represent important ecological indicators of the health of the estuary. Additionally these species are particularly vulnerable to anthropogenic and climatic changes effecting estuarine flow dynamics.

This report serves to document interim progress of a multi-year study on the effects of flow dynamics, salinity, and water quality on the Atlantic sturgeon, the shortnose sturgeon, and the eastern oyster in the Delaware Estuary. The purpose of the study is to gather information and develop a model for planning, in support of managing and restoring sturgeon, oysters, and other salinity dependent resources of the Delaware Estuary. The study focuses on habitats at the fresh/brackish water interface, the turbidity maximum zone (TMZ), ranging from the Marcus Hook area south to the Maurice River. The TMZ is vulnerable to anthropogenic and climatic changes. This oligohaline zone supports essential habitats for juvenile anadromous fish, such as sturgeons, and provides critical disease refuge for oysters. Evaluations of oyster population dynamics, water quality and food web dynamics, and sturgeon habitats will be integrated in a circulation-biogeochemical model (ROMS v.3), which has been developed to identify dominant circulation phenomena in Delaware Bay and on the adjacent continental shelf. The model's temperature, salinity, and flow velocity outputs force oyster larval transport, as well as other biological and environmental interactions occurring in the Estuary.

Ultimately the study and its products will provide information and modeling capabilities, for Estuary resource managers and users to develop thoughtful, proactive policies to plan for and mitigate sea-level rise impacts on important estuarine natural resources. This work will augment efforts to restore and protect oyster and sturgeon habitats in the Delaware Bay. Refinement of the ROMS v.3 model will enhance its utility for examining a wide variety of questions relating to the effects of climatic shifts and flow alterations on the biological resources of the Estuary.

The study reported here (referred to as the Delaware Estuary Study (DES)) represents an interdisciplinary collaborative effort involving several institutions and organizations. Experts of various disciplines have independently gathered information during the first year of this project on three main study areas: (1) sturgeon distribution, (2) water and oyster food quality, and (4) hydrodynamic modeling. In subsequent years these efforts will come together as they are interrelated through analyses and modeling efforts. To this end the study has three main objectives:

1) To track juvenile sturgeon using acoustic telemetry to examine seasonal distribution and movements in relation to water quality and hydrodynamic factors.
2) To gather information on spatial and temporal variability in water quality and food supply parameters to better ground truth and enhance the utility of the ROM v.3 model for modeling hydrodynamic influences, specifically freshwater inflow, on oyster population dynamics.
3) To apply the ROMS v.3 model as a tool for examining the relationship of juvenile sturgeon distribution and environmental parameters with a view toward identifying essential habitats and examining the sensitivity of essential habitats to past, present, and future anthropogenic and natural alterations in flow and water quality.

The interim results of this first-year study are presented here as three separate chapters. The integration of the "independent" study efforts will evolve in Project Year 2.

CHAPTER 1

Acoustic Telemetry Studies of the Distribution and Movement of Juvenile Sturgeons in the Delaware River and Estuary

Harold M. Brundage III[1] and John C. O'Herron, II[2]

[1]Environmental Research and Consulting, Inc., 126 Bancroft Rd., Kennett Square, PA 19348

[2]Amitrone O'Herron, Inc., P.O. 173, Cornwall, PA 17016-0173

1.0 INTRODUCTION

In October 2008, Environmental Research and Consulting, Inc. (ERC) in collaboration with Delaware Estuary Study project partners initiated a program to capture and acoustically tag juvenile Atlantic sturgeon (*Acipenser oxyrinchus oxyrinchus*) and juvenile shortnose sturgeon (*Acipenser brevirostrum*) in the Delaware River. The objective of this program is to study the distribution and movements of juvenile sturgeons, as determined by acoustic telemetry, in relation to water temperature, salinity, dissolved oxygen concentration, and river flow. The ultimate goal of the project is to integrate juvenile sturgeon distribution/movement data into a water quality model (ROMS v.3) being developed by Rutgers University, and use this model to explore the effects of natural and anthropogenic changes in river flow and water quality on the availability and suitability of sturgeon habitat in the Delaware River Estuary. This juvenile sturgeon study is part of a larger project, known as the Delaware Estuary Study (DES), funded by the U.S. Army Corps of Engineers, Philadelphia District. This draft interim report presents the results of the first year of the juvenile sturgeon study.

2.0 MATERIALS AND METHODS

2.1 Sturgeon Collection and Processing

Sampling to collect juvenile sturgeon for acoustic tagging was performed in the lower tidal Delaware River from the lower Cherry Island Flats, near Wilmington, DE (river kilometer (rkm) 110; river kilometer references based on DRBC, 1969), to the upper Marcus Hook, PA anchorage (rkm 130) during October-November 2008 and May-November 2009. Sampling was conducted using anchored gill nets of various lengths and mesh sizes (100 x 1.8 m with 33 m panels of 2.5, 5.1 and 7.6 cm mesh; 66 x 1.8 m with 33 m panels of 5.1 and 7.6 cm mesh; 100 x 1.8 m with 25 m panels of 2.5, 5.1, 7.6, and 10.2 cm mesh; and 100 x 1.8 m of 12.7 cm mesh). Sampling was performed in a

non-systematic fashion, whereby gill netting locations and the types of nets fished during each sampling event were selected to maximize the number of sturgeon collected.

Water depth during net deployment was measured using a Hummingbird Model 100SX digital depth finder. Surface and bottom water temperature, dissolved oxygen concentration, specific conductance, and salinity were measured using a Yellow Springs Instrument Company (YSI) Model 85 handheld meter at the beginning and end of each sampling day.

Sturgeons were removed from the nets and placed in an out-board live car or an on-board tank containing river water at ambient temperature and dissolved oxygen levels. Sturgeon were identified to species, measured for fork length (FL) and total length (TL) to the nearest millimeter, and weighed to the nearest gram. Sturgeon of sufficient size were tagged with a numbered T-bar tag (Floy Tag and Manufacturing, Inc.) and/or a passive integrated transponder (PIT) tag. Destron 14 mm PIT tags activated at a radio frequency of 125 kHz were used in this study.

All sampling and handling of sturgeon followed established protocols (Moser *et al.*, 2000) and were performed in accordance with Permit to Take Endangered Species for Scientific Purposes No. 1486, issued by the National Marine Fisheries Service (NMFS).

2.2 Acoustic Telemetry

Selected sturgeon were surgically implanted with a VEMCO acoustic transmitter (model V7, V9, V13, or V16) matched to their body weight. Tags with different combinations of battery size, output power, and delay interval were used to maximize tag life and power, while maintaining tag weight at less than 2% of body weight (Table 1). Each acoustic transmitter was coded with a unique pulse series/tag number and pulsed at 69.0 kHz.

Sturgeon for acoustic tag implantation were anesthetized using tricane methanesulfonate (MS-222) at a dose of 50 mg/L and then held upside down in a cradle where the gills were perfused with aerated flowing water. A sterile scalpel was used to make a small longitudinal abdominal incision and a transmitter was inserted into the body cavity. The incision was closed with interrupted sutures of 3-0 polydioxanone (PDS) and treated with povidone iodine (10 percent solution) and petrolatum to prevent infection. Post surgery, fish were held in an aerated holding tank and released upon recovery from anesthesia. The surgical procedure required approximately five minutes to complete, with a total holding time (surgery plus recovery) of 15 minutes or less per individual.

The movements of acoustically tagged sturgeon were monitored using a network of 86 VEMCO VR2 and VR2W single-channel receivers, deployed in the Delaware River and Bay from Yardley, PA (rkm 221) to the bay mouth (rkm 0), in the eastern Chesapeake and Delaware (C&D) Canal, in the Elk River, MD near the western terminus of the C&D Canal, and in the nearshore ocean from Cape May, NJ to Ocean City, MD (Fig. 1). The receiver network was established and cooperatively maintained by Environmental

Research and Consulting, Inc. (ERC), Delaware State University (DSU), and the Delaware Department of Natural Resources and Environmental Control (DNREC).

Tag Type	Battery Option	Length (mm)	Diameter (mm)	Weight in Air (g)	Weight in Water (g)	Power Output (dB re 1uPa @1m)	Delay (sec)	Calculated Battery Life (days)
V7	4L	22.5	7.0	1.8	1.0	136	60-180	248
	4L	22.5	7.0	1.8	1.0	136	110-250	337
V9	6L	21.0	9.0	2.9	1.6	142	60-180	147
	1L	24.0	9.0	3.6	2.2	142	60-180	291
	2L	29.0	9.0	4.7	2.9	142	60-180	537
V13	1H	36.0	13.0	11.0	5.0	153	60-180	372
	P-1H[1]	45.0	13.0	12.0	4.0	158	20-60	120
V16	1L	54.0	16.0	20.0	9.0	150	60-180	739
	4H	68.0	16.0	25.0	11.0	152	60-180	1625
	6H	95.0	16.0	36.0	16.0	153	60-180	3003

[1]equipped with depth sensor

Table 1. Specifications of VEMCO acoustic tags used in the study.

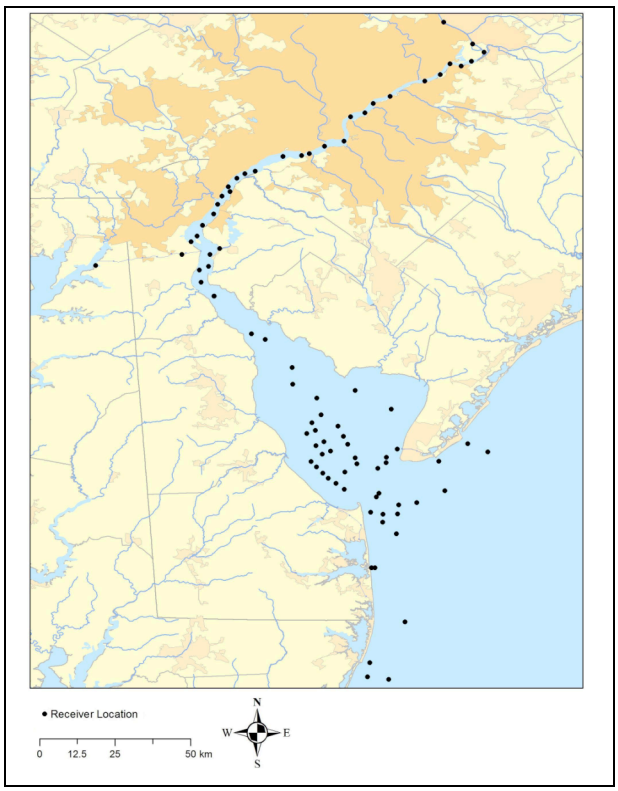

Figure 1. Acoustic telemetry receiver network in the Delaware-River, Bay, and nearshore ocean.

Acoustic tag transmissions were decoded by a receiver and stored in its flash memory. The data stored by a receiver included receiver identification number, transmitter identification number, date/time of signal detection, and the number of detections received during the period the sturgeon was present. Records of the occurrence of each

tagged sturgeon were extracted from the receiver files and compiled in EXCEL spreadsheets for analysis. Metrics of relative occurrence and site fidelity calculated for this study were the total number of calendar days a sturgeon was recorded at each receiver and the total number of individual detections received.

3.0 RESULTS

3.1 Atlantic Sturgeon

Gill net sampling for the DES program was conducted on 28 days during October-November 2008 and May-November 2009 (total fishing effort - 465.9 net hours). This sampling yielded 59 juvenile Atlantic sturgeon (Table 2). This total includes the recapture of one previously tagged fish in each of September and October 2009. Atlantic sturgeon were captured during July through November 2009, at water temperatures ranging from 11.0-27.1ºC, dissolved oxygen concentrations ranging from 6.2-9.6 mg/l, specific conductances ranging from 208-665 µS/cm, and salinities ranging from 0.1-0.3‰ (Chapter 1 Appendix: Table 1).

	No. Sampling Events	No. Net Hours	No. Atlantic Sturgeon	No. Shortnose Sturgeon
Oct-08	2	38.6	0	0
Nov-08	4	78.6	0	1
May-09	1	14.8	0	0
Jun-09	3	61.1	0	0
Jul-09	5	111.8	1	3
Aug-09	1	13.0	2	1
Sep-09	2	29.8	23[a]	3
Oct-09	7	85.7	18[a]	4
Nov-09	3	32.5	15	0
Total	28	465.9	59	12

[a]Includes 1 recapture

Table 2. Monthly sampling effort and catch of Atlantic and shortnose sturgeons.

Collection information and vital statistics for the 57 Atlantic sturgeon collected during this study and six Atlantic sturgeon obtained from the Delaware Department of Natural Resources and Environmental Control (DNREC) are presented in Chapter 1 Appendix, Table 1 (see DNREC (2009) for information on their Atlantic sturgeon sampling program). Atlantic sturgeon ranged from 220-1,148 mm in total length, 189-970 mm in fork length, and 38-8,640 g in weight. The length-frequency distribution for these fish is presented in Figure 2 and the length-weight relationship is shown in Figure 3.

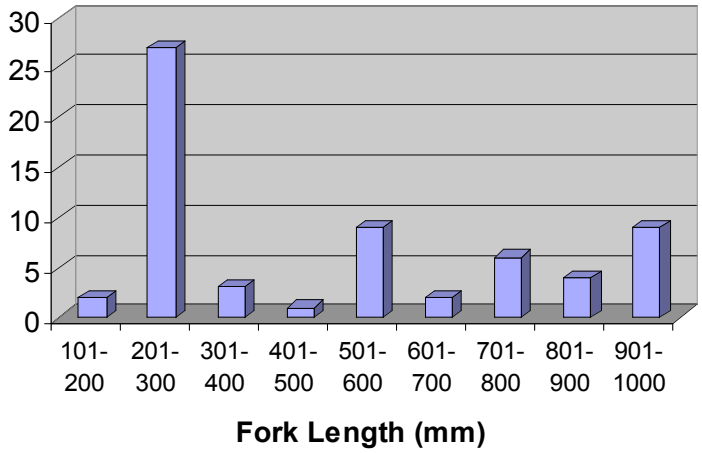

Figure 2. Length-frequency distribution of Atlantic sturgeon collected in the lower tidal Delaware River, July-November 2009.

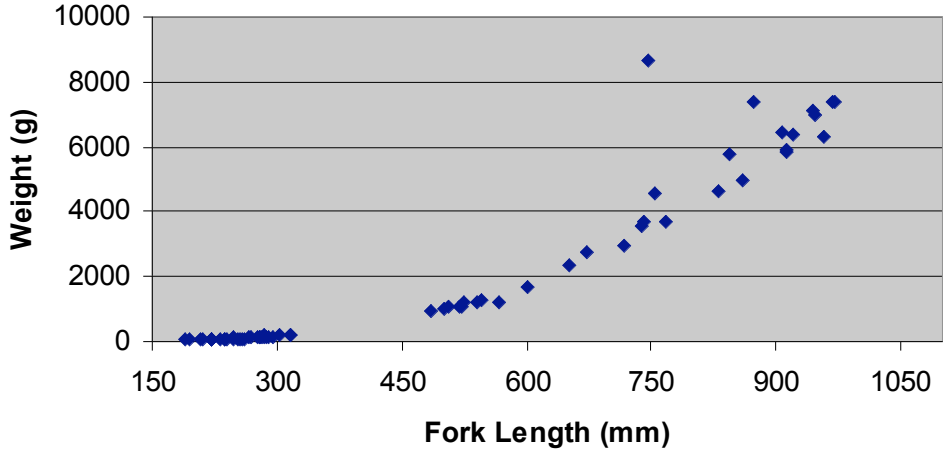

Figure 3. Length-weight relationship of Atlantic sturgeon collected in the lower tidal Delaware River, July-November 2009.

Thirty-two of the Atlantic sturgeon were young-of-the-year (YOY), ranging from 220-367 mm in total length, 189-315 mm in fork length, and 38-220 g in weight (Chapter 1 Appendix: Table 1). Atlantic sturgeon YOY were collected from late September through November. The length-weight relationship for YOY Atlantic sturgeon is presented in Figure 4. Lengths of the YOY Atlantic sturgeon are plotted by collection date in Figure 5. An average growth rate of approximately 1.08 mm/day can be inferred from this plot.

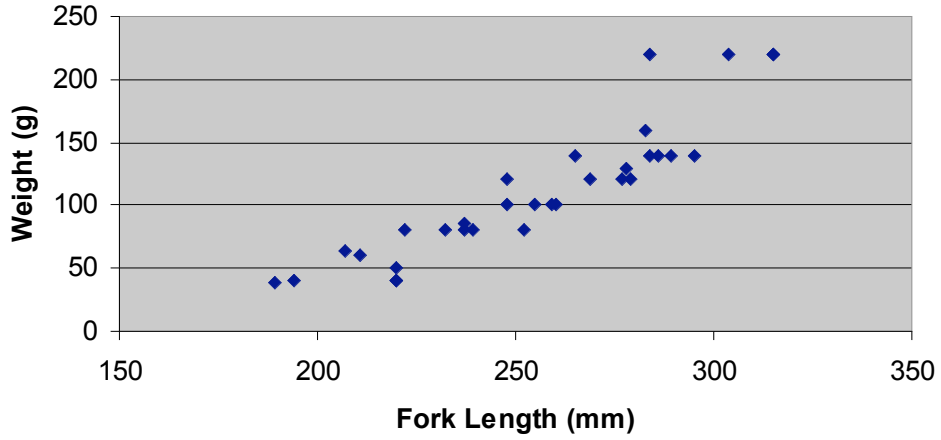

Figure 4. Length-weight relationship of young-of-the-year Atlantic sturgeon collected in the lower tidal Delaware River, September-November 2009.

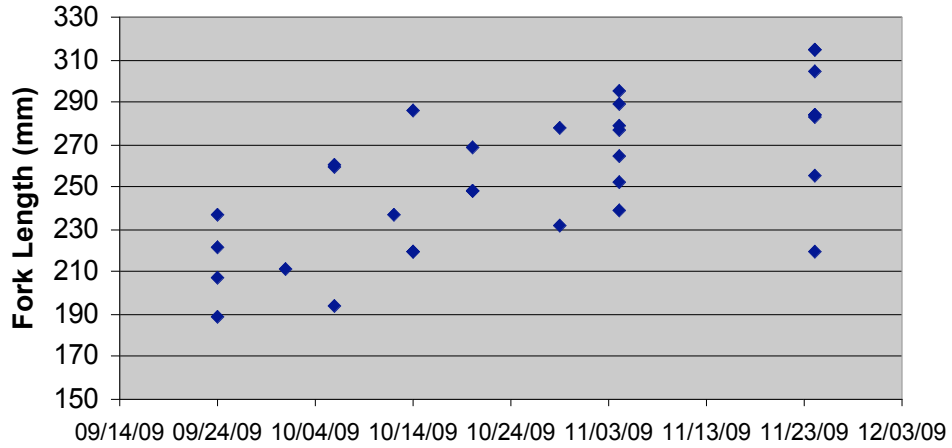

Figure 5. Lengths of young-of-the-year Atlantic sturgeon plotted against collection date.

Acoustic transmitters were implanted in 26 juvenile Atlantic sturgeon, six of which were YOY. Occurrence data for each acoustically-tagged Atlantic sturgeon are given in Chapter 1 Appendix: Table 2 and river kilometer-date plots are presented in Figures A-1 through A-25. One transmitter (acoustic tag A109) was detected for only a few days, and data from this tag were not included.

Acoustically-tagged subadult (i.e., juveniles older than YOY) Atlantic sturgeon ranged from the nearshore ocean off of Ocean City, NJ to Philadelphia, PA (rkm 148), with most detections occurring in the lower tidal Delaware River from the middle Liston Range (rkm 70) to Tinicum Island (rkm 141) (Chapter 1 Appendix: Table 2).

The movements of subadult Atlantic sturgeon were generally localized during the summer and early fall, with areas of particular concentration noted in the Marcus Hook (rkm 123-129) and Cherry Island Flats (rkm 112-118) regions of the river (Chapter 1 Appendix: Table 2). Later in the fall, movement increased and fish typically evidenced one of three generalized movement/ detection patterns. Nine (47.4%) of the 19 acoustically-tagged subadults made rapid directed movements to lower Delaware Bay or the ocean, 4 (21.1%) evidenced directed movements toward the bay, but were not detected below the Liston Range, and 6 (31.6%) appeared to have remained in the tidal river into the winter. Examples of these three movement patterns are provided in Chapter 1 Appendix: Figures A-1, A-3, and A-5, respectively. It is possible fish that evidenced the second pattern continued seaward, but were not detected by any receivers. The bay widens considerably below the Liston Range and the receiver network becomes more porous, thusly allowing fish to move through an area without being detected.

There appears to be a relationship between length and the movement pattern demonstrated by subadult Atlantic sturgeon, with smaller, presumably younger, fish more likely to remain in the tidal river. The fork length of fish that made defined movements to the lower bay and ocean averaged 815 mm (range 651-970 mm); those that moved towards the bay but were not detected below Liston Range averaged 716 mm (range 505-947 mm) and those that appear to have remained in the tidal river into the winter averaged 524 mm (range 485-566 mm).

Acoustically-tagged YOY Atlantic sturgeon, all of which were captured in the Marcus Hook anchorage (rkm 127) during late October-late November 2009, ranged from Deepwater, NJ (rkm 105) to Roebling, NJ (rkm 199) (Chapter 1 Appendix: Table 2). Two of the YOY Atlantic sturgeon (acoustic tags A120 and A124) remained in the Marcus Hook to Chester, PA reach of the river between rkm 123-130 (Chapter 1 Appendix: Figs. A-20 and A-25). Atlantic sturgeon YOY acoustic tag A121 was detected over a somewhat wider range of the lower tidal river between Deepwater (rkm 105) and Tinicum Island (rkm 141) (Chapter 1 Appendix: Fig. A-21). Three of the acoustically-tagged YOY (acoustic tags A122, A123, and A125) made more extensive movements and moved progressively upriver to the Torresdale, PA (rkm 176) to Roebling (rkm 199) reach of the upper tidal river in January 2010 (Chapter 1Appendix: Figs. A-22 through A-24).

3.2 Shortnose Sturgeon

Gill net sampling in the lower tidal Delaware River during October-November 2008 and May-November 2009 yielded 12 shortnose sturgeon (Table 2 and Chapter 1 Appendix: Table 3). Based on length and/or examination of gonads during tag implantation, 1 was a juvenile, 3 were probable juveniles, 1 had recently matured, and 7 were adults. Two juvenile shortnose sturgeon were collected in the upper tidal Delaware River during sampling for another project in June 2008 and June 2009. Both of these fish were acoustically tagged and are included in the results below. Shortnose sturgeon were captured during June and November 2008, and June through October 2009 at water

temperatures ranging from 12.8-26.4ºC, dissolved oxygen concentrations ranging from 5.8-8.8 mg/l, specific conductances ranging from 102-2,881 µS/cm, and salinities ranging from 0.1-1.6‰ (Chapter 1 Appendix: Table 3). Shortnose sturgeon ranged from 438-796 mm in total length, 381-702 mm in fork length, and 410-3,480 g in weight (Chapter 1 Appendix: Table 3). The length-frequency distribution for these fish is presented in Figure 6 and the length-weight relationship is shown in Figure 7.

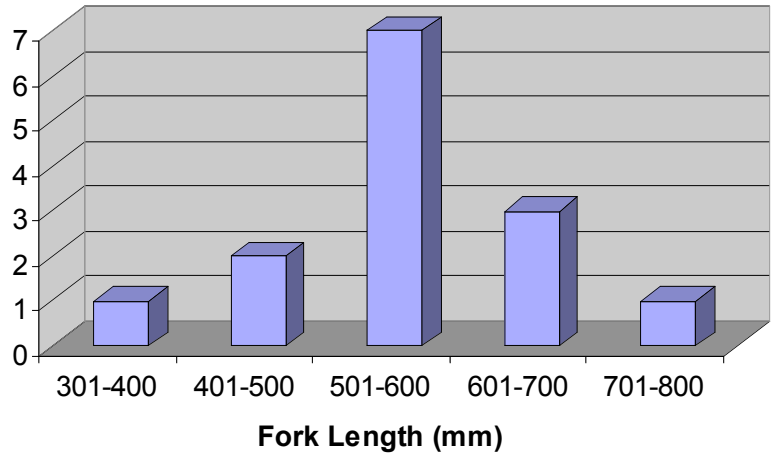

Figure 6. Length frequency distribution of shortnose sturgeon collected in the lower tidal Delaware River, June 2008-October 2009.

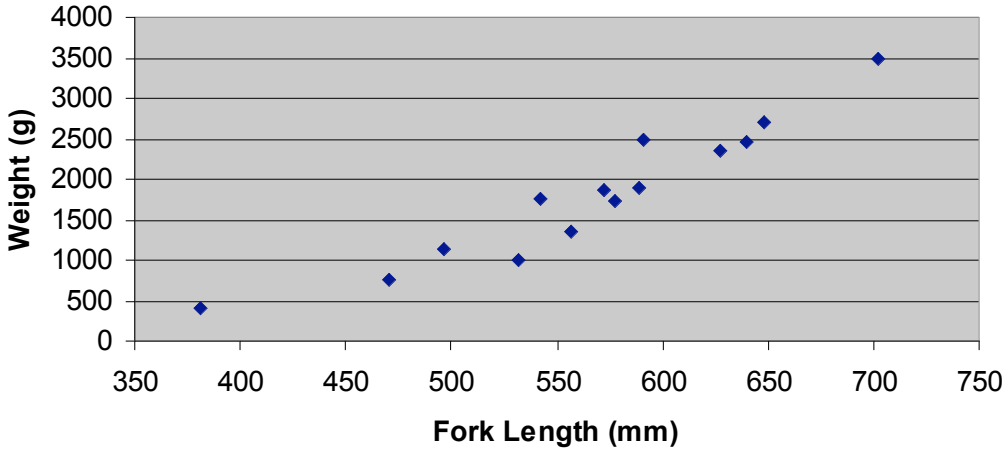

Figure 7. Length-weight distribution of shortnose sturgeon collected in the lower tidal Delaware River, June 2008-October 2009.

Acoustic transmitters were implanted in six shortnose sturgeon. Two of these were juveniles (acoustic tags A126 and A128), 3 were probable juveniles (acoustic tags A127, A129, and A131), and one had recently matured (acoustic tag A130). Occurrence data for each acoustically-tagged shortnose sturgeon are given in Chapter 1 Appendix: Table 4 and river kilometer-date plots are presented in Chapter 1 Appendix: Figures B-1 through B-6.

Acoustically-tagged shortnose sturgeon ranged from upper Liston Range (rkm 77) to Trenton (rkm 211), with most detections occurring in the upper tidal Delaware River from Torresdale (rkm 176) to Trenton (rkm 211) and the lower tidal river from Deepwater (rkm 105) to Marcus Hook (rkm 125) (Chapter 1 Appendix: Table 4). Varying patterns of movement were evidenced by the acoustically tagged shortnose sturgeon. Shortnose sturgeon acoustic tag A126, a juvenile tagged in the upper tidal Delaware River in June 2008, remained there where it ranged between rkm 163 and 211 (Chapter 1 Appendix: Fig. B-1). Shortnose sturgeon acoustic tag A128, a juvenile tagged in the upper tidal river in June 2009, moved rapidly to the lower tidal river and spent most of its time in the Cherry Island Flats-Marcus Hook reach (Chapter 1 Appendix: Fig. B-3). Shortnose sturgeon acoustic tag A127, a probable juvenile tagged in the lower tidal river in October 2008, remained in the lower tidal river (rkm 83-134) through the winter, and moved rapidly to the upper reaches of the tidal river (rkm 211) in early May 2009, remaining there only a few days before moving back downriver (Chapter 1 Appendix: Fig. B-2).

Shortnose sturgeon acoustic tag A129, a probable juvenile tagged in the lower tidal river in July 2009, moved to the upper tidal river (rkm 86-201) where it spent most of the summer and early fall. This fish moved rapidly back to the lower tidal river (rkm 108-134) in mid-October, where it appears to have overwintered (Chapter 1 Appendix: Fig. B-4). Acoustic tag A130, a recently matured shortnose sturgeon tagged in the lower tidal river in July 2009, demonstrated the opposite pattern of movement, remaining in the lower tidal river (rkm 99-134) through the summer and early fall. In mid-October, this sturgeon moved to the upper tidal river (rkm 176-207), where, with the exception of several brief downriver excursions, it spent the remainder of the fall and early winter (Chapter 1 Appendix: Fig. B-5). Shortnose sturgeon acoustic tag A131, a probable juvenile tagged in the lower tidal Delaware River in July 2009, moved slowly upriver in early August, and remained in the upper tidal river until it was last detected at rkm 207 in early November 2009 (Chapter 1 Appendix: Fig. B-6).

4.0 DISCUSSION

4.1 Atlantic Sturgeon

The occurrence and movement patterns of subadult Atlantic sturgeon in the present study is consistent with those observed in others studies in the Delaware River Estuary (Brundage and Meadows, 1982; Brundage and O'Herron, 2009; Lazzari *et al*., 1986; DNREC, 2009) and the Hudson River (Dovel and Berggren, 1983, Bain 1997).

Subadults move upriver into the seasonally brackish and tidal freshwater reaches during the summer and may move downriver to overwintering areas in the lower estuary and nearshore ocean in fall-early winter. Younger subadult Atlantic sturgeon appear less likely to move down bay, and may overwinter in the lower tidal river. Results of the present study indicate that YOY Atlantic sturgeon utilize the lower tidal Delaware River in fall, probably as a foraging area, and may expand their range into the upper tidal river in winter.

The collection of 32 YOY Atlantic sturgeon in the present study and the capture of an additional 34 YOY by DNREC (2009) is evidence of a successful and, perhaps, significant spawn of Atlantic sturgeon in the Delaware River in 2009. The literature contains only a few prior records of YOY Atlantic sturgeon in the Delaware River. Burton *et al.* (2005) captured a 342 mm FL Atlantic sturgeon in the Marcus Hook anchorage in February 2005. Based on the date of capture and length, this fish was probably a YOY. The only other reported captures of presumed YOY Atlantic sturgeon in the Delaware River, summarized in Table 3 below, were from the 1970s (Brundage and Meadows, 1982).

Capture Date	Location	River km	Total Length (mm)
9/24/73	Newbold Island	203	196
8/15/78	Burlington Island	190	157
8/28/78	Burlington Island	190	175
9/6/78	Burlington Island	190	175
8/9/79	N of Pea Patch Island	101	128

Table 3. Summary of captures of presumed young-of-the-year Atlantic sturgeon in the Delaware River.

Studies in the Hudson River (Dovel and Berggren, 1983) and other systems indicate that Atlantic sturgeon remain in their natal river until at least age 2 and may be resident for up to 6 years. Lazzari *et al.* (1986) reported the capture of one age 1 and two age 2 Atlantic sturgeon in the upper tidal Delaware River during 1981-1984. Of the five juvenile Atlantic sturgeon captured in the lower tidal river by Brundage and O'Herron (2009) the youngest was probably age 2. It is likely that all of these young fish were spawned in the Delaware River.

The results reported herein, while promising in respect to the capture of YOY Atlantic sturgeon, must be interpreted cautiously due to the lack of comparable sampling efforts in the past. Sampling in this project was intensive and targeted to maximize the number of sturgeon captured (as opposed to sampling with standardized effort at regular stations).

4.2 Shortnose Sturgeon

Juvenile and probable juvenile shortnose sturgeon in the present study ranged throughout the entire tidal Delaware River and demonstrated a diversity of movement patterns. Dispersion of juvenile shortnose sturgeon through the tidal freshwater and seasonally

brackish river zones was reported in a previous study in the Delaware River (Brundage and O'Herron, 2009), as well as studies in the St. John (Dadswell, 1979), Connecticut (Kynard, 1997), and Hudson (Bain, 1997) Rivers.

Juvenile and probable juvenile shortnose sturgeon in this study appeared to preferentially utilize the upper tidal Delaware River from Torresdale to Trenton and the lower tidal river from Deepwater to Marcus Hook. The middle reach of the tidal river was utilized to a lesser extent. This may be related to the quality and/or quantity of food resources in the preferred reaches and/or lower habitat quality in the less utilized middle reach, which includes the cities of Philadelphia and Camden.

4.3 Year 2 Scope of Work

The juvenile sturgeon tracking program will be continued during the second year of the DES project. Many of tags implanted during the first year of the study will be active after the period covered in this report and data from these tags will be collected and analyzed. Additional juvenile sturgeon will be captured and tagged. Tagging and tracking of Atlantic sturgeon of the 2009 year class will be of particular interest. Moreover, possible relationships between the distribution and movements of juvenile sturgeon and water quality variables will be investigated using the ROMS v.3 model during the second year of the project.

5.0 LITERATURE CITED

Bain, M. B. 1997. Atlantic and shortnose sturgeons of the Hudson River: common and divergent life history attributes. Environmental Biology of Fishes 48: 347-358.

Brundage, H. M., and R. E. Meadows. 1982. The Atlantic sturgeon, *Acipenser oxyrhynchus,* in the Delaware River estuary. Fishery Bulletin 80:337-343.

Brundage, H. M., and J. C. O'Herron. 2009. Investigations of juvenile shortnose and Atlantic sturgeons in the lower tidal Delaware River. Bulletin of the New Jersey Academy of Science 54:1-8.

Burton, W. H., H. M. Brundage, and J. C. O'Herron. 2005. Delaware River adult and juvenile sturgeon survey - winter 2005. Prepared for the U.S. Army Corps of Engineers, Philadelphia District. Versar, Inc., Columbia, MD. 36 pp.

Dadswell, M. J. 1979. Biology and population characteristics of the shortnose sturgeon, *Acipenser brevirostrum* LeSueur 1818 (Oesteichthyes: Acipenseridae), in the Saint John River Estuary, New Brunswick, Canada. Canadian Journal of Zoology 57: 2186-2210.

DNREC (Delaware Department of Natural Resources and Environmental Control). 2009. Atlantic sturgeon progress report. State Wildlife Grant. Project T-4-1. Delaware Department of Natural Resources and Environmental Control. Dover, DE. December 2009.

Dovel, W. L., and T. J. Berggren. 1983. Atlantic sturgeon of the Hudson River estuary, New York. New York Fish and Game Journal 30:140-172.

DRBC (Delaware River Basin Commission). 1969. The Delaware River basin stream mileage system. Staff Paper 105, Revision 1. January 30, 1969.

Kynard, B. 1997. Life history, latitudinal patterns, and status of the shortnose sturgeon, *Acipenser brevirostrum*. Environmental Biology of Fishes 48: 319-334.

Lazzari, M. A., J. C. O'Herron, and R. W. Hastings. 1986. Occurrence of juvenile Atlantic sturgeon, *Acipenser oxyrhynchus*, in the upper tidal Delaware River. Estuaries 9:358-361.

Moser, M. L., M. Bain, M. R. Collins, N. Haley, B. Kynard, J. C. O'Herron, G. Rogers, and T. S. Squiers. 2000. A protocol for use of shortnose and Atlantic sturgeon. NOAA Technical Memorandum NMFS-OPR-18. 18 pp.

USCG (United States Coast Guard). 2007. Light List. Vol. II. Atlantic coast. Shrewsbury River, New Jersey to Little River, South Carolina. United States Department of Homeland Security, Washington, D. C. COMDTPUB P16502.2. 376 pp.

CHAPTER 2

Spatial and Temporal Variability in Water and Oyster Food Quality in the Delaware Estuary

Danielle Kreeger,[1] Roger Thomas,[1] Eric Powell[2], Jason Morson[2]

[1]Patrick Center for Environmental Research, The Academy of Natural Sciences, 1900 Ben Franklin Parkway, Philadelphia, PA 19103

[2]Haskin Shellfish Research Laboratory, Institute of Marine and Coastal Sciences, Rutgers, the State University of New Jersey, 5969 Miller Avenue, Port Norris, NJ 08349

1.0 INTRODUCTION

1.1 Effects of Food Availability on Bivalve Productivity

Worldwide, suspension-feeding bivalves are considered as "ecosystem engineers" that, where abundant, can regulate key processes such as biofiltration and its attendant effects on water quality, exerting top-down control of phytoplankton and pathogens (Officer, *et al*., 1982; Ulanowicz and Tuttle, 1992; Dames and Prins, 1998; Grabowski and Peterson, 2007). Factors that in turn regulate bivalve population dynamics include the recruitment of young individuals into the population, the mortality of animals due to predation, harvest pressure and disease, and the productivity (growth) of the population (MacKenzie, 1996; Shumway, 1996; Smaal, *et al*., 1998; Newell, 2004). In cases where the productivity and recruitment are high relative to mortality, bivalve populations increase up to a system's carrying capacity; whereas, populations that experience higher mortality and loss of biomass than that which can be replaced will decline (Dame and Prins, 1998; Smaal, *et al*., 1998).

Much more is known about the various factors that contribute to bivalve mortality than the factors that regulate recruitment (examined here in Chapter 3) and productivity (this Chapter.) To develop an understanding of bivalve production requires careful analysis of the organismal-level physiological ecology and nutrition of bivalves (Newell and Langdon, 1996) as well as an understanding of resource dynamics in the system within which they reside (Grant, 1996; Grant and Bacher, 1998; Grizzle *et al*., 2008.). Most bivalves, including oysters, are obligate suspension-feeders that take advantage of the rich suite of microparticulate material in aquatic ecosystems. Although they bulk filter suspended material indiscriminately, they are capable of sorting particles prior to ingestion as well as biochemically fractionating ingested material to optimize assimilated rations (Newell and Jordon, 1983).

The concentration and composition of microparticulate material (seston) is known to be highly variable on small time scales (Berg and Newell 1986, Huang *et al.,* 2003a, 2003b). Moreover, the specific nutritional demands of bivalves can vary widely with changing physiological status (e.g., with age, body size, and reproductive state; for example, see Whyte, *et al*., 1990; Kreeger, 1993. Kreeger and Langdon, 1994; Kreeger *et al.*1997). Therefore, actual rates of secondary productivity by bivalves such as oysters result from the interplay between the nutritional demands and the available foods, both of which change in time and space and are rarely in balance (Kreeger and Newell, 2000; ANSP, 2004). The "carrying capacity" of the system is in large measure determined by spatial and temporal variation in seston quantity and quality relative to the demands of the animals and the efficiency with which they can assimilate captured foods, defined as the net "scope for growth" (Beiras *et al*., 1994; Widdows *et al*., 1995; Bayne, 1998).

1.2 Effects of Food on Delaware Bay Oysters

Oysters are euryhaline, living along salinity gradients with upper limits in the oligohaline zone. In Delaware Bay there has been a consistent body of long-term oyster research that has generated a wealth of data and knowledge enabling the development of sophisticated oyster population models. However, the spatial and temporal variability in oyster food quality in the Delaware Bay is poorly understood. Implementation of oyster growth models requires a realistic representation of available food supply (e.g., Langdon and Newell, 1996; Rheault and Rice, 1996). Measurements of the temporal and spatial distribution and variability of food in the Delaware Bay are limited to a single study (Powell, *et al*., 2001).

A biogeochemical/food web model has been incorporated into the ROM v3.0 circulation-biogeochemical model; however, this model was implemented, calibrated, and verified for the continental shelf. Additional measurements of water quality and food supply are required to further improve and calibrate the model for the Delaware Estuary. Here we examine water and food quality during an 8-month period (January and March-November, 2009). Water samples were collected monthly by grab at up to eighteen oyster bed locations along the salinity gradient from Hope Creek to the Maurice River. Samples were collected from 18 locations representing both inshore and offshore beds.

Water quality measurements included temperature, salinity, and dissolved oxygen. Food quality and quantity (for oysters; i.e. total suspended solids, and particulate carbohydrate, protein, and lipid) were examined. The condition (meat quality) of oysters along the salinity gradient was also evaluated at a single time point. Patterns in food availability and composition were correlated with water quality and oyster condition. Due to expected changes in climate, precipitation, and sea level (PDE, 2010), it is important to also understand how basic environmental parameters such as temperature and salinity interact with resource dynamics to affect oysters (Hutchinson and Hawkins, 1992; Kimmel and Newell, 2007).

2.0 MATERIALS AND METHODS

2.1 Collection of Water samples

To examine food availability and water quality, water samples were collected at eighteen sites in the Delaware Bay and River once every month in 2009, with the exception of February and December (Fig. 1, Chapter 2 Appendix: Table 1). Sites were accessed via the F/V Dredge Monster. At each site three, replicate, 1-gallon jugs of water were retrieved from one foot below the surface with an *Eheim Universal Model 1048* submersible pump and flexible rubber tubing. In addition, using a *YSI 85 Instrument* and a refractometer, data were collected on temperature, salinity, and dissolved oxygen at all sites (Table 1). Jugs of water were kept at ambient temperature in coolers while being transported back to the lab.

	Number Possible	**Number Analyzed and OK Data**			
		Weight	Protein	Lipid	CHO
Station-Month Samplings	**171**	171	170	171	171
Total Filters (with blanks)	**523**	518	510	513	522
Percent Successfully Analyzed		**99%**	**98%**	**98%**	**100%**

Table 1. Summary of sample analysis success.

2.2 Seston Collection – Vacuum Filtration of Microparticulate Material

Methods for collecting seston from water samples are described in detail in DK-SOP-23 (Rev. 2, 8/06). This is a standard operating procedure prepared by D. Kreeger and it is available upon request. The following is a shorter version.

Seston is defined as microparticulate material too small to be seen by the human eye. These are suspended particles that are large enough to be retained on a glass fiber filter having an approximate retention of 0.7 µm (particle diameter) and small enough to pass through a 100 µm sieve.

Seston was collected on prepared glass fiber filters using vacuum filtration of water collected in 4 L jugs from field sampling stations. To ensure sufficient material was captured for the various analyses, a sufficient volume of water was filtered to almost clog the filter, noted by a slowing rate of water volume passing through a filter. The volume required depends on the density of particulate organic matter (POM). For seston, the volume typically ranges between 100-1000 ml per filter. To maximize captured seston, a test filter was used for each water sampling site to purposefully clog a filter, and the volume needed to do so was recorded. For the balance of the subsamples from that sampling, 90% of this clogging volume was used. Each filter containing captured seston

was added to a Petrislide™ for storage in a freezer at -20°C until laboratory analysis. Filters were frozen until laboratory analysis. Generally, for each water sampling (collection station sampled at a given time), 3 replicate jugs were filled. From each jug, four replicate seston samples were collected on 0.7 µm retention glass fiber filters (47 mm diameter; Whatman type GF/F or the VWR equivalent). The replicate filtration of each water sample (jug) onto 4 filters allowed for the separate analysis of seston weight, protein content, carbohydrate content, and lipid content. Since three replicate jugs of water were collected per sampling, there were therefore twelve seston filters prepared from each sampling, leading to triplicate analyses for each of the four parameters of interest.

Filters were pre-combusted at 450°C for at least 24 hours prior to seston filtration. A sufficient number of pre-weighed (to 0.01 mg) filters were also prepared in advance of sampling. For each bottle of water, one of the four filter replicates were used for weight-on-ignition and the remaining three filter replicates will be used for biochemistry. The replicate to be used for weight-on-ignition was pre-weighed. The same balance was used before and after filtering seston. Weights were measured only on desiccated samples.

2.3 Seston Analysis - Proximate Biochemical Composition and Weight

One of the four replicate seston-coated filters per water jug was used for weight-on-ignition analysis, one for protein content, one for lipid content and one for carbohydrate content. Therefore, since three replicate containers of water were collected per stream sampling, this resulted in three replicate filters to be used for each of the four assays.

2.3.1. Weight-on-Ignition Analysis

The weight-on-ignition assay assessed the total seston weight per unit volume (*i.e.,* total suspended solid concentration) and the seston organic content. Calculations for seston particulate material (PM, also known as total suspended solids), particulate organic matter (POM), and the percentage organic content (%OC) are given below.

Seston filters for weight analysis were dried at 60°C for >2 days and weighed (±.01mg; Sartorius M-9001). Filters were then combusted in a muffle furnace for 48 hr at 450°C and weighed again. Concentrations of PM and POM were then calculated with the following formulae:

$$\text{PM (mg/L)} = \frac{[(\text{mg dry weight of filter+seston}) - (\text{dry filter pre-weight})]}{\text{ml filtered volume}}$$

$$\text{POM} = \text{PM} - \frac{[(\text{mg ash weight of filter+seston}) - (\text{filter pre-weight})]}{\text{ml filtered volume}}$$

The percentage organic content was calculated as follows:

Organic Content of seston = [POM] / [PM] * 100%

2.3.2. Analysis of Seston Biochemical Composition

The concentration of particulate protein, carbohydrate and lipid was measured on separate replicate filters from each water sample. This proximate biochemical composition was determined using various published methods that have been adapted by Kreeger *et al.* (1997). Provide below is a brief summary of each method, but full details are given by Kreeger *et al.* (1997).

Protein content was measured spectrophotometrically using the bicinchonic acid modification (Pierce test kit, 23225) of the procedure of Lowry *et al.*(1951), standardized with bovine serum albumen (Pierce 23210). A microplate reader was used for spectrophotometry at a wavelength of 640 nm.

Carbohydrates were quantified spectrophotometrically (wavelength 480 nm) using the method of Dubois *et al.*(1956), standardized with potato starch (Sigma S 4561).

Lipids were measured gravimetrically according to a modification of the technique of Folch *et al.*(1957), whereby dried seston filters were suspended in 10 ml of 2:1 v/v chloroform/methanol, ground for 1 min in a Potter Elvehjem tissue grinder tube with PTFE pestle (Wheaton #358039), and then centrifuged at 1000 x g for 5 min. The supernatant (containing lipid) was collected and received a 20% v/v (final concentration) aliquot of 0.88% KCl to promote phase separation. The bottom layer was transferred by pipette to a pre weighed vial, dried at 60°C until constant weight was achieved, and weighed. Hexadecanone was used to standardize the lipid procedure.

The concentration of particulate protein, lipid, and carbohydrate in each water sample was then expressed relative to the total dry weight of particulate material in the same water sample to calculate the percentage protein, lipid and carbohydrate contents, respectively. In addition, the relative proportions of each constituent were compared to each other as ratios (e.g. protein:carbohydrate). The proportion of POM that is comprised of protein, lipid and carbohydrate is considered helpful for indicating nutritional value of the organic fraction, for example.

2.4 Oyster Condition Index

Condition was measured as the ratio of dry meat weight to right valve length. Comparison of length as the method of normalization to the multiple of length X width X height reveals that length is an adequate divisor for comparison of condition between bay regions and over time. The survey is typically conducted in late October of each year.

3.0 RESULTS

3.1 Seston Analyses and Data Format

3.1.1. Seston Analysis Success

Of the total 523 seston filters available to analyze from 2009 sampling, more than 98% were successfully analyzed for weight, protein, lipid and carbohydrate (Table 1.) This is higher than is typical (<5% loss) as sometimes test tubes break in the centrifuge, etc.

3.1.2. Orientation to Seston Metrics

For each sample, the following parameters were assessed:

Concentrations (measured):

- Particulate Matter (PM) Concentration (mg/L)
- Particulate Organic Matter (POM) Concentration (mg/L)
- Particulate Inorganic Matter (PIM) Concentration (mg/L)
- Particulate Protein (PRO) Concentration (mg/L)
- Particulate Lipid (LIP) Concentration (mg/L)
- Particulate Carbohydrate (CHO) Concentration (mg/L)

Relative Percentage Contents Data (calculated):

- Seston Organic Content (OC) (%)
- Seston Inorganic Content (ASH) (%)
- Seston Protein Content (PRO/PM, %)
- Seston Lipid Content (LIP/PM, %)
- Seston Carbohydrate Content (CHO/PM, %)

Additional information can be extracted by examining ratios such as for PRO:CHO.

To achieve normality for statistical analysis, logarithmic transformation was typically used to compare concentration data; whereas, arcsine square root transformation was used to compare percentage data.

3.1.3 Orientation to Seston Database

An Excel database file was created, which is titled DES_2009_Seston_v2-28-10.xls. The first tab provides the dataset, showing which samplings (a date/station water collection) were performed and indicating any specific replicates or samples that were problematic during sample filtration or lab analysis. The second tab consists of the same dataset, but simplified without notes for use in statistical analyses. The third tab shows examples of graphical results.

3.2 Temporal and Spatial Variation in Seston

Preliminarily data analyses were performed with Statgraphics V.5. Only parametric tests were used, including one-way and two-way ANOVAs (main effects = month, station.) Regressions were also performed.

3.2.1. Temporal Variation in Seston Quantity (Total Suspended Solids)

Total suspended solids (TSS) are also referred to as the concentration of particulate material (PM). Overall seston concentration (PM) tended to be highest in spring and fall but with a July spike as well (Fig. 1a).

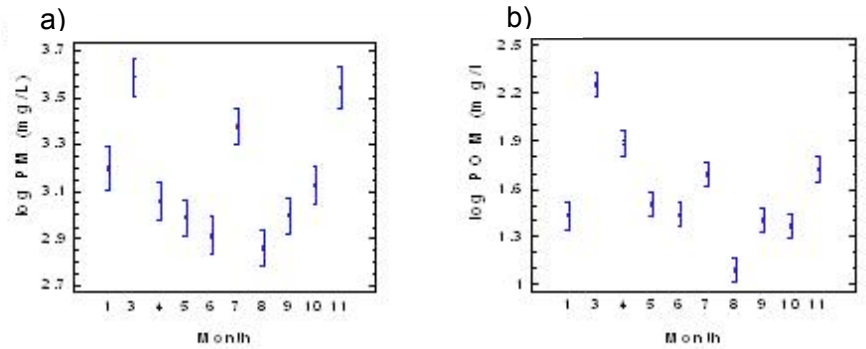

Figure 1. Mean ± SE (pooled) concentration of a) particulate matter (total suspended solids) and b) particulate organic matter averaged across eighteen stations in the Delaware Estuary during various months in 2009.

3.2.2. Temporal Variation in Seston Quality (Particulate Organic Material)

These results suggest that the proportion of seston that might be of nutritional importance for oysters was much greater in spring to early summer. The particle organic matter (POM) concentration was higher in March and April, as expected from spring blooms and river runoff (Fig. 1b). Moreover, the proportion of organic matter that was in the form of analyzable protein, lipid and carbohydrate varied temporally as well, also being greater from January to June (Figs. 2a, 2b). This suggests that humic geopolymers and other likely indigestible organic molecules associated with detritus and organic flocs were more prevalent in the organic fraction from July on (not unexpected but shows how biochemical analyses can provide more nutritional information than bulk organic content.

3.2.3. Temporal Variation in Compound-Specific Seston Quality

Higher concentrations of protein, lipid and carbohydrate occurred in the earlier part of the year, with a small late fall increase (Figs. 3a-5a). However, the relative proportions (e.g., protein:carbohydrate ratio) varied as well (Figs. 3-5b). This could be particularly important with regard to the timing of specific nutritional demands for oysters (e.g., protein for gametogenesis and growth; carbohydrate for fall conditioning).

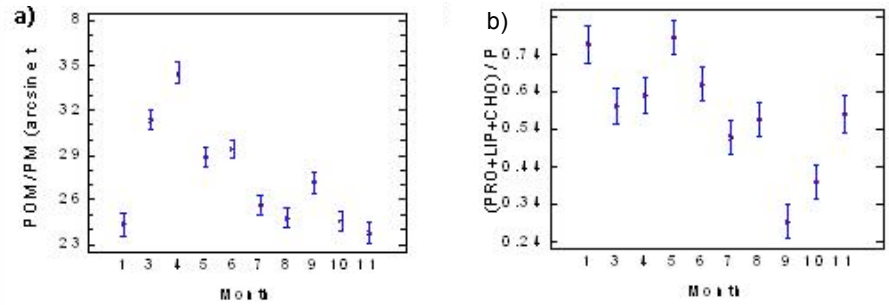

Figure 2. Mean ± SE (pooled) seston a) organic proportion (arcsine square root transformed percentage) and b) proportion of organic fraction represented by either protein, lipid or carbohydrate (fraction) averaged across eighteen stations in the Delaware Estuary during various months in 2009.

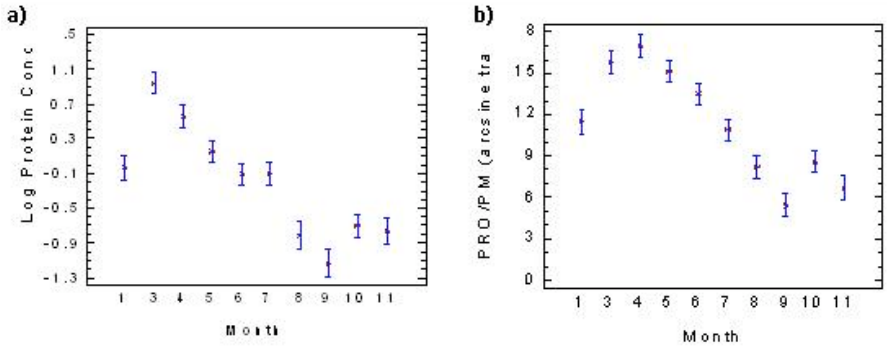

Figure 3. Seston protein concentration a) (mean±pooled SE) and b) the percentage protein content of seston, arcsine square root transformed) averaged across eighteen stations in the Delaware Estuary during various months during 2009.

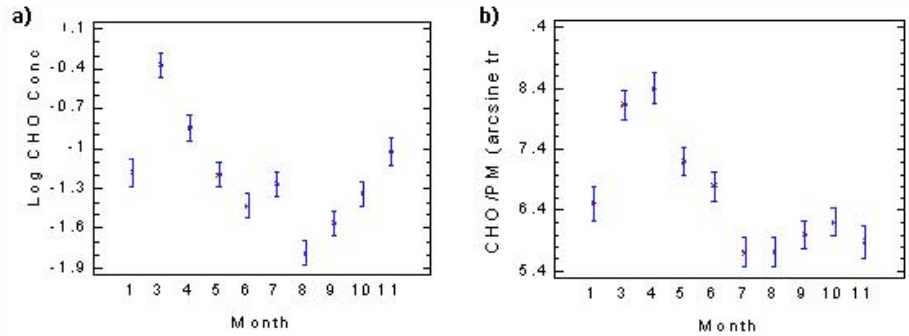

Figure 4. Seston carbohydrate concentration a) (mean±pooled SE) and b) the percentage carbohydrate content of seston, arcsine square root transformed) averaged across eighteen stations in the Delaware Estuary during various months during 2009.

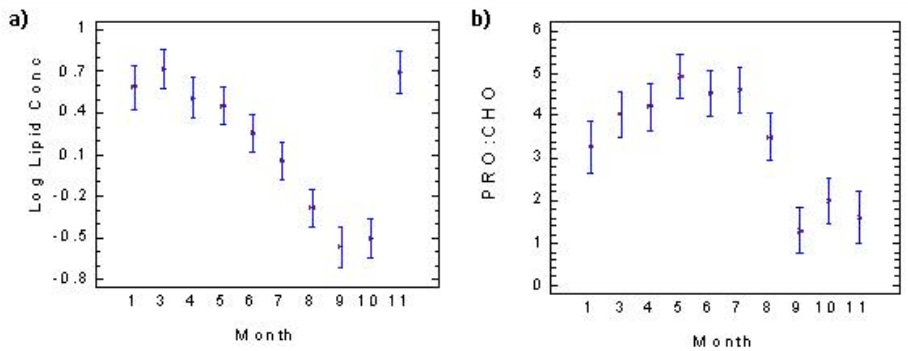

Figure 5. Seston lipid concentration a) (mean±pooled SE) and b) the percentage lipid content of seston, arcsine square root transformed) averaged across eighteen stations in the Delaware Estuary during various months during 2009.

3.2.4. Spatial Variation in Seston

Seston quantity and quality varied widely among the eighteen stations sampled. Some stations appeared to have generally high quantity (Fig. 6) but low quality seston (Fig. 7; e.g. see Reedy Point), whereas others were characterized by low quantity but high quality seston (Maurice River Cove). Typically, POM decreases as PM increases, an inverse relationship. These data should enable us to characterize the eighteen stations along the natural gradient, such as in the context of the turbidity zone and salinity gradients.

Caveat: Only preliminary, parametric statistics have been performed, and the dataset has not been scrutinized for extreme outliers or anomalies. A station-by-station characterization of temporal changes in the palette of seston metrics will be undertaken after additional years of data are collected to ensure that no extreme values are biasing the summary statistics.

Various biochemical constituents within the seston also varied significantly among stations, as exemplified by the percentage content of particulate protein (Fig. 8) and carbohydrate (Fig. 9).

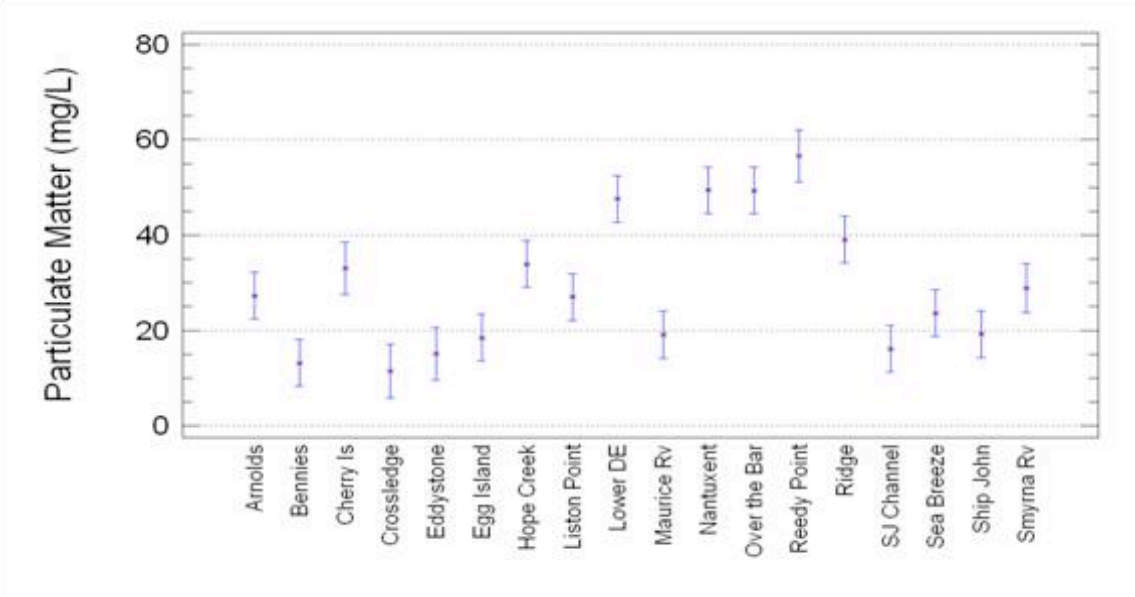

Figure 6. Seston particulate matter concentration (mean±pooled SE) for eighteen stations in the Delaware Estuary averaged among the various months sampled during 2009.

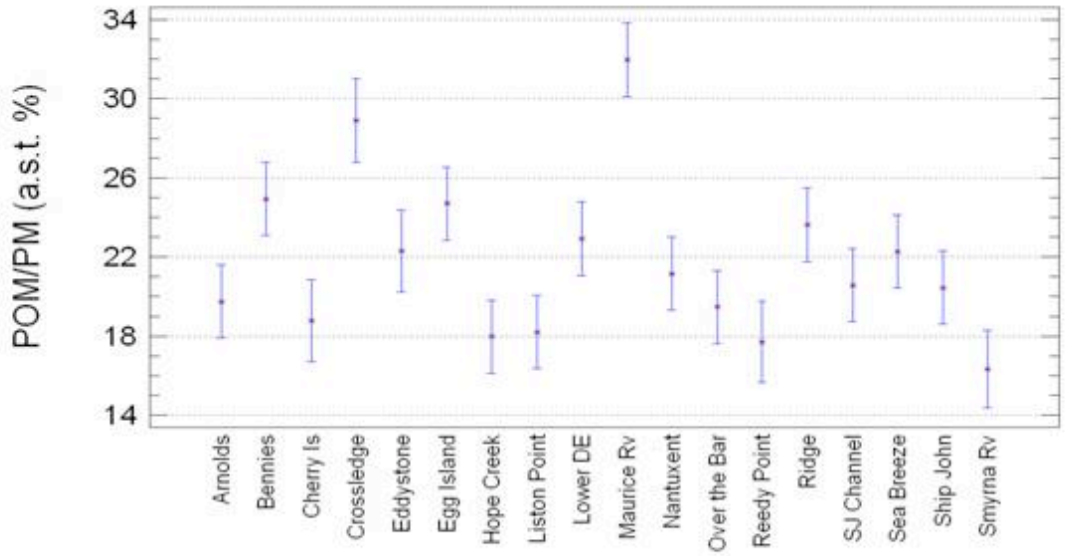

Figure 7. Percentage organic content (mean±pooled SE; arcsine square root transformed) for eighteen stations in the Delaware Estuary averaged among the various months sampled during 2009.

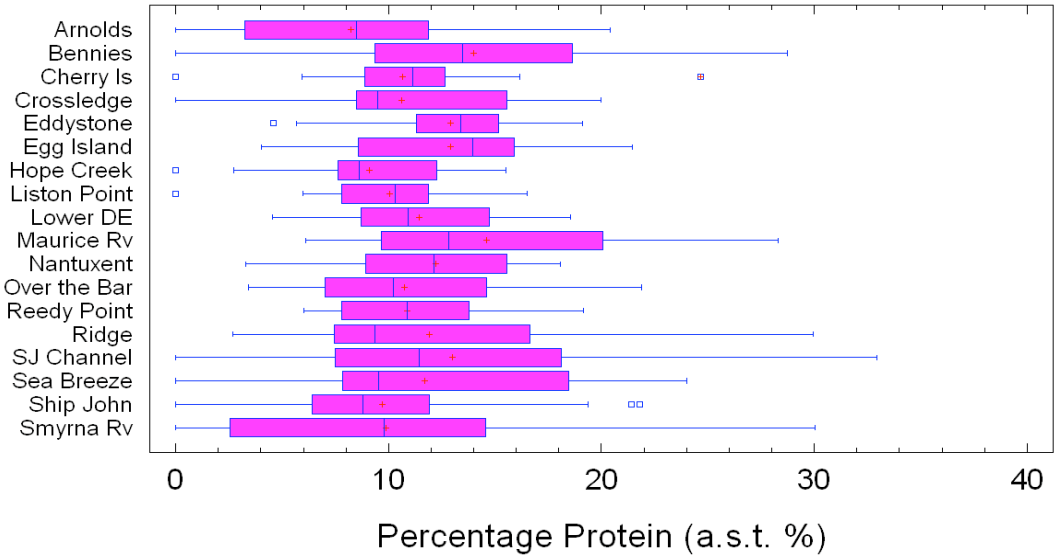

Figure 8. Percentage protein content (box and whisker plot, median and quartiles; arcsine square root transformed) for eighteen stations, averaged among the various months sampled during 2009.

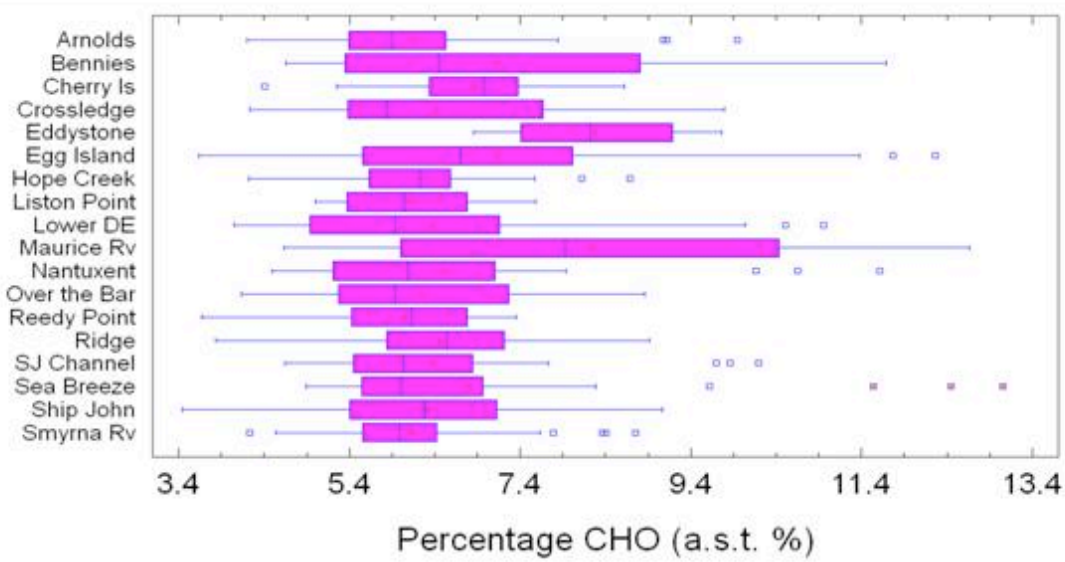

Figure 9. Percentage carbohydrate content (box and whisker plot, median and quartiles; arcsine square root transformed) for eighteen stations, averaged among the various months sampled during 2009.

3.2.5. Additional Descriptive Analyses

Stations were grouped along a downbay to upbay gradient as follows:

i) LB = Lower Bay

ii) HM = High Mortality
iii) MHM = Med-High Mortality
iv) LM = Low Mortality
v) VLM = Very Low Mortality
vi) D = Delaware
vii) R = River

Downbay—Upbay. Averaged over the year, Delaware stations had the greatest overall seston material, and particulate matter was lowest in the lower estuary and bay. Organic content was generally inversely proportional with highest values in Delaware Bay. Therefore, seston quality does tend to vary along the upbay to downbay gradient (Figs. 10 and 11). More refined analysis should be undertaken to discern seasonal relationships in

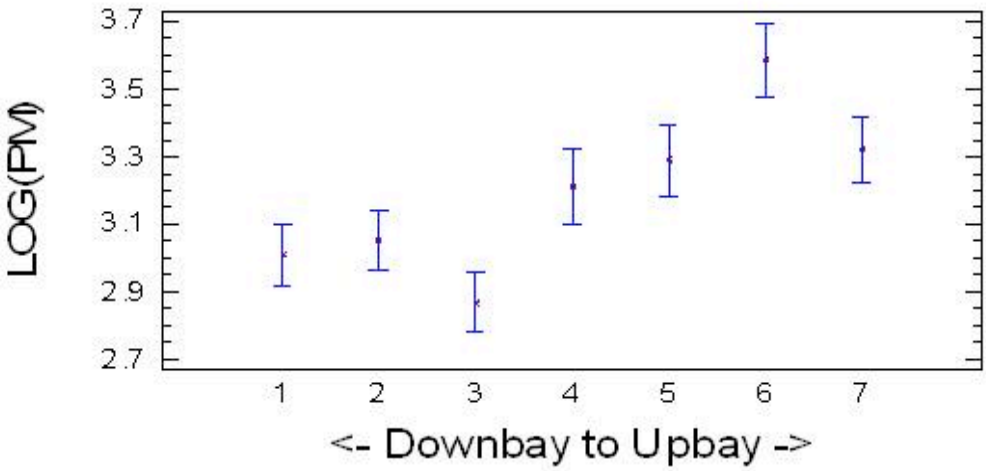

Multiple Range Tests for LOG(PM) by Downbay

Method: 95.0 percent LSD

Downbay	Count	Mean	Homogeneous Groups
3	90	2.86644	X
1	81	3.01067	XX
2	90	3.04958	X
4	57	3.21246	XX
5	60	3.2873	X
7	72	3.32155	X
6	59	3.58573	X

Figure 10. Concentration of seston particulate material (mean±pooled SE) averaged across months for stations located along the downbay to upbay axis of the Delaware Estuary, sampled between January and November 2009.

these trends. For example, the generally higher carbohydrate concentrations upbay only occurred later in the year, and the proximate biochemical composition varied along the gradient, possibly in relation to the turbidity maximum (e.g., protein, see Fig. 12). Seston metrics were also compared among the eighteen stations simply based on their latitude along the upbay to downbay gradient. The percentage organic content (proxy for seston

quality) decreased with increasing latitude, i.e., moving from downbay to upbay. Salinity also was inversely correlated with latitude.

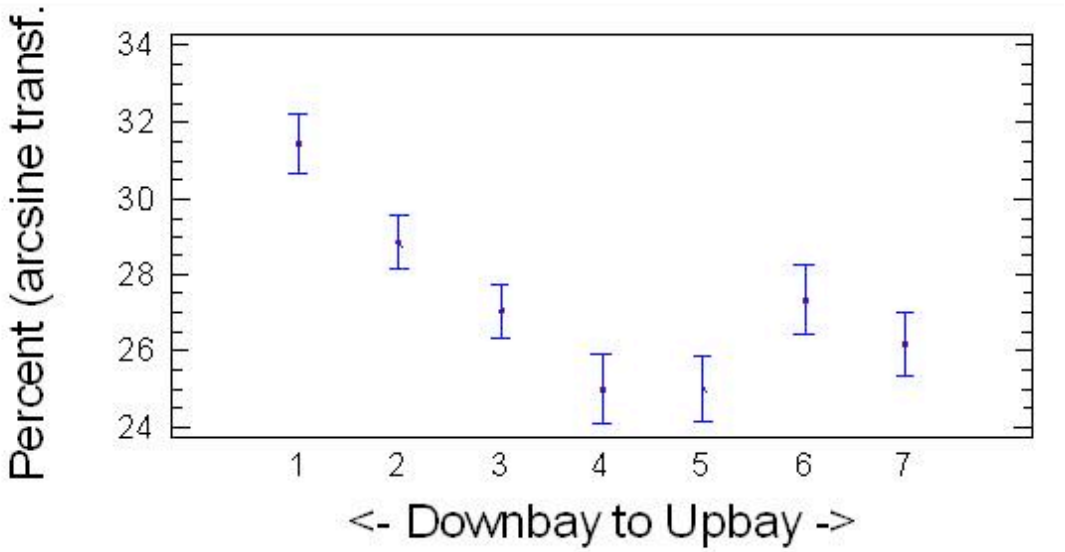

Figure 11. Concentration of organic content of seston material (mean±pooled SE; arcsine square root transformed) averaged across months for stations located along the downbay to upbay axis of the Delaware Estuary, sampled between January and November 2009.

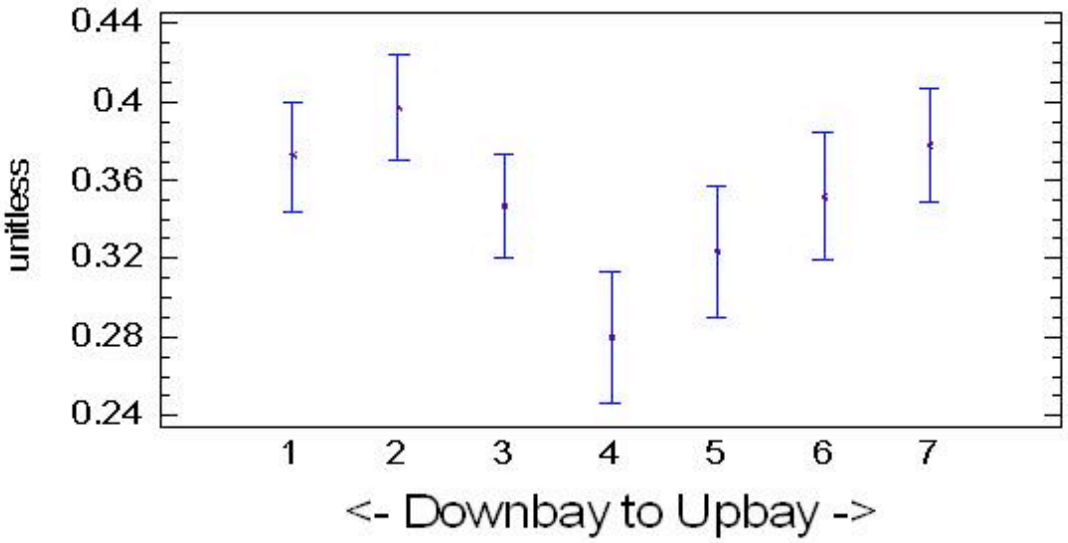

Figure 12. Ratio of the protein concentration to the sum of protein, lipid and carbohydrate concentrations (i.e., PRO/(PRO+UP+CHO) for seston collected along the downbay to upbay axis of the Delaware Estuary, sampled January-November 2009.

Inshore – Offshore. There was much more particulate matter at inshore stations (Nantuxent and Sea Breeze) than in the adjacent offshore stations (Bennies and Ship John, respectively; Fig. 13). Seston organic content did not differ inshore versus offshore, however. So there was much more bioavailable food quantity available inshore, averaged across the year. The same was true for the absolute concentration of particulate protein, lipid and carbohydrate, all of which were markedly greater inshore than offshore.

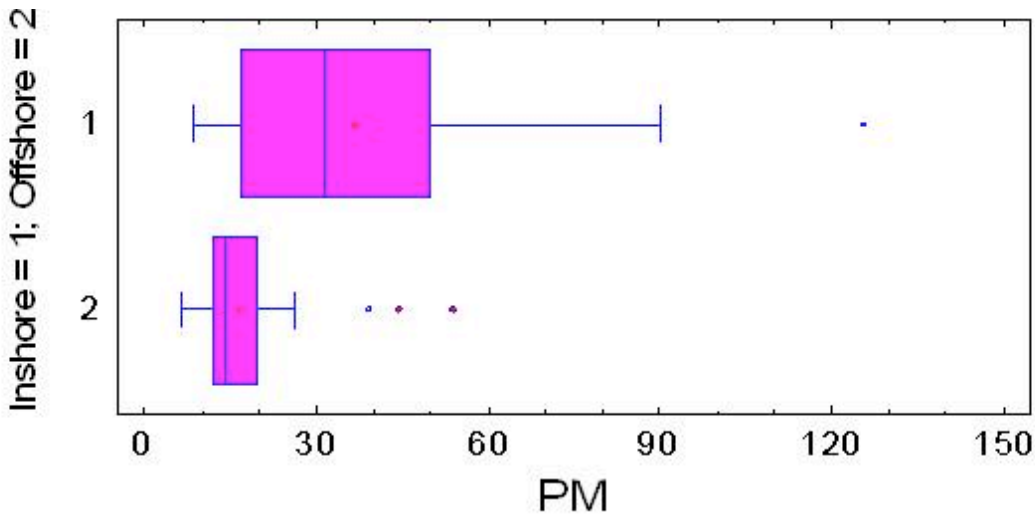

Figure 13. Concentration of seston particulate material (box and whisker plot medians and quartiles) averaged across months for paired stations located inshore versus offshore (see text) within the Delaware Estuary, sampled January-November 2009.

3.2.6. Relationships Between Seston and Water Quality

Preliminary comparison of seston composition and water quality (dissolved oxygen, salinity, temperature) yielded no substantive relationships. As noted above, salinity varied with latitude and along downbay-upbay gradient (Fig. 14), and so some seston patterns were related to salinity (Figs. 15 and 16). However, no notable food quality metrics appeared to scale with temperature. Detailed comparisons for specific sites and months remain to be completed.

3.2.7. Seston versus Tide Stage

Significantly (ANOVA, p=0.0002) more particulate matter was evident in 182 samples that were collected during ebb tide compared to 220 samples that were collected during flood tide and 35 that were collected during slack tide (Fig. 17). Interestingly, some food quality parameters also varied with tide stage. For example, the percentage protein content was higher on slack tide (significant, p=0.01). This suggests that tidal stage should be carefully considered during seston studies. It is unclear why seston varied with

tide stage, however resuspension of bottom sediments, outwelling from adjacent wetlands, and phytoplankton bloom dynamics could all be factors.

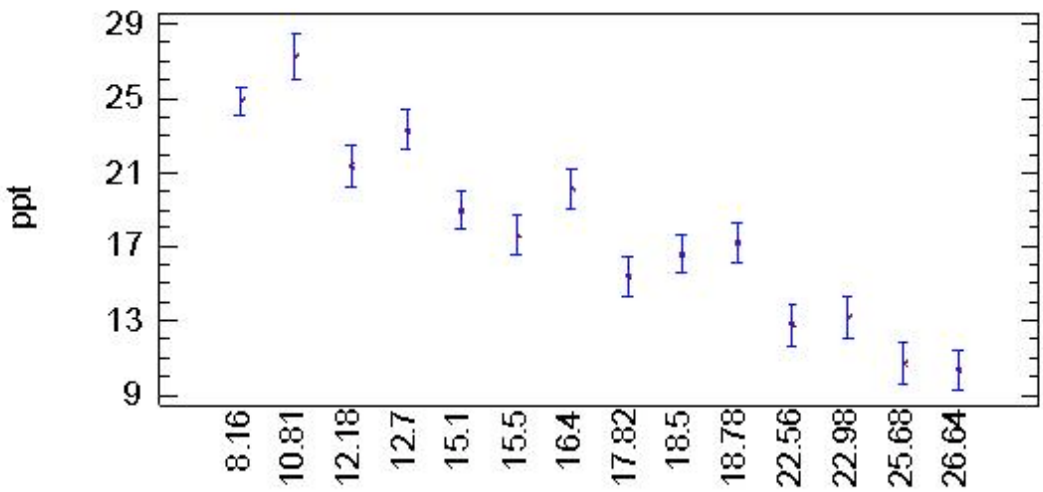

Figure 14. Salinity (mean+pooled SE) versus the decimal latitude within Delaware Bay sampled between January and November 2009.

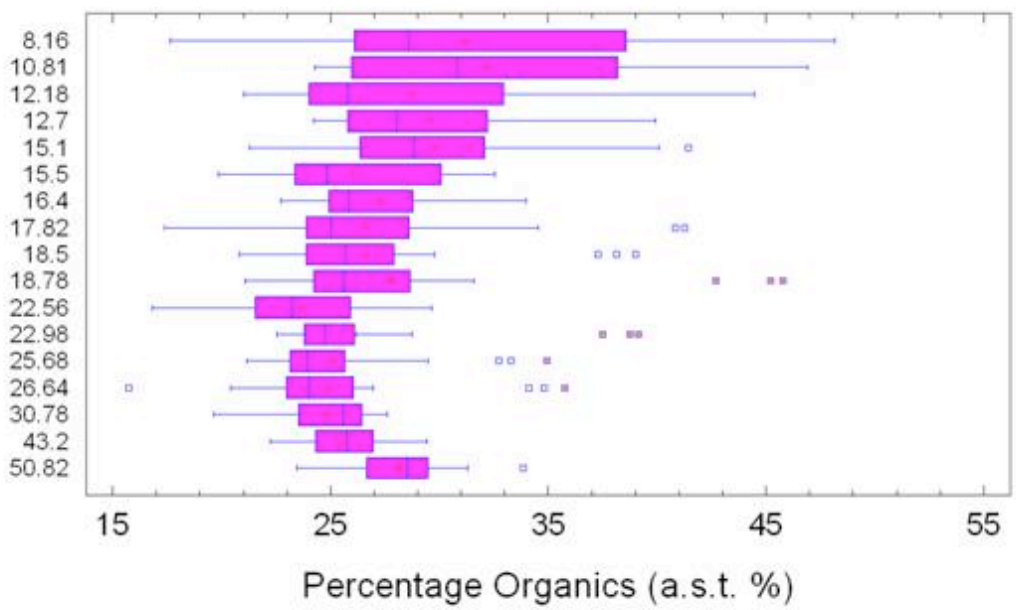

Figure 15. Percentage organic content of seston (mean±pooled SE; arcsine square root transformed) versus the decimal latitude within Delaware Bay, sampled between January and November 2009.

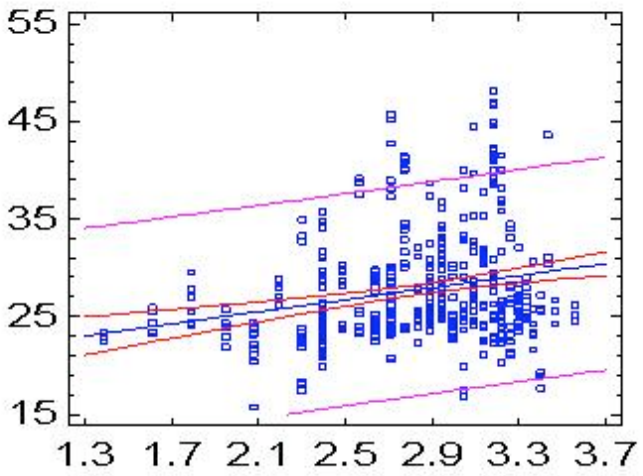

Figure 16. Least squares linear regression of the percentage organic content of seston (y-axis; arcsine square root transformed) asa function of salinity (x-axis; logarithm transformed) within Delaware Bay, sampled between January and November 2009.

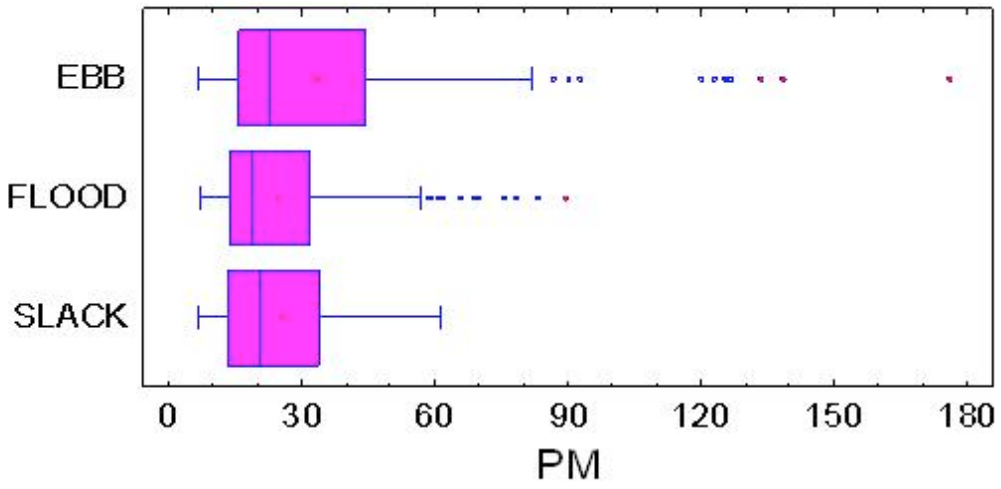

Figure 17. Concentration of seston particulate material (box and whisker plot medians and quartiles) averaged across months for stations within Delaware Bay that were sampled on different tide stages between January-November 2009.

3.3 Oyster condition

The oyster stock in the New Jersey waters of Delaware Bay is partitioned into twenty-three oyster beds that are sufficiently large to be included in the sampling program. These

beds have been apportioned into four bay groups based on the long-term average rates of natural mortality, productivity, and influence on survey catchability.

Analyses of condition of the Delaware Bay oyster resource of New Jersey routinely reveal a division between the upbay group of eight beds (Round Island, Upper Arnolds, Arnolds, Upper Middle, Middle, Sea Breeze, Cohansey, and Ship John and the downbay group of twelve beds (Shell Rock, Bennies Sand, Bennies, New Beds, Nantuxent Point, Hog Shoal, Hawk's Nest, Strawberry, Vexton, Beadons, Egg Island, and Ledge) (Fig. 18)) . Salinity, natural mortality rate, and growth rate are higher downbay. Dredge efficiencies are significantly higher downbay (Powell *et al*., 2002, 2007). Both regions can be subdivided based on natural mortality rate and productivity. In the upbay region, natural mortality rates and growth rates are significantly lower for the upper three beds, Round Island, Upper Arnolds and Arnolds, than for the remainder. This trend is dictated by the salinity gradient. Over the long term, salinity averages around 12ppt on the upper group of beds and closer to 15ppt on the lower group of beds (Haskin and Ford, 1982).

In assessment documents, these two upbay groups are termed the low-mortality and medium-mortality beds. In the downbay region, growth rates and mortality rates are lower for Shell Rock, leading to its designation as a medium-mortality bed; the remainder being high-mortality beds. Salinities for most beds downbay of Shell Rock average around 18ppt with salinities tending to exceed 20ppt on the lower-most two, Egg Island and Ledge (Haskin and Ford, 1982). Shell Rock is unique in consistently achieving the highest productivity today of any New Jersey bed. This is due to an auspicious coincidence of relatively high recruitment and growth and relatively low mortality on this bed. In addition, three newly-surveyed beds are found upbay of Round Island. These beds do not have long-term time series associated with them as they were first surveyed in 2007. They (Liston Range, Fishing Creek, Hope Creek) have been designated as very-low-mortality beds in the most recent stock assessment based on two years of mortality data.

Condition is tracked in the stock assessment as the ratio of dry meat weight to right valve length. Comparison of length as the method of normalization to the multiple of length by width by height reveals that length is an adequate divisor for comparison of condition between bay regions and over time. The survey is conducted in late October of each year. Hence, the time series of condition is for year-ending condition well after spawning has ceased. In years, when a fall phytoplankton bloom occurs, the bloom normally occurs prior to the survey, so that year-ending condition includes a fall fattening phase.

Condition index fell in 2009 in comparison to three of the last four years to levels typical of the late 1990s-early 2000s (Fig. 18). Although data on food supply is insufficient to evaluate in any but a general way, as the 2009 field season represents one of only two years in which data are available, the low condition in October coincides with a multi-month period of low food supply that began certainly by August if not before. The time series of condition suggests that food levels this low are not rare, though clearly below normal.

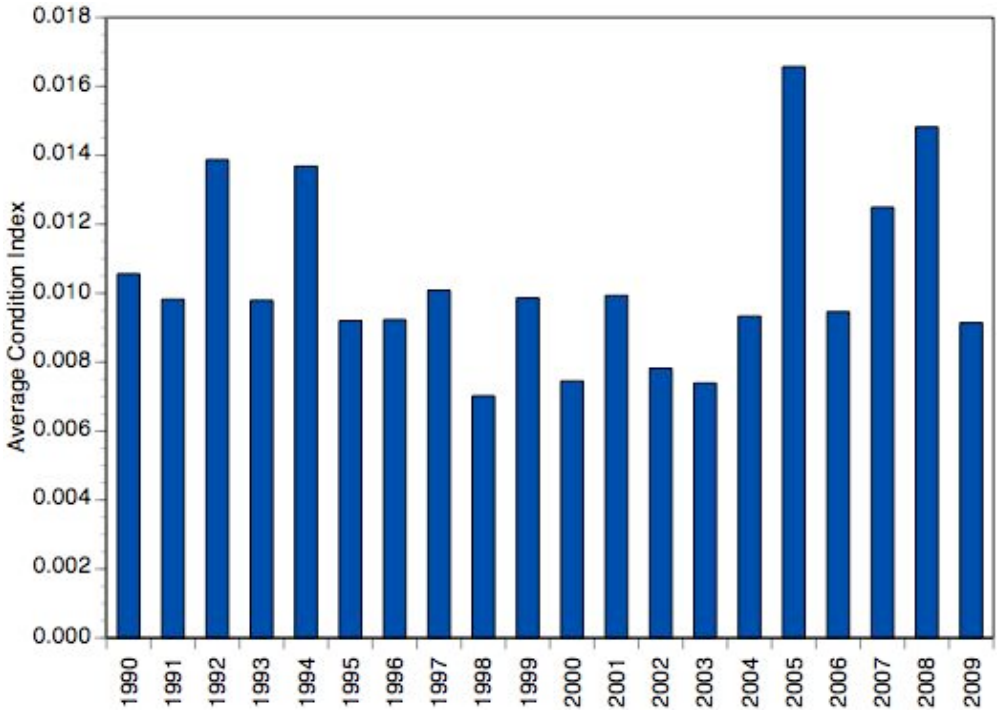

Figure 18. Annual average condition index [dry meat weight (g) / hinge-to-lip shell length (mm)], excluding the very low mortality beds.

Condition index normally declines upbay. This trend is consistently present every year (Fig. 19). The variation between years is generated by the differential between the upbay and downbay beds. In some years, such as 2003 and 2004, the differential is large and increases stepwise down-estuary. In other cases, such as 1990 and 1991, the upper half of the bay tends to be of similar condition and lower than the downbay regions. In a few cases, such as 2007 and 2008, the downbay-upbay gradient is clearly muted. Normally, high condition over the entire bay is associated with the latter trend. Thus, bay wide trends in condition are primarily driven by the condition index of animals in the low-mortality and medium-mortality regions. Bed distributions by group are given in Chapter 2 Appendix: Figure 1.

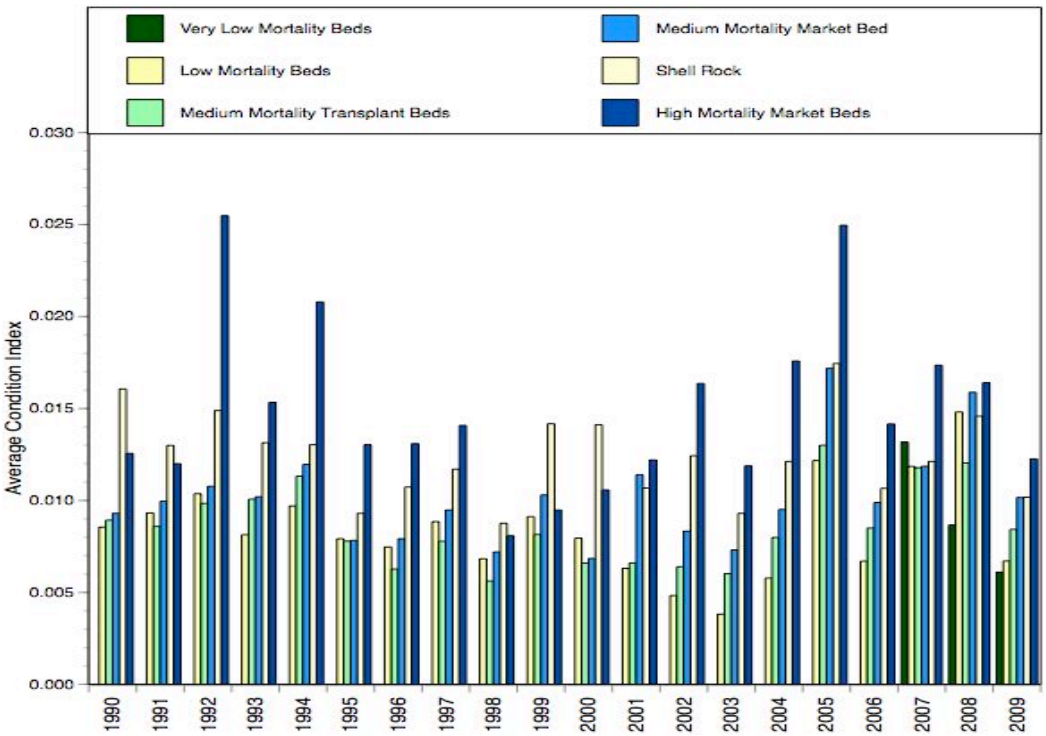

Figure 19. Annual average condition index [dry meat weight (g) / hinge-to-lip shell length (mm)] by bay group.

In 2009, condition declined throughout the bay, although marginally less strongly on the high-mortality beds (Fig. 19). Nevertheless, condition has not been this low bay-wide since 2003. Furthermore, condition was particularly low in the upbay regions of the stock and increased in stepwise fashion downestuary. Once again, food supply data are available only for two years, 2000 and 2009, so that interpretation of condition index data in terms of trends in food supply must be considered tentative. However, trends in food supply show high values over the year for the high-mortality beds, intermediate values for the medium-mortality beds, and low-values for the low-mortality beds. This gradient approximates a factor of over 1.5 for protein. Moreover, the protein content of the food likewise declines by a factor of about 1.4. Thus upbay-downbay trends in food supply track upbay downbay trends in condition and the stepwise change in protein content (fraction) and protein concentration follow the stepwise change observed in condition. Although the data are still inadequate, from a time series perspective, to evaluate the promise of using food supply to explain trends in oyster population dynamics, the results from the 2009 sampling support the belief that such an outcome may occur.

4.0 SUMMARY AND NEXT STEPS

Many interesting spatial and temporal patterns in oyster food quantity and quality were documented in the seston survey in 2009, which constitutes the most thorough study of

its kind ever for Delaware Bay. Preliminary analyses suggest that seston variation is associated with many factors, including the proximity to riverine and marshland inputs of particulate matter, the turbidity gradient, the salinity gradient, and water quality. Due to extensive grazing of particulate matter by oysters, the oyster reefs themselves might affect seston availability and composition. River flows, climate conditions, and nutrient inputs also likely govern phytoplankton bloom dynamics, likely explaining some of the variability in seston quality. Due to the complexity of these relationships between environmental conditions and the food supply for oysters, our understanding will be greatly facilitated by extended monitoring and surveys of seston spanning multiple years and climate/flow conditions. Contingent upon funding, we therefore plan to continue this effort for 2010 and beyond.

Oyster condition (sampled in the fall) appeared to be related to the availability and composition of food during 2009, especially late summer seston quantity and quality. If confirmed with additional years of surveys, this would provide important new insights into the principal factors governing the effect of bottom-up resource dynamics on oyster productivity in Delaware Bay.

5.0 LITERATURE CITED

Academy of Natural Sciences of Philadelphia (ANSP). 2004. 2002-03 San Antonio Bay Oyster Population Health Assessment, Rept. No. 04-01. Acad. Nat. Sci. Phila. 80 pp.

Bayne, B.L. 1998. The physiology of suspension feeding bivalve molluscs: an introduction to the Plymouth "TROPHEE" workshop. J. Exp. Mar. Biol. Ecol. 219: 1-19.

Beiras, R., A. Perez Camacho and M. Albentosa. 1994. Comparison of the scope for growth with the performance of (*Ostrea edulis*) seed reared at different food concentrations in an open-flow system. Marine Biology 119:227-233.

Berg, J.A. and R.I.E. Newell. 1986. Temporal and spatial variations in the composition of seston available to the suspension feeder, *Crassostrea virginica*. Estuar. Coastal Shelf Sci. 23:375-386.

Dame, R. F. & Prins, T. C. 1998. Bivalve carrying capacity in coastal ecosystems. Aquatic Ecology. 31: 409-421.

Dubois M., K. A. Gilles, J. K. Hamilton, P.A. Rebers, and F. Smith. 1956. A calorimetric method for the determination of sugars and related substances. Analytical Chemistry 28: 350 356.

Folch, J., M. Lees, and G. H. Sloane Stanley. 1957. A simple method for the isolation and purification of total lipids from animal tissue. Journal of Biological Chemistry 226: 497 509.

Grabowski, J.H., and C.H. Peterson, 2007. Restoring oyster reefs to recover ecosystem services. Ch. 15, pp. 281-298, in Ecosystem Engineers: Concepts, Theory and Applications, Eds., K. Cuddington, J.E. Byers, W.G. Wilson, and A. Hastings, Elsevier/Academic Press, Netherlands.

Grant, J. & Bacher. 1998. Comparative models of mussel bioenergetics and their validation at field culture sites. J. Mar. Biol. Ecol. 219: 21-44

Grant, J. 1996. The relationship of bioenergetics and the environment to the field growth of cultured bivalves. J. Exp Mar. Biol. Ecol. 200: 239-256.

Grizzle, R.E., J.K. Greene, and L.D. Coen, 2008. Seston removal by natural and constructed intertidal eastern oyster (*Crassostrea virginica*) reefs: a comparison with previous laboratory studies, and the value of in situ methods. Estuaries and Coasts 31:1208-1220.

Haskin, H. H , Ford, S E. (1982). *Haplosporidium nelsoni* (MSX) on Delaware Bay seed oyster beds: a host-parasite relationship along a salinity gradient. J. Invertebr Pathology 40: 388-405.

Huang, S.-C., D.A. Kreeger and R.I.E. Newell. 2003a. Tidal and seasonal variations in the quantity and composition of seston in a North American, mid-Atlantic saltmarsh. Estuarine Coastal Shelf Science 56: 547-560.

Huang, S.-C., D.A. Kreeger and R.I.E. Newell. 2003b. Seston available as a food resource for the ribbed mussel (*Geukensia demissa*) in a North American, mid-Atlantic saltmarsh. Estuarine Coastal Shelf Science 56: 561-571.

Hutchinson, S. and L.E. Hawkins. 1992. Quantification of the physiological responses of the European flat oyster *Ostrea edulis* L. to temperature and salinity. J. Moll. Stud. 58: 215-226.

Kimmel, D.G., and R.I.E. Newell, 2007. The influence of climate variation on eastern oyster (*Crassostrea virginica*) juvenile abundance in Chesapeake Bay. Limnol. Oceanogr. 52:959–965.

Kreeger, D.A. 1993. Seasonal patterns in the utilization of dietary protein by the mussel, *Mytilus trossulus*. Mar. Ecol. Progr. Ser. 95:215-232. Kreeger, D. A., C. E. Goulden, S. S. Kilham, S. G. Lynn, S. Datta, and S. J. Interlandi. 1997. Seasonal changes in the biochemistry of lake seston. Freshwater Biology 38: 539 554.

Kreeger, D.A., C.E. Goulden, S.S. Kilham S.G. Lynn, S. Datta and S.J. Interlandi. 1997. Seasonal changes in the biochemistry of lake seston. Freshwater Biology 38: 539-554.

Kreeger, D.A. and C.J. Langdon. 1994. Digestion and assimilation of protein by *Mytilus trossulus* (Bivalvia: Mollusca) fed mixed carbohydrate/protein microcapsules. Mar. Biol. 118: 479-488.

Kreeger, D.A. and R.I.E. Newell. 2000. Trophic complexity between producers and invertebrate consumers in salt marshes. In: M.A. Weinstein and D.A. Kreeger (eds.), Concepts and Controversies in Tidal Marsh Ecology. Kluwer Publishing. New York. pp. 183-216.

Langdon C.J. and R.I.E. Newell. 1996. Digestion and nutrition in larvae and adults. Chapter 6 in The Eastern Oyster *Crassostrea virginica*. Kennedy V. S., Newell R. I. E. and A. E. Eble eds. Maryland Sea Grant, College Park, MD.

Lowry, O. H., N. J. Rosebrough, A.L. Farr, and R. J. Randall. 1951. Protein measurement with the folin phenol reagent. Journal of Biological Chemistry 193: 265 275.

MacKenzie, C.L. 1996. Management of natural populations. Chapter 21 in The Eastern Oyster *Crassostrea virginica*. Kennedy V. S., Newell R. I. E. and A. E. Eble eds. Maryland Sea Grant, College Park, MD.

Newell, R.I.E. 2004. Ecosystem influences of natural and cultivated populations of suspension-feeding bivalve mollusks: A review. J. Shellfish Res. 23: 51-61.

Newell, R.I.E. and S.J. Jordon. 1983. Preferential ingestion of organic material by the American oyster *Crassostrea virginica*. Mar. Ecol. Prog. Ser. 13:47-53.

Newell, R.I.E. and C.J. Langdon. 1996. Mechanisms of physiology and larval and adult feeding. Pages 185-229 in V.S. Kennedy, R.I.E. Newell and A.F. Eble, eds. The Eastern Oyster *Crassostrea virginica*. Maryland Sea Grant, College Park, MD.

Officer, C.B., T.J. Sayda and R. Mann. 1982. Benthic filter feeding: a natural eutrophication control. Mar. Ecol. Prog. Ser. 9: 203-210.

Powell, E. N., S. E. Ford, M. Cummings, R. B. Barber, B. D. Brewster, F. Kelley, K. Sillett, and R. J. Diaz. 2001. Pre-Construction Oyster and Water Quality Monitoring Study for the Main Channel Deepening Project, Delaware Bay, New Jersey and Delaware . Report to the US Army Corp of Engineers by Versar, Inc. December, 2001.

Powell, E.N., Ashton-Alcox, K.A., Dobarro, J.A. Cummings, M., Banta, S.E. 2002. The inherent efficiency of oyster dredges in survey mode. Journal of Shellfish Research, 21:2, 691-695.

Powell, E.N., Ashton-Alcox, K.A., Kraeuter, J.N.. 2007. Re-evaluation of oyster dredge efficiency in survey mode: application in stock assessment. North American Journal of Fisheries Management, 27:2, 492-511. Prins, T.C., A.C. Smaal and R.F. Dame. 1998. A review of the feedbacks between bivalve grazing and ecosystem processes. Aquat. Ecol. 31: 349-359.

Rheault, R.B. and M.A. Rice. 1996. Food-limited growth and condition index in the eastern oyster *Crassostrea virginica* (Gmelin 1791), and the bay scallop, *Argopecten irradians irradians* (Lamarck 1819). J. Shellfish Res. 15:271-283.

Shumway, S. E. 1996. Natural environmental factors. Chapter 13 in The Eastern Oyster *Crassostrea virginica*. Kennedy V. S., Newell R. I. E. and A. E. Eble eds. Maryland Sea Grant, College Park, MD.

Smaal, A.C., T.C. Prins, N. Dankers and B. Ball. 1998. Minimum requirements for modelling bivalve carrying capacity. Aquat. Ecol. 31: 423-428.

Ulanowicz, R.E. and J.H. Tuttle. 1992. The trophic consequences of oyster stock rehabilitation in Chesapeake Bay. Estuaries 15: 298-306.

Whyte, J.N.C., J.R. Englar and B.L. Carswell. 1990. Biochemical composition and energy reserves in *Crassostrea gigas* exposed to different levels of nutrition. Aquaculture, 90:157-172.

Widdows, J., P. Donkin, M.D. Brinsley, S.V. Evans, P.N. Salkeld, A. Franklin, R.J. Law and M.J. Waldock. 1995. Scope for growth and contaminant levels in North Sea mussels *Mytilus edulis*. Mar. Ecol. Prog. Ser. 127: 131-148.

CHAPTER 3

Implementation and Validation of a Coupled Hydrodynamic-Larval Transport Model for the Delaware Estuary

Dale Haidvogel[1], Bob Chant[1], Maria Aristizabal[1], Joseph Wang[1] and Eric Powell[1]
Eileen Hofmann[2], John Klinck[2] and Diego Narvaez[2]

[1]Institute of Marine and Coastal Sciences, Rutgers University, 71 Dudley Road, New Brunswick NJ 08901

[2]Center for Coastal Physical Oceanography, 4111 Monarch Way, Old Dominion University, Norfolk, VA 23508

1.0 INTRODUCTION

The Haskin Shellfish Research Laboratory (HSRL) and its partners (IMCS, Rutgers University; Old Dominion University) are presently engaged in a multi-institutional National Science Foundation funded study to understand how oyster host genetics, population dynamics, and environment interact with disease organisms to structure host populations, and how climate change may interact with these inter-related processes. An initial emphasis has been placed on understanding the mechanisms by which molluscan populations maintain themselves in the face of disease, particularly in a spatially structured environment.

As part of this effort, an existing circulation model for the continental shelf was extended to the Delaware Estuary. The model, based upon the Regional Ocean Modeling System (ROMS, v.3), is being applied to identify dominant circulation phenomena in Delaware Bay and on the adjacent continental shelf that affect general changes in oyster parasite distribution and larval transport. The circulation model output also provides temperature, salinity, and flow velocities, which are not only essential to modeling oyster population dynamics, but are also valuable in modeling and examining other biological and environmental interactions occurring in the Estuary.

Included in this program is the development of a larval model subroutine for ROMS to be used to track larvae in Delaware Bay. Numerical particle-tracking experiments using the simulated circulation fields provide potential transport pathways of oyster larvae (and free-living disease pathogens), illustrating the importance of freshwater discharge rates

and wind in determining these transport pathways, and highlighting the importance of oyster-larvae behavior in determining retention and final settling region.

Of particular interest are the biological and environmental interactions taking place in the low-salinity region of the Bay. This zone (0-10 ppt) supports essential habitats for juvenile anadromous fish and provides critical disease refuge for oyster brood stocks. The low-salinity zone is also especially vulnerable to long-term and short-term climatic shifts, which greatly impact flow dynamics, salinity, and water quality.

The work described herein builds upon this NSF-sponsored research to investigate interactions of flow dynamics, salinity, and water quality on three species inhabiting the oligohaline zone of the Delaware Estuary—the Atlantic sturgeon (*Acipenser oxyrinchus*), the shortnose sturgeon (*Acipenser brevirostrum*), and the eastern oyster (*Crassostrea virginica*). The purpose of this work is to gather information which will be used to develop and to refine a model for managing and restoring sturgeon, oysters, and other salinity-dependent resources of the Delaware Estuary.

A serious regional concern of global warming is the acceleration of sea-level rise in the Delaware Estuary. Associated increases in salinity could have a major impact on critical estuarine processes and species. This project will provide coastal-decision makers and managers the critical information and modeling capabilities enhancing the development of thoughtful, proactive policies to plan for and to mitigate sea-level rise impacts on critical estuarine natural resources and uses. This work will also serve to augment the work being conducted to restore oyster habitat in Delaware Bay initiated in 2005.

2.0 METHODS

2.1 The Regional Ocean Modeling System (ROMS)

ROMS (http://www.myroms.org/) is a free-surface, terrain-following, primitive equations ocean model widely used by the scientific community for a diverse range of applications (e.g., Haidvogel *et al*., 2000; Marchesiello *et al*., 2003; Peliz *et al*., 2003; Di Lorenzo, 2003; Dinniman *et al*., 2003; Budgell, 2005; Warner *et al*., 2005a, b; Wilkin *et al*., 2005). The algorithms that comprise the ROMS computational nonlinear kernel are described in detail in Shchepetkin and McWilliams (2003, 2005), and the tangent linear and adjoint kernels and platforms are described in Moore *et al.*(2004). ROMS includes accurate and efficient physical and numerical algorithms and several coupled models for biogeochemical, bio-optical, sediment, and sea ice applications. The sea ice model is

described in Budgell (2005). It also includes several vertical mixing schemes (Warner *et al*., 2005a), multiple levels of nesting and composed grids.

For computational economy, the hydrostatic primitive equations for momentum are solved using a split-explicit time-stepping scheme which requires special treatment and coupling between barotropic (fast) and baroclinic (slow) modes. A finite number of barotropic time steps, within each baroclinic step, are carried out to evolve the free-surface and vertically integrated momentum equations. In order to avoid the errors associated with the aliasing of frequencies resolved by the barotropic steps but unresolved by the baroclinic step, the barotropic fields are time averaged before they replace those values obtained with a longer baroclinic step. A cosine-shape time filter, centered at the new time level, is used for the averaging of the barotropic fields. In addition, the separated time-stepping is constrained to maintain exactly both volume conservation and consistency preservation properties which are needed for the tracer equations. Currently, all 2D and 3D equations are time-discretized using a third-order accurate predictor (Leap-Frog) and corrector (Adams-Molton) time-stepping algorithm which is very robust and stable. The enhanced stability of the scheme allows larger time steps, by a factor of about four, which more than offsets the increased cost of the predictor-corrector algorithm.

In the vertical, the primitive equations are discretized over variable topography using stretched terrain-following coordinates (Song and Haidvogel, 1994). The stretched coordinates allow increased resolution in areas of interest, such as the thermocline and bottom boundary layers. The default stencil uses centered, second-order finite differences on a staggered vertical grid. Options for higher-order stencils are available via a conservative, parabolic spline reconstruction of vertical derivatives. This class of model exhibits stronger sensitivity to topography which results in pressure gradient errors. These errors arise due to splitting of the pressure gradient term into an along-sigma component and a hydrostatic correction (for details, see Haidvogel and Beckmann, 1999). The numerical algorithm in ROMS is designed to reduce such errors.

In the horizontal, the primitive equations are evaluated using boundary-fitted, orthogonal curvilinear coordinates on a staggered Arakawa C-grid. The general formulation of curvilinear coordinates includes both Cartesian (constant metrics) and spherical (variable metrics) coordinates. Coastal boundaries can also be specified as a finite-discretized grid via land/sea masking. As in the vertical, the horizontal stencil utilizes centered, second-order finite differences. However, the code is designed to make the implementation of higher order stencils easy.

ROMS has various options for advection schemes: second- and forth-order centered differences; and third-order, upstream biased. The later scheme is the model default and it has a velocity-dependent hyper-diffusion dissipation as the dominant truncation error (Shchepetkin and McWilliams, 1998). These schemes are stable for the predictor-corrector methodology of the model. In addition, there is an option for conservative parabolic spline representation of vertical advection which has dispersion properties similar to an eight-order accurate conventional scheme.

There are several subgrid-scale parameterizations in ROMS. The horizontal mixing of momentum and tracers can be along vertical levels, geopotential (constant depth) surfaces, or isopycnic (constant density) surfaces. The mixing operator can be harmonic (3-point stencil) or biharmonic (5-point stencil).

The vertical mixing parameterization in ROMS can be either by local or nonlocal closure schemes. The local closure schemes are based on the level 2.5 turbulent kinetic energy equations by Mellor and Yamada (1982) and the Generic Length Scale (GLS) parameterization (Umlauf and Burchard, 2003). The nonlocal closure scheme is based on the K-profile, boundary layer formulation by Large *et al.*(1994). The K-profile scheme has been expanded to include both surface and bottom oceanic boundary layers. The GLS is a two-equation turbulence model that allows a wide range of vertical mixing closures, including the popular k-kl (Mellor-Yamada level 2.5), k-e, and k-w schemes. Several stability functions (Galperin *et al*., 1988; Kantha and Clayson, 1994; Canuto *et al*., 2001) have been also added to provide further flexibility. A recent study (Warner *et al*., 2005a) evaluated the performance of these turbulence closures in ROMS in terms of idealized sediment transport applications. In addition, there is a wave/current bed boundary layer scheme that provides the bottom stress (Styles and Glenn, 2000) and sediment transport which become important in coastal applications.

Currently, the air-sea interaction boundary layer in ROMS is based on the bulk parameterization of Fairall *et al.*(1996). It was adapted from the COARE (Coupled Ocean-Atmosphere Response Experiment) algorithm for the computation of surface fluxes of momentum, sensible heat, and latent heat. This boundary layer is used for one or two-way coupling with atmospheric models.

ROMS is a very modern code and uses C-preprocessing to activate the various physical and numerical options. The code can be run in either serial or parallel computers. The code uses a coarse-grained parallelization paradigm which partitions the computational 3D grid into tiles. Each tile is then operated on by different parallel threads. Originally, the code was designed for shared-memory computer architectures and the parallel compiler-dependent directives (OpenMP Standard) are placed only in the main

computational routine of the code. An MPI version of the code has been developed so both shared and distributed-memory paradigms coexist together in a single code.

ROMS has extensive pre- and post-processing software for data preparation, analysis, plotting, and visualization. The entire input and output data structure of the model is via NetCDF which facilitates the interchange of data between computers, the user community, and other independent analysis software.

2.2 Larval tracking sub-model

The model used to simulate the growth of larvae of *Crassostrea virginica* is based on the model presented in Dekshenieks *et al.*(1993, 1996, 1997). This model simulates the time-dependent change in oyster larva size based on ambient temperature, salinity, food supply and turbidity conditions. A larval behavior model, which is based on Dekshenieks *et al.*(1996), was coupled with the growth model to calculate the vertical displacement of the larva as a function of swimming rate, sinking rate and larval activity. These biologically determined displacement processes are dependent upon the age of the larva and are modified by the vertical advective velocities. The simulated oyster larvae set when a length of 330 μm is reached.

The larval growth and behavior models have been embedded successfully into the Delaware Bay circulation model. The coupled circulation-oyster larvae model was implemented for Delaware Bay to do a series of particle tracking (Lagrangian) simulations. The Lagrangian simulations use the particle tracking module that is available as part of the ROMS setup. In these simulations the trajectory of a particle in time and space is calculated based on the three-dimensional velocity field obtained from the circulation model and the biological displacement obtained from the larva behavioral sub-model. This code structure facilitates computations over nested and composed grids. The parallel framework is coarse-grained with both shared- and distributed-memory paradigms coexisting in the same code. The shared-memory option follows OpenMP 2.0 standard. ROMS has a generic distributed-memory interface that facilitates the use of several message passage protocols. Currently, the data exchange between nodes is done with MPI. However, other protocols like MPI2, SHMEM, and others can be coded without much effort. Simulations were done with and without larval behavior to isolate the effect of circulation and biological processes on the retention and/or export of oyster larvae from Delaware Bay.

3.0 RESULTS

3.1 Validation of the Delaware Estuary circulation model: in situ water level, temperature and salinity

The first year of this project was devoted to validation of the circulation component of the Delaware Bay model. Quantitative comparisons were conducted using available water level, temperature, salinity and velocity datasets. The results of these activities, obtained by our two DuPont-supported Graduate Research Assistants (GRA), are described next.

Our first DuPont-supported GRA (Joseph Wang) has been comparing the ROMS Delaware Bay model output with data obtained in the year 2000 (Versar, 2001). The ROMS Delaware Bay model used for this comparison has 98x386 grid points in the horizontal and 20 vertical terrain-following levels. Tidal inputs from a global tidal model are applied at the open boundary segments; daily fresh water input is supplied by six rivers; three-hourly atmospheric fluxes are obtained from the North American Regional Reanalysis (NARR). For the year 2000, concurrent observations are available at 12 water level (WL) and 9 temperature (T) and salinity (S) stations. Grid spacing, bathymetry, and river and observing locations are shown in Figure 1.

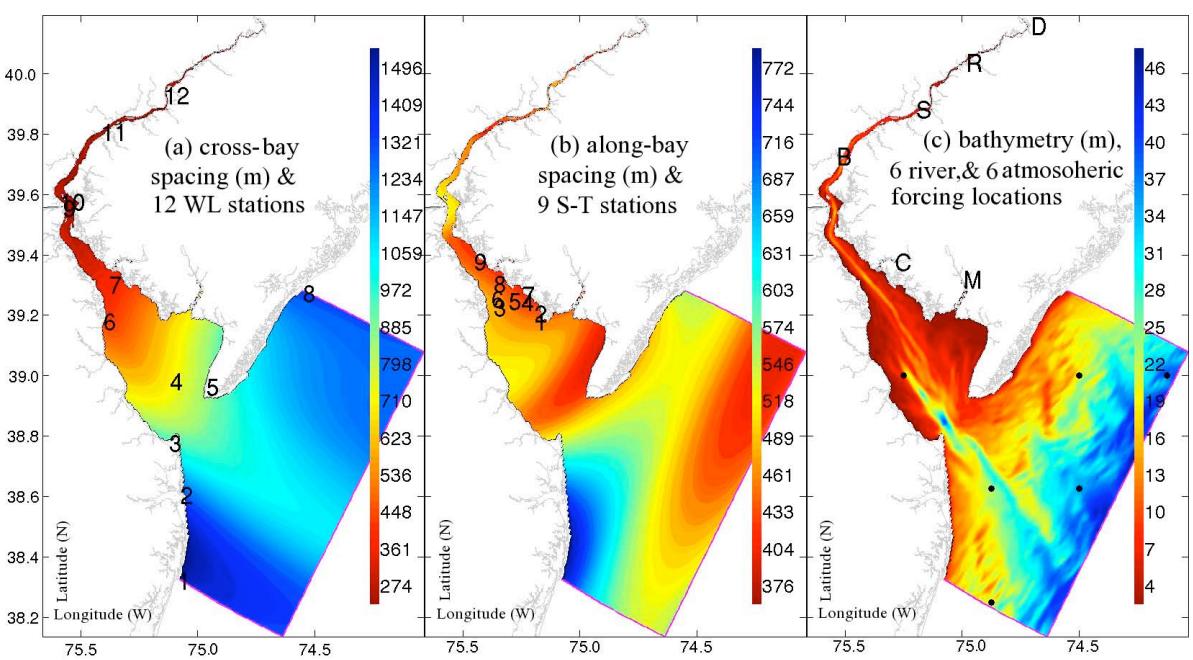

Figure 1. (a) cross-bay (along-shelf) grid spacing in meters and the 12 locations where water level data was obtained; (b) along-bay (cross-shelf) grid spacing and the 9 temperature-salinity stations; (c) bathymetry in meters, the locations of the 6 rivers (the letters) and atmospheric forcing stations (the black dots).

Early simulations showed the Delaware Bay model to be too warm, especially in the summer months. This discrepancy was traced to the incoming solar short-wave radiation.The SSWR from NARR is systematically higher than measured regional values from the Delaware Environmental Observation System (DEOS). An example of two time series of SSWR averaged over the years 2005-2009 is given in Figure 2. For the model results shown below, the NARR SSWR was reduced by 20%.

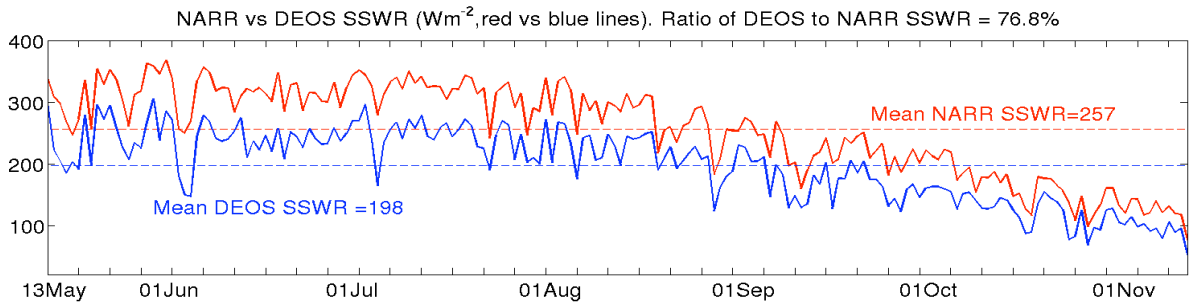

Figure 2. Comparison of time series for incoming solar short wave radiation as given by the North American Regional Reanalysis (red line) and by the Delaware Environmental Observation System (blue).

For the year 2000, we have identified 4896 hourly water level (11 June-31 December) and 4416 hourly salinity-temperature (13 May-12 November) samples at the stations shown in Figure 1. Time series of water level, temperature and salinity at these locations were obtained from the Delaware Bay model output. Model hindcast skill may then be assessed in many ways. Here we show results in terms of the Taylor Diagram (Figure 3). On a Taylor diagram, the radial distance R_t from the "test" point measures the normalized standard deviation of the model (test) field. The correlation between model and observations is given by the angle from the x-axis [cos(α)]. Finally, the distance (R_m) from the reference point (1,0) is the centered-pattern RMS difference between model and observations.

Model-data comparisons for water level, temperature and salinity are shown in Figures 4, 5 and 6, respectively. Color bars have been added to quantify any bias in M2 tidal amplitude (Fig. 4) or in predicted temperature and salinity values (Figs. 5 and 6). Correlations between observed and predicted time series are uniformly high: in excess of 0.9 for both water level and temperature at all stations, and in excess of 0.8 at all but one of the salinity stations. The bias is typically low in all 3 quantities.

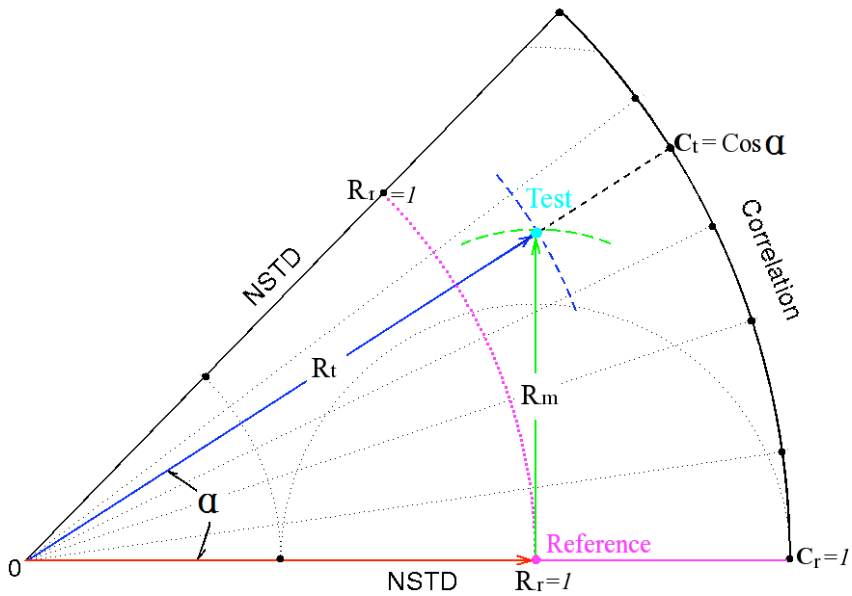

Figure 3. Schematic of the Taylor diagram (see text for explanation).

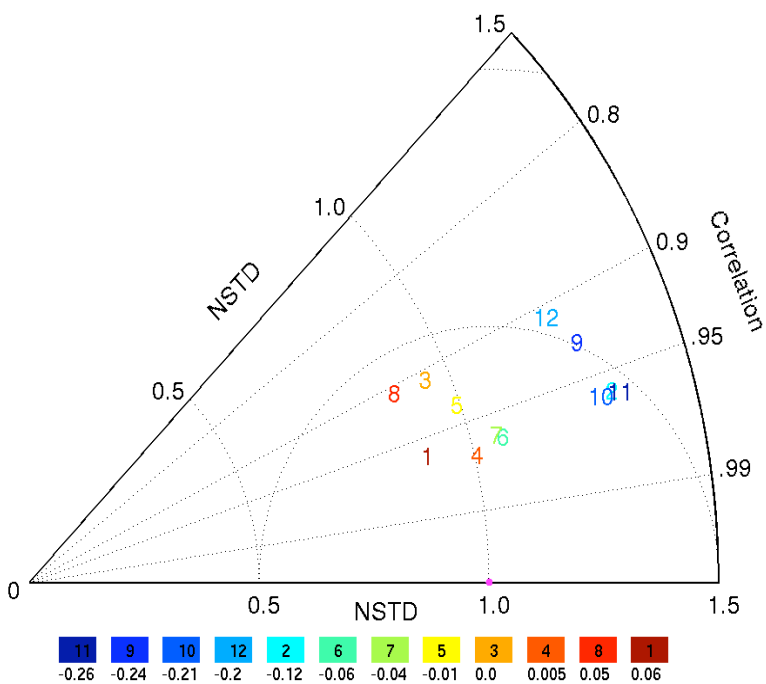

Figure 4. Taylor diagram for model-data comparisons at the 12 water level stations.

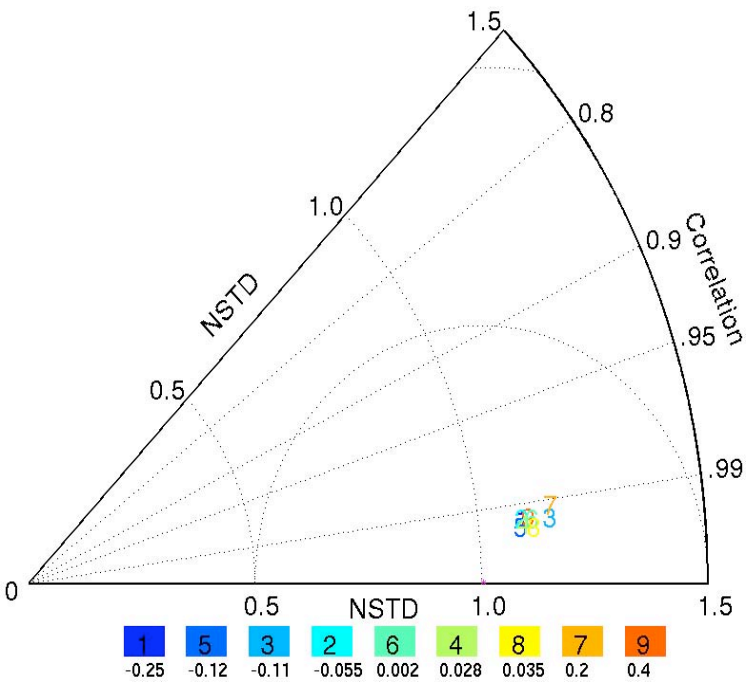

Figure 5. Taylor diagram for model-data comparisons at the 9 temperature stations.

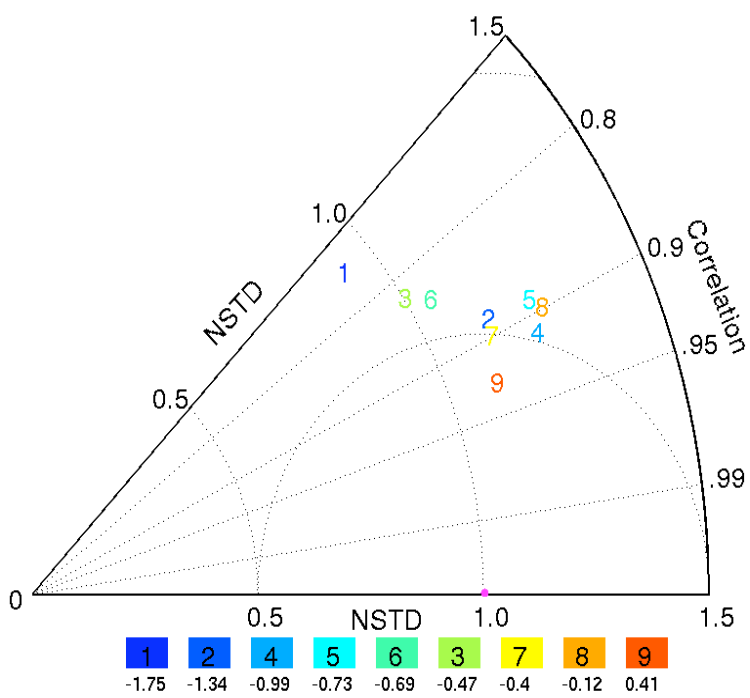

Figure 6. Taylor diagram for model-data comparisons at the 9 salinity stations.

By examining the low- and high-passed time series, it can be shown that the variability in temperature is dominated by the seasonal cycle, whereas the variability in salinity is dominated by the high-frequency (tidal) fluctuations. Hence, we conclude that the Delaware Bay model has substantial skill in its replication of both the seasonal and tidal dynamics regimes.

3.2 Validation against in situ velocity and salinity data

Our second DuPont-supported GRA (Maria Aristizabal) has been comparing numerical simulations of the tidally averaged mean flow (i.e., the exchange flow) to available observations obtained in the year 2005 by Chris Sommerfield of the University of Delaware. The configuration of the ROMS model is the same as that shown in Figure 1.

Comparison between observed and modeled exchange flow are promising but there appears to be a bias for the model to underestimate the velocity of the inflowing layer (Fig. 7). In contrast, the model appears to be more skilled in the upper layer velocity. A comparison between modeled and measured salinity stratification at the same location as the current meter observations are also promising wth the notable exception of a significant over-prediction of stratification following a large discharge event in April 2005 (Fig. 8).

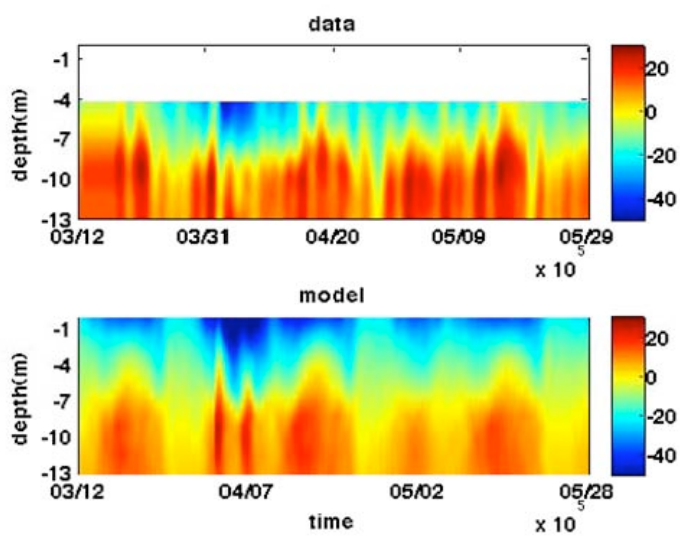

Figure 7. Comparison between tidally averaged along channel flow from 2005 mooring deployment (upper panel) and model (lower panel).

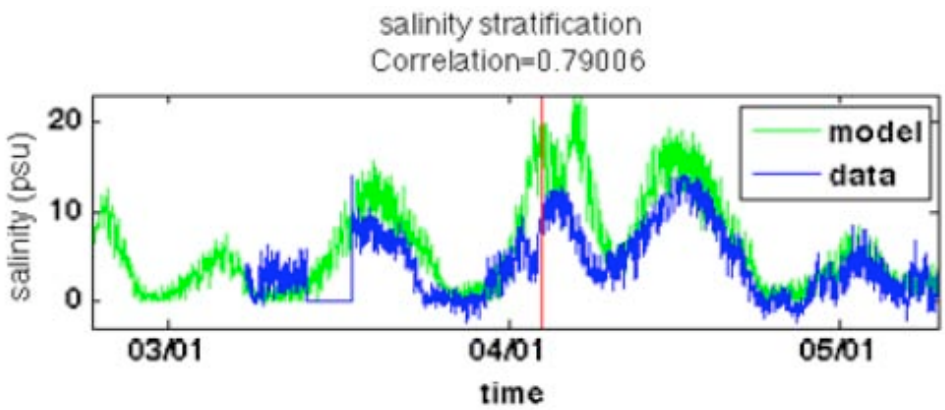

Figure 8. Vertical salinity stratification from model (green) and observed (blue) from 2005 deployment. Red line indicates peak of April 2005 Delaware River discharge

Examples of a comparison between modeled and observed cross-channel structure of the exchange flow are shown in Figure 9. The observed mean flow is based on a 12- hour tidal cycle survey conducted with a shipboard Acoustic Doppler Current Profiler conducted in August of 2005. While both the modeled and observed flow are broadly similar with both depicting a mean outflow at the surface and an inflow at depth in the main channel and on the flank, the cross-channel structure of the observed exchange flow is asymmetric relative to the channel while the modeled exchange flow is more symmetric with the outflow over the main channel.

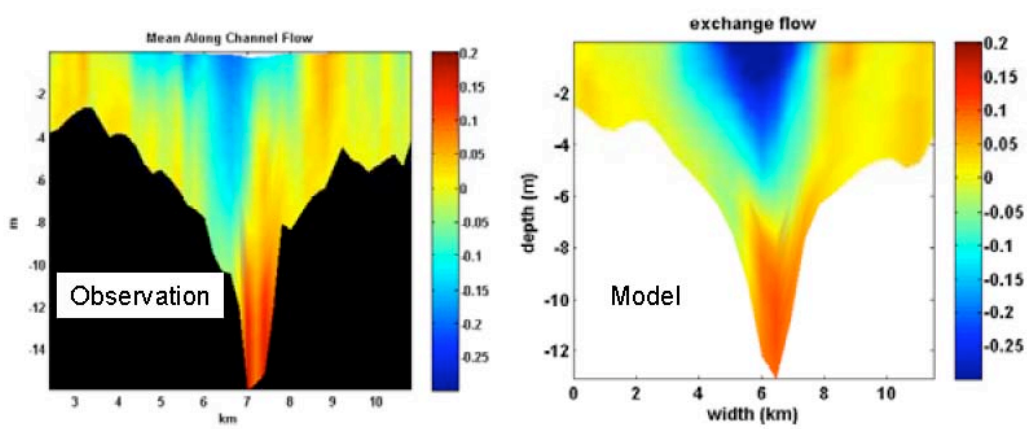

Figure 9. Comparison between observed along-channel tidally mean flow from observations (left) and model (right). Negative velocity (blue) is landward, positive (yellow/red) is seaward.

3.3 Larval tracking simulations

Particles were released in the simulated circulation fields at locations that correspond to those of the primary oyster reefs (Fig. 10). The circulation simulation supporting results presented here was obtained using conditions that were from 1984-1985. Simulation of years in the 2000s provided essentially equivalent patterns and are not presented. Particle releases started in June and continued throughout the summer at weekly intervals. This period coincides with oyster spawning and hence oyster larvae production.

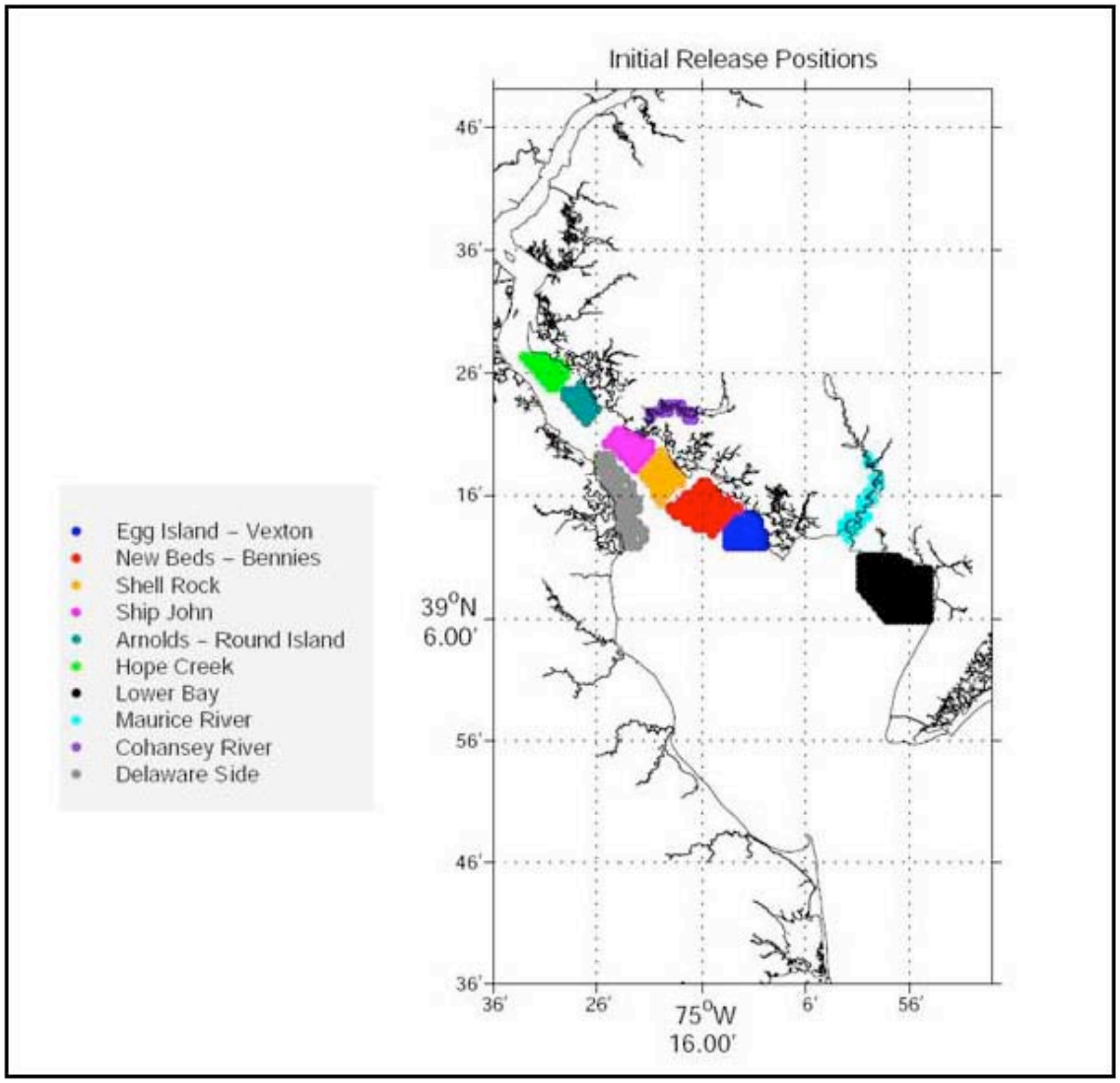

Figure 10. Particle release locations for the Lagrangian particle tracking simulations. The colors correspond to the locations of known oyster reefs in Delaware Bay.

The importance of larval behavior in determining the final settling location is illustrated by a comparison of the particle distribution in July obtained from simulations that did not include larval behavior (Fig. 11, left panel) and that did include larval behavior (Fig.11, right panel). Passive particles tend to escape the bay, ending up on the continental shelf. Larval behavior, which includes vertical migration as a function of size and salinity, is critical for retaining the larvae in Delaware Bay. Simulations show, overall, that larvae reach settlement size in 10-20 days as observed in the field (and hatchery). Thus, the larval subroutine in ROMS provides results anticipated from known observations of larval growth rates and behavior.

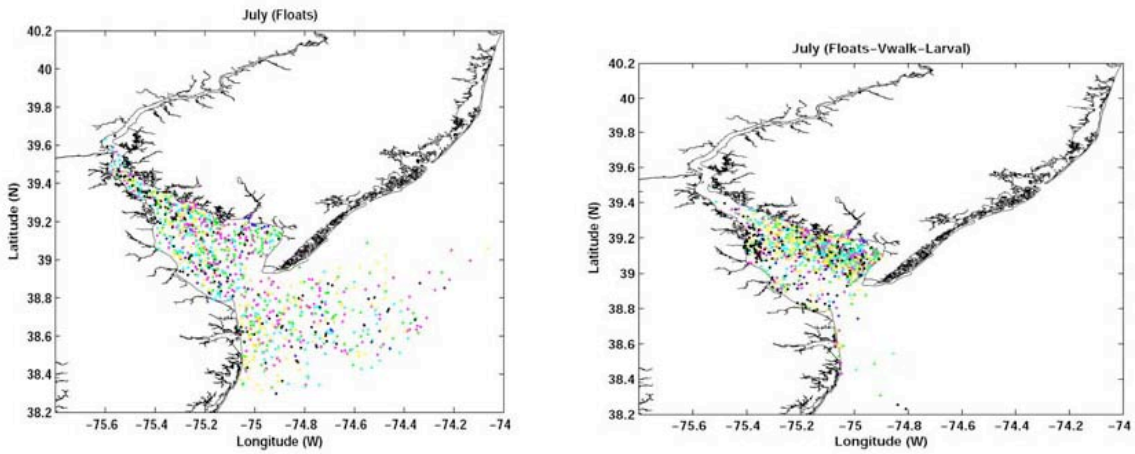

Figure 11. Comparison of larval transport without (left panel) and with (right panel) behavior.

The distribution of larvae that set between June and August (Fig. 12) shows considerable variability in the location at which they reach settlement size. Particles released in July tend to remain on the New Jersey side of the Bay. Note in particular, the tendency for particles to accumulate in the bayshore region below Egg Island Point. This is an area famous for persistently high recruitment year after year (though survival is always poor). The region acts as a larval trap. Particles released later in the summer, particularly in August, are more dispersed in the Bay with particles tending to settle at higher frequencies along the Delaware side of the Bay. This behavior is consistent with results from the 2005-2008 shell-planting program that show that the two sides of the bay rarely have good recruitment events in the same year. Very likely, from the simulations, this is due in large part to the timing of the spawn.

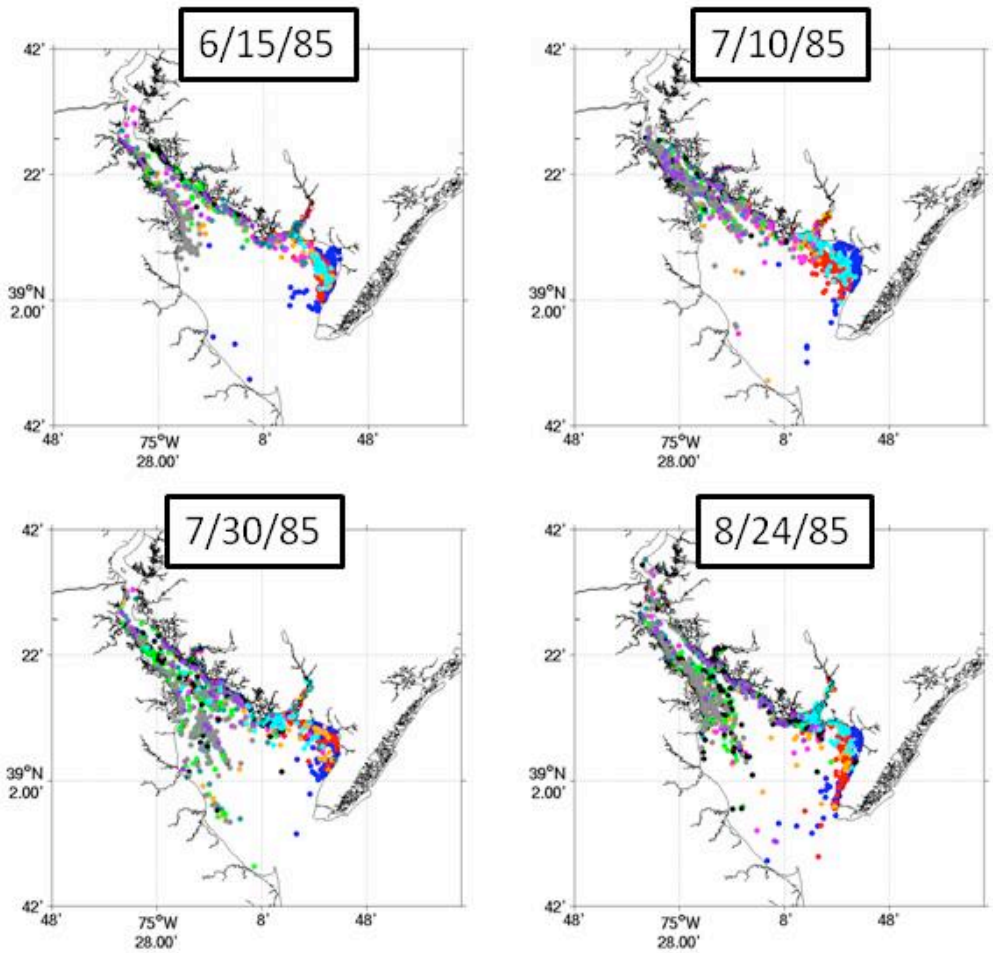

Figure 12. Final settling location of particles released between June and August.

The connectivity between the particle release point and the final settling location (Fig. 13) provides an estimate of the exchange between individual reefs and throughout the Bay. The simulations show a number of features that relate to known patterns from stock assessment survey data. First, there is a net downbay drift of larvae. This is shown clearly in Figure 12 and also in Figure 13. The downbay drift is more apparent in the upper bay. That is, larvae spawned from the upper bay reefs are more likely to drift downbay and fail to recruit back to those reefs than larvae released from reefs further downbay. A comparison between the Ship John/Shell Rock area and the Hope Creek area is most insightful. The stock assessment time series for the New Jersey beds shows this same behavior. Note in Figure 14 the tendency for recruitment events of consequence to be much less frequent or predictable upbay relative to downbay. This is clear evidence of the net downbay larval drift that is typical of the larval dynamics in Delaware Bay. Note also in Figure 13 that the area from Ship John through Bennies is characterized by a tendency

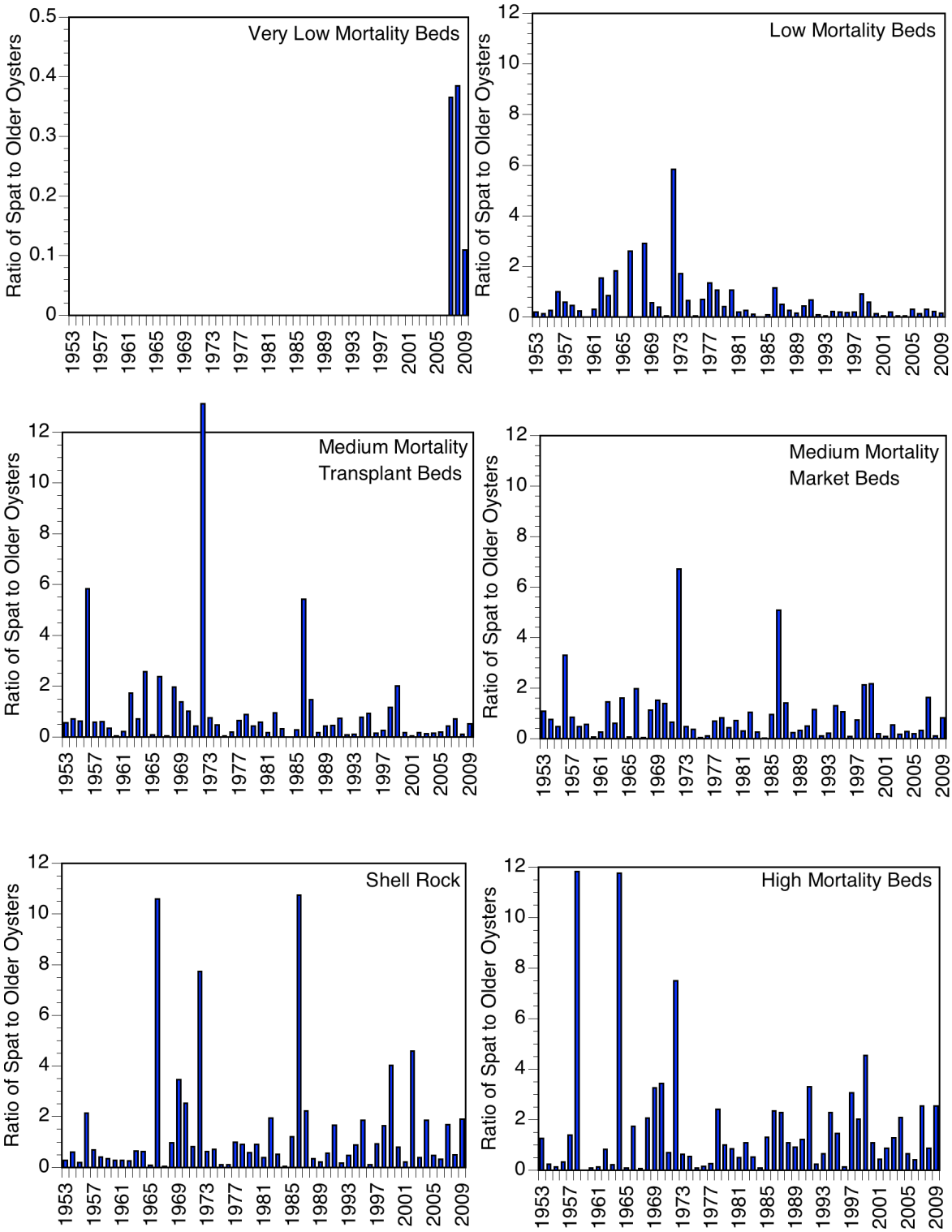

Figure 13. The percent of simulated particles (oyster larvae) released from a particular reef that settle at various locations in Delaware Bay.

for larvae spawned in this region to remain nearby and recruit to the same general region. This explains the much more consistent recruitment observed on the high-mortality beds as documented in Figure 14. Finally, note that larvae rarely move back upbay. Thus, beds upbay are more likely to be self-supporting than beds downbay which can attract larvae from local spawns as well as upbay spawns. Moreover, note the strong tendency for Delaware beds to be more self-recruiting than New Jersey beds. This explains the greater uncertainty in recruitment on the Delaware side of the bay observed in comparisons between the New Jersey and Delaware stock assessment time series.

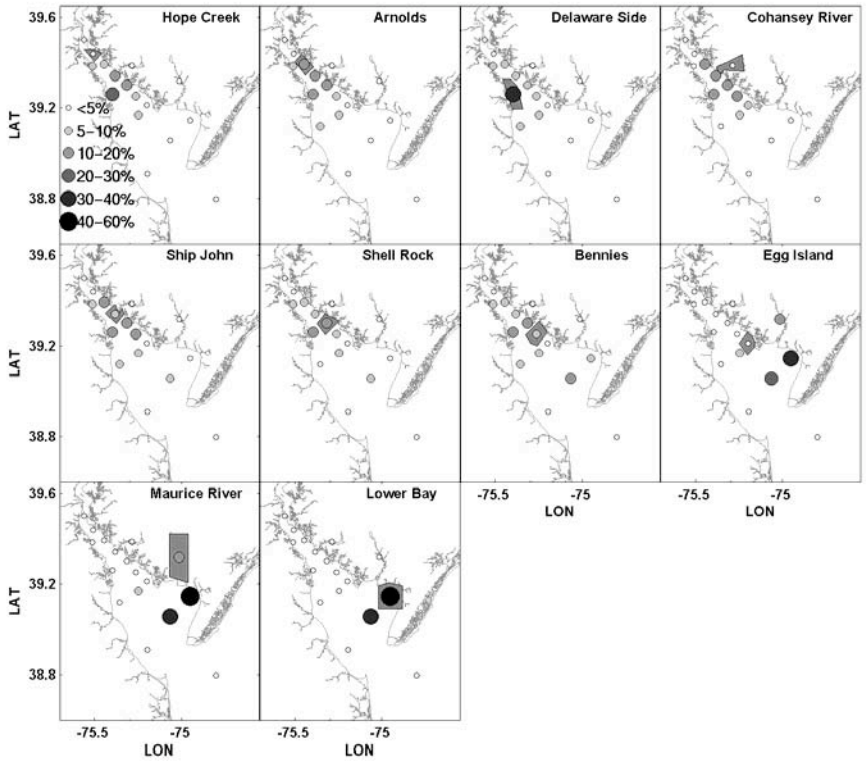

Figure 14. Spat-to-adult oyster ratio for each Bay region. Bed distributions by Bay region are shown in Figure 15.

The model simulations that have been presented here come with an important caveat. Food supply is an important controlling factor behind larval success. As an adequate time series of food supply has not been available, the simulations have been run with food present continuously in all bay regions at a level conducive to larval success. The provision of a geographically-detailed time series of food supply from sampling conducting during this funding year will provide the basis for a much improved series of simulations in the coming year. Once the food supply data are integrated into model runs, the model will be useful to evaluate the influence of factors varying environmental

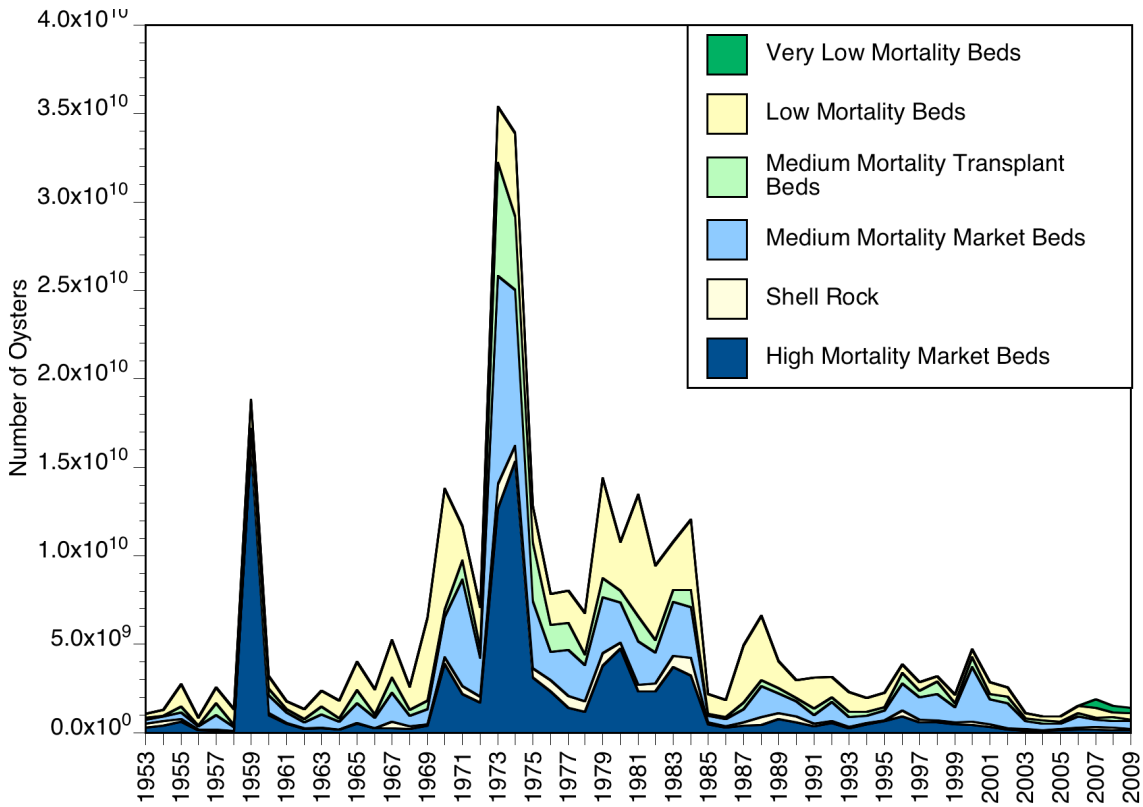

Figure 15. Time series of oyster abundance by bay region. High Mortality: Bennies Sand, Nantuxent Point, Bennies, Strawberry, Hog Shoal, Vexton, Hawk's Nest, New Beds, Beadons, Egg Island, Ledge; Medium Mortality Market (less Shell Rock): Ship John, Cohansey, Sea Breeze; Medium Mortality Transplant: Middle, Upper Middle; Low Mortality: Arnolds, Upper Arnolds, Round Island; Very Low Mortality: Hope Creek, Fishing Creek, Liston Range. No data are available for the Very Low Mortality beds prior to 2007.

conditions on larval transport and recruitment dynamics. Of some importance will be the evaluation of the impact of wet and dry years on larval transport and the influence of variations in summer and fall food levels on recruitment.

4.0 CONCLUSIONS

The ROMS hydrodynamic model for the Delaware Estuary successfully reproduces many features of the observed water level, circulation and tracer fields for datasets obtained in the years 2000 and 2005. The larval growth/behavior sub-model has been coupled to ROMS, and initial coupled hydrodynamic/larval transport simulations have been conducted.

In the second year of this project, we will: 1) begin to consider the nutrient cycle within the Delaware Bay model domain, and its influence on larval transport; 2) seek possible environmental relationships with the acoustically derived positions of sturgeon; 3) begin

to conduct climate change scenario simulations to assess the potential impacts of future changes in (e.g.) sea level and river flow; and 4) continue to characterize fundamental processes that drive the exchange flow and stratification in the Bay.

5.0 LITERATURE CITED

Budgell, W.P., 2005: Numerical simulation of ice-ocean variability in the Barents Sea region, *Ocean Dynamics*, DOI 10.1007/s10236-005-0008-3.

Canuto, V.M., A. Howard, Y. Cheng, M.S. Dubovikov, 2001: Ocean turbulence I: one-point closure model. Momentum and heat vertical diffusivities. *J. Phys. Oceanogr. 31, 1413-1426.*

Dekshenieks, M. M., E. E. Hofmann, and E. N. Powell (1993), Environmental effects on the growth and development of eastern oyster, *Crassostrea virginica* (Gmelin, 1791), larvae: A modeling study, *J. Shellfish Res*., 12 (2), 241-254.

Dekshenieks, M. M., E. E. Hofmann, J. M. Klinck, and E. N. Powell (1996), Modeling the vertical distribution of oyster larvae in response to environmental conditions, *Mar. Ecol. Prog. Ser*., 136, 97-110.

Dekshenieks, M. M., E. E. Hofmann, J. M. Klinck, and E. N. Powell (1997), A modeling study of the effects of size- and depth-dependent predation on larval survival, *J. Plankton Res*., 19 (11), 1583-1598.

Di Lorenzo, E., 2003: Seasonal dynamics of the surface circulation in the southern California Current System, *Deep-Sea Res., Part* II, **50**, 2371-2388.

Dinniman, M. S., J. M. Klinck, and W. O. Smith Jr. (2003), Cross shelf exchange in a model of the Ross Sea circulation and biogeochemistry, *Deep-Sea Res., Part* II, **50**, 3103-3120.

Fairall, C.W., E.F. Bradley, D.P. Rogers, J.B. Edson and G.S. Young, 1996: Bulk parameterization of air-sea fluxes for tropical ocean-global atmosphere Coupled-Ocean Atmosphere Response Experiment, *J. Geophys. Res.*, **101**, 3747-3764.

Galperin, B., L. H. Kantha, S. Hassid, and A. Rosati, 1988: A quasi-equilibrium turbulent energy model for geophysical flows. *J. Atmos. Sci.*, **45**, 55-62.

Haidvogel, D. B., H. G. Arango, K. Hedstrom, A. Beckmann, P. Malanotte-Rizzoli, and A. F. Shchepetkin (2000), Model evaluation experiments in the North Atlantic Basin: Simulations in nonlinear terrain-following coordinates, *Dyn. Atmos. Oceans*, **32**, 239-281.

Haidvogel, D. B. and A. Beckmann, 1999: *Numerical Ocean Circulation Modeling*. Imperial College Press.

Kantha, L.H., C.A. Clayson, 1994: Nermerical Models of Oceans and Oceanic Processes. In: International Geophysics Seris, Vol. 66. *Academic Press*, San Diego. 940 pp.

Large, W. G., J. C. McWilliams, and S. C. Doney, 1994: Oceanic vertical mixing: a review and a model with a nonlocal boundary layer parameterization. *Rev. Geophys.*, **32**, 363-403.

Marchesiello, P., J.C. McWilliams, and A. Shchepetkin, 2003: Equilibrium structure and dynamics of the California Current System, *J. Phys. Oceanogr.*, **33**, 753-783.

Mellor, G. L. and T. Yamada, 1982: Developement of a turbulence closure model for geophysical fluid problems. *Rev. Geophys. Space Phys.*, **20**, 851-875.

Moore, A.M., H.G. Arango, A.J. Miller, B.D. Cornuelle, E. Di Lorenzo and D.J. Neilson, 2004: A Comprehensive Ocean Prediction and Analysis System Based on the Tangent Linear and Adjoint Components of a Regional Ocean Model. *Ocean Modelling*, **7**, 227-258.

Peliz, A., J. Dubert, D. B. Haidvogel, and B. Le Cann (2003), Generation and unstable evolution of a density-driven Eastern Poleward Current: The Iberian Poleward Current, *J. Geophys. Res.*, **108**(C8), 3268, doi:10.1029/2002JC001443.

Shchepetkin, A. F., and J. C. McWilliams (1998), Quasi-monotone advection schemes based on explicit locally adaptive dissipation, *Monthly Weather Review*, **126**, 1541-1580.

Shchepetkin, A. F., and J. C. McWilliams (2003), A method for computing horizontal pressure-gradient force in an oceanic model with a nonaligned vertical coordinate, *J. Geophys. Res.*, **108**(C3), 3090, doi:10.1029/2001JC001047.

Shchepetkin, A. F., and J. C. McWilliams (2005), The Regional Ocean Modeling System: A split-explicit, free-surface, topography following coordinates ocean model, *Ocean Modelling*, **9**, 347-404.

Song, Y. and D. B. Haidvogel, 1994: A semi-implicit ocean circulation model using a generalized topography-following coordinate system. *J. Comp. Phys.*, **115(1)**, 228-244.

Styles, R. and S.M. Glenn, 2000: Modeling stratified wave and current bottom boundary layers in the continental shelf. *J. of Geophys. Res.*, **105**, 24119-24139.

Umlauf, L., H. Burchard, 2003: A generic length-scale equation for geophysical turbulence models. *J. MArine Res.*, **61**, 235-265.

Warner, J.C, C.R. Sherwood, H.G. Arango, and R.P. Signell, 2005a: Performance of four Turbulence Closure Methods Implemented using a Generic Length Scale Method. *Ocean Modelling*, **8**, 81-113.

Warner, J. C., W. R. Geyer, and J. A. Lerczak, 2005b: Numerical modeling of an estuary: A comprehensive skill assessment, *J. Geophys. Res.*, **110**, C05001, doi: 10.1029/2004JC002691.

Wilkin, J.L., H.G. Arango, D.B. Haidvogel, C.S. Lichtenwalner, S.M. Durski, and K.S. Hedstrom, 2005: A regional Ocean Modeling System for the Long-term Ecosystem Observatory. *J. Geophys. Res.*, **110**, C06S91, doi:10.1029/2003JC002218.

CHAPTER 1 APPENDIX

Table 1. Juvenile Atlantic sturgeon collected in the lower tidal Delaware River, July-November 2009.

Date	Location	Gear[1]	Depth (m)	Total length (mm)	Fork length (mm)	Weight (g)	Water temp. (ºC)	Dissolved oxygen (mg/L)	Specific conductance (µS/cm)	Salinity (‰)	Acoustic Tag	Acoustic Tag Type
7/15/2009	Upper Cherry Isl. Flats	C	8.1	865[2]	747	8640	24.7	7.2	236	0.1	A100	V16-4H
8/18/2009	Marcus Hook anchorage	C	13.9	791	673	2760	26.4	7.4	208	0.1	A101	V16-6H
8/18/2009	Marcus Hook anchorage	C	13.9	1085	947	6980	26.4	7.4	208	0.1	A102	V16-6H
8/25/2009	Upper Cherry Isl. Flats	DNREC1	6.7	855	754	4540	27.1	---	220	0.1	A103	V16-6H
9/1/2009	Marcus Hook anchorage	A	13.7	568[3]	485	940	24.8	6.8	221	0.1	A104	V9-6L
9/1/2009	Marcus Hook anchorage	B+B	14.0	588	502	1000	24.8	6.8	221	0.1	A105	V9-1L
9/1/2009	Marcus Hook anchorage	C	13.7	593	505	1100	24.8	6.8	221	0.1	A106	V13-1H
9/1/2009	Marcus Hook anchorage	C	13.7	598	519	1080	24.8	6.8	221	0.1	---	---
9/1/2009	Marcus Hook anchorage	A	13.7	607	524	1180	24.8	6.8	221	0.1	A107	V13-1H
9/1/2009	Marcus Hook anchorage	C	13.9	626	540	1180	24.8	6.8	221	0.1	---	---
9/1/2009	Marcus Hook anchorage	C	13.7	629	545	1250	24.8	6.8	221	0.1	A108	V16-1L
9/1/2009	Marcus Hook anchorage	C	13.7	691	600	1680	24.8	6.8	221	0.1	A109	V16-1L
9/1/2009	Marcus Hook anchorage	C	13.9	775	651	2360	24.8	6.8	221	0.1	A110	V16-4H
9/1/2009	Marcus Hook anchorage	B+B	14.0	834	718	2960	24.8	6.8	221	0.1	A111	V16-4H
9/1/2009	Marcus Hook anchorage	C	13.9	862	742	3710	24.8	6.8	221	0.1	---	---
9/1/2009	Marcus Hook anchorage	C	13.7	964	830	4660	24.8	6.8	221	0.1	---	---
9/1/2009	Marcus Hook anchorage	C	13.9	981	860	5000	24.8	6.8	221	0.1	---	---
9/1/2009	Marcus Hook anchorage	C	13.7	1044	920	6360	24.8	6.8	221	0.1	---	---
9/1/2009	Marcus Hook anchorage	C	13.7	1054	908	6440	24.8	6.8	221	0.1	---	---
9/1/2009	Marcus Hook anchorage	C	13.7	1112	945	7140	24.8	6.8	221	0.1	---	---
9/1/2009	Marcus Hook anchorage	C	13.7	1128	958	6280	24.8	6.8	221	0.1	---	---
9/1/2009	Marcus Hook anchorage	C	13.7	1148	872	7380	24.8	6.8	221	0.1	---	---
9/24/2009	Marcus Hook anchorage	A	13.0	220	189	38	21.8	6.2	282	0.1	---	---
9/24/2009	Marcus Hook anchorage	A	13.0	240	207	63	21.8	6.2	282	0.1	---	---
9/24/2009	Marcus Hook anchorage	A	13.0	263	222	80	21.8	6.2	282	0.1	---	---
9/24/2009	Marcus Hook anchorage	A	13.0	277	237	86	21.8	6.2	282	0.1	---	---
9/24/2009	Marcus Hook anchorage	DNREC2	12.5	902	768	3660	21.8	6.2	282	0.1	A112	V16-1L
9/24/2009	Marcus Hook anchorage	DNREC2	12.5	1008	843	5760	21.8	6.2	282	0.1	A113	V16-4H
9/24/2009	Marcus Hook anchorage	DNREC2	12.5	1074	913	5860	21.8	6.2	282	0.1	A114	V16-4H
9/24/2009	Marcus Hook anchorage	DNREC2	12.5	1112	967	7380	21.8	6.2	282	0.1	A115	V16-4H
9/24/2009	Marcus Hook anchorage	DNREC2	12.5	1131	970	7360	21.8	6.2	282	0.1	A116	V16-4H
10/1/2009	Marcus Hook anchorage	A	13.9	245	211	60	19.3	6.6	327	0.2	---	---
10/1/2009	Marcus Hook anchorage	C	13.6	600	523	1060	19.3	6.6	327	0.2	A117	V16-1L
10/1/2009	Marcus Hook anchorage	C	13.4	655	566	1180	19.3	6.6	327	0.2	A118	V16-1L
10/1/2009	Marcus Hook anchorage	C	13.4	1062	913	5920	19.3	6.6	327	0.2	---	---
10/6/2009	Marcus Hook anchorage	B+B	14.6	223	194	40	18.9	6.7	331	0.2	---	---
10/6/2009	Marcus Hook anchorage	C	13.9	303	259	100	18.9	6.7	331	0.2	---	---
10/12/2009	Marcus Hook anchorage	B+B	12.8	282	237	80	17.9	7.3	357	0.2	---	---
10/14/2009	Marcus Hook anchorage	B+B	13.0	257	220	40	17.4	6.8	665	0.3	---	---
10/14/2009	Marcus Hook anchorage	A	13.4	258	220	40	17.4	6.8	665	0.3	---	---
10/14/2009	Marcus Hook anchorage	B+B	13.0	319	286	140	17.4	6.8	665	0.3	---	---
10/20/2009	Marcus Hook anchorage	A	14.0	297	248	120	13.7	7.2	378	0.2	---	---
10/20/2009	Marcus Hook anchorage	A	14.0	291	248	100	13.7	7.2	378	0.2	---	---
10/20/2009	Marcus Hook anchorage	B+B	14.9	316	269	120	13.7	7.2	378	0.2	---	---
10/29/2009	Marcus Hook anchorage	B+B	13.3	274	232	80	14.3	8.5	325	0.2	---	---
10/29/2009	Marcus Hook anchorage	B+B	13.3	323	278	130	14.3	8.5	325	0.2	A120	V7-4L
11/4/2009	Marcus Hook anchorage	B	14.0	280	239	80	13.2	7.6	232	0.1	---	---

Table 1. Continued.

Date	Location	Gear[1]	Depth (m)	Total length (mm)	Fork length (mm)	Weight (g)	Water temp. (ºC)	Dissolved oxygen (mg/L)	Specific conductance (µS/cm)	Salinity (‰)	Acoustic Tag	Acoustic Tag Type
11/4/2009	Marcus Hook anchorage	B+B	14.9	304	265	140	13.2	7.6	232	0.1	---	---
11/4/2009	Marcus Hook anchorage	B	14.0	309	252	80	13.2	7.6	232	0.1	---	---
11/4/2009	Marcus Hook anchorage	B+B	14.9	320	277	120	13.2	7.6	232	0.1	---	---
11/4/2009	Marcus Hook anchorage	B	14.0	324	279	120	13.2	7.6	232	0.1	---	---
11/4/2009	Marcus Hook anchorage	B	14.0	337	289	140	13.2	7.6	232	0.1	A121	V7-4L
11/4/2009	Marcus Hook anchorage	B	14.0	345	295	140	13.2	7.6	232	0.1	---	---

[1]Gear
A = 100- x 1.8-m, 33 m panels of 2.5-, 5.1- and 7.6 cm mesh
B = 66- x 1.8-m, 33 m panels of 5.1 and 7.6 cm mesh
C = 100- x 1.8-m, 12.7 cm mesh
DNREC1 = 100- x 3.7-m, 7.6 cm mesh
DNREC2 = 100- x 3.7-m, 5.1 cm mesh

[2]Recaptured 9/24/09 in Marcus Hook anchorage

Table 2. Occurrence of acoustically tagged Atlantic sturgeon in the Delaware River-Estuary and nearshore ocean.

Acoustic tag		A100		A101		A102		A103		A104		A105	
Fork length (mm)		747		673		947		754		485		502	
Life stage		subadult		subadult		subadult		subadult		subadult		subadult	
Date tagged		7/15/09		8/18/09		8/18/09		8/25/09		9/1/09		9/1/09	
Period of detection		7/15-11/15/09		8/18-12/15/09		8/18-10/9/09		8/25-10/28/09		9/2/09-1/14/10		9/1/09-1/14/10	
Location[1]	km[2]	No. Days	No. Detects	No. Days	No. Detects	No. Days	No. Detects	No. Days	No. Detects	No. Days	No. Detects	No. Days	No. Detects
LL# 4120 Upper DE River CB 66	199												
LL# 3920 Upper DE River CLB 36	186												
LL# 3775 Upper DE River CLB 18	176												
LL# 3605 DE River LB 50	163												
LL# 3565 Horseshoe Bend LB 39	154												
LL# 3405 Elbow LBB 44	148												
LL# 3395 Mantua Creek Anchorage Buoy B	147												
LL# 3380 Mifflin Range LB 1F	144											2	8
LL# 3315 Tinicum Island Range LB 5T	141			1	12					3	37	5	83
LL# 3270 Tinicum Island Range LB 2T	135									2	52		
LL# 3255 Chester Range LB 6C	134	1	3	2	7					31	531	4	39
LL# 3215 Chester Range LGB 1C	130									1	2	46	5442
LL# 3240 Chester Range Buoy 2C	130												
LL# 3210 Marcus Hook Range LB 9M	129	63	1724	16	342	3	193	1	1	24	248	38	237
LL# 3180 Marcus Hook Anchorage Buoy B	127									4	151	4	28
LL# 3160 Marcus Hook Range LB 6M	125	72	1468	22	660	36	174	17	96	31	1671	15	211
LL# 3130 Marcus Hook Range LBB 2M	123	21	688	17	513	40	3512	35	1335	9	112	6	54
LL# 3105 Bellevue Range Buoy 4B	120	7	33	14	157	8	77	20	73			4	108
LL# 3045 Bellevue Range LB 2B	118									1	13		
LL# 3065 Cherry Is. Flats E Channel B 4	118	22	955	20	608	5	43	19	234			1	1
LL# 3030 Cherry Island Range Red 4C	116	25	1743	33	1375	3	54	6	33	5	40	3	13
LL# 2995 Cherry Is. Range Buoy 3C	112	14	78	27	439	3	10	2	17	5	17		
LL# 2960 New Castle Flats Buoy 29	108			1	17					8	111		
LL# 2945 Deepwater Point Range LB 4D	105	1	22	6	148	1	15	1	6	9	73	1	1
LL# 2820 Bulkhead Shoal Channel B 10	99			1	3			2	28	2	28		
LL# 2835 New Castle Range Buoy 7N	99			4	47	1	2			4	28	1	16
LL# 2725 New Castle Range Buoy 2N	93			9	141	6	157	3	16	3	34	10	139
LL# 2630 Artificial Is Anchorage Buoy B	89			7	65	9	492	2	2			1	3
LL# 2515 Baker Range Buoy 3B	83	1	2	16	109	3	29	3	36	3	27	1	2
LL# 2470 Liston Range LB 8L	77			4	32					3	23	2	53
LL# 2455 Liston Range Buoy 4L	70	3	95	5	140	1	5	5	27	3	27	3	41
LL# 2235 Blake Channel Buoy 1	41	3	15					1	7				
LL# 1700 Maurice River Entrance LB 1	30												
LL# 2230 Joe Flogger Shoal Jct Buoy J	29												
LL# 2220 Channel Crossing Buoy 1	28							1	1				
LL# 2195 Tanker Anchorage LB D	27	1	20					3	16				
LL# 2200 Tanker Anchorage Buoy E	25												
LL# 1570 DE Bay Main Channel LBB 16	23							1	1				
LL# 2190 Tanker Anchorage Buoy C	21	1	20					3	13				
LL# 1565 DE Bay Main Channel LB 14	19												
LL# 2185 Tanker Anchorage LB B	19							1	3				
LL# 2210 Tanker Anchorage Buoy G	18												
Shark Array 2B	18												
LL# 1550 DE Bay Main Channel LBB 12	17												

Table 2 continued.

Acoustic tag Fork length (mm) Life stage Date tagged Period of detection Location[1]	km[2]	A100 747 subadult 7/15/09 7/15-11/15/09 No. Days	No. Detects	A101 673 subadult 8/18/09 8/18-12/15/09 No. Days	No. Detects	A102 947 subadult 8/18/09 8/18-10/9/09 No. Days	No. Detects	A103 754 subadult 8/25/09 8/25-10/28/09 No. Days	No. Detects	A104 485 subadult 9/1/09 9/2/09-1/14/10 No. Days	No. Detects	A105 502 subadult 9/1/09 9/1/09-1/14/10 No. Days	No. Detects
Shark Array 3B	16												
LL# 1540 DE Bay Main Channel LB 10	13												
LL# 95 Hereford Inlet LWB H	13												
Shark Array 4B	13												
LL# 2180 Tanker Anchorage Appr LB A	11												
LL# 1660 Cape May W Ent Approach LB 5	8	2	2										
LL# 1665 Cape May Canal W Ent App LB 8	7												
LL# 1650 Cape May W Ent Approach LB 2	6	2	22										
Shark Array 7B	5							2	5				
LL# 160 McCrie Shoal LGB 2MS	4												
LL# 1515 DE Bay Entrance Channel LB 8	1							1	6				
LL# 1525 South Shoal Lump Buoy 8A	1	1	1										
LL# 1483 DE Bay Entrance Junction LB DF	0												
LL# 1485 DE Bay Approach LWB CH	0												
LL# 1495 Hen and Chickens Shoal LB 3HC	0												
LL# 1505 DE Bay Entrance Channel LGB 5	0							3	22				
LL# 190 Hen and Chickens Shoal LGB 1HC	0												
LL# 220 Great Gull Bank LB 4	0												
LL# 240 Ocean City Inlet LBB 2	0												
LL# 4360 Indian River Inlet LGB 1	0												
LL# 4365 Indian River Inlet LGB 2	0												

[1]Location - aid to navigation name and light list (LL) number from USCG, 2007
[2]River km based on DRBC, 1969

Table 2. Continued.

Acoustic tag		A106		A107		A108		A110		A111		A113	
Fork length (mm)		505		524		545		651		718		843	
Life stage		subadult		subadult		subadult		subadult		subadult		subadult	
Date tagged		9/1/09		9/1/09		9/1/09		9/1/09		9/1/09		9/24/09	
Period of detection		9/1-10/4/09		9/1-12/2/09		9/1-12/18/09		9/1-11/15/09		9/2-10/17/09		9/24-10/27/09	
Location[1]	km[2]	No. Days	No. Detects	No. Days	No. Detects	No. Days	No. Detects	No. Days	No. Detects	No. Days	No. Detects	No. Days	No. Detects
LL# 4120 Upper DE River CB 66	199												
LL# 3920 Upper DE River CLB 36	186												
LL# 3775 Upper DE River CLB 18	176												
LL# 3605 DE River LB 50	163												
LL# 3565 Horseshoe Bend LB 39	154												
LL# 3405 Elbow LBB 44	148											2	29
LL# 3395 Mantua Creek Anchorage Buoy B	147												
LL# 3380 Mifflin Range LB 1F	144	7	223									1	3
LL# 3315 Tinicum Island Range LB 5T	141	27	1127			2	36	1	10			2	175
LL# 3270 Tinicum Island Range LB 2T	135					1	7						
LL# 3255 Chester Range LB 6C	134	6	69	2	3	2	4	4	46			2	9
LL# 3215 Chester Range LGB 1C	130					1	43						
LL# 3240 Chester Range Buoy 2C	130												
LL# 3210 Marcus Hook Range LB 9M	129	4	26	3	58	4	37	18	201	1	44	3	40
LL# 3180 Marcus Hook Anchorage Buoy B	127					2	42						
LL# 3160 Marcus Hook Range LB 6M	125	2	15	8	222	23	206	39	1856	4	19	5	86
LL# 3130 Marcus Hook Range LBB 2M	123	1	5	5	55	55	2605	40	1807	11	187	6	299
LL# 3105 Bellevue Range Buoy 4B	120			5	24	19	186	38	385	18	96	6	71
LL# 3045 Bellevue Range LB 2B	118									26	2923		
LL# 3065 Cherry Is. Flats E Channel B 4	118	1	4	6	336	29	589	37	1253			5	273
LL# 3030 Cherry Island Range Red 4C	116	1	9	7	103	26	367	19	292	24	280	5	134
LL# 2995 Cherry Is. Range Buoy 3C	112	1	11	13	326	11	67	13	96	8	97	2	27
LL# 2960 New Castle Flats Buoy 29	108					5	118						
LL# 2945 Deepwater Point Range LB 4D	105	1	7			6	27	2	50	2	27	1	8
LL# 2820 Bulkhead Shoal Channel B 10	99							2	43				
LL# 2835 New Castle Range Buoy 7N	99	2	84			4	46	1	9	1	21	1	12
LL# 2725 New Castle Range Buoy 2N	93					2	6	1	1			1	3
LL# 2630 Artificial Is Anchorage Buoy B	89	1	1			2	2	2	2			3	134
LL# 2515 Baker Range Buoy 3B	83					4	105	5	71	1	5	2	197
LL# 2470 Liston Range LB 8L	77					4	22	4	24				
LL# 2455 Liston Range Buoy 4L	70					2	4	4	26	1	42		
LL# 2235 Blake Channel Buoy 1	41					2	14	2	10				
LL# 1700 Maurice River Entrance LB 1	30									2	4		
LL# 2230 Joe Flogger Shoal Jct Buoy J	29											1	2
LL# 2220 Channel Crossing Buoy 1	28											1	5
LL# 2195 Tanker Anchorage LB D	27					1	6					2	17
LL# 2200 Tanker Anchorage Buoy E	25											2	5
LL# 1570 DE Bay Main Channel LBB 16	23												
LL# 2190 Tanker Anchorage Buoy C	21											2	10
LL# 1565 DE Bay Main Channel LB 14	19												
LL# 2185 Tanker Anchorage LB B	19												
LL# 2210 Tanker Anchorage Buoy G	18											1	1
Shark Array 2B	18												
LL# 1550 DE Bay Main Channel LBB 12	17												

Table 2. Continued.

Acoustic tag Fork length (mm) Life stage Date tagged Period of detection		A106 505 subadult 9/1/09 9/1-10/4/09		A107 524 subadult 9/1/09 9/1-12/2/09		A108 545 subadult 9/1/09 9/1-12/18/09		A110 651 subadult 9/1/09 9/1-11/15/09		A111 718 subadult 9/1/09 9/2-10/17/09		A113 843 subadult 9/24/09 9/24-10/27/09	
Location[1]	km^2	No. Days	No. Detects	No. Days	No. Detects	No. Days	No. Detects	No. Days	No. Detects	No. Days	No. Detects	No. Days	No. Detects
Shark Array 3B	16												
LL# 1540 DE Bay Main Channel LB 10	13												
LL# 95 Hereford Inlet LWB H	13												
Shark Array 4B	13							1	1				
LL# 2180 Tanker Anchorage Appr LB A	11												
LL# 1660 Cape May W Ent Approach LB 5	8												
LL# 1665 Cape May Canal W Ent App LB 8	7									1	2		
LL# 1650 Cape May W Ent Approach LB 2	6												
Shark Array 7B	5							2	15				
LL# 160 McCrie Shoal LGB 2MS	4									1	6		
LL# 1515 DE Bay Entrance Channel LB 8	1											1	6
LL# 1525 South Shoal Lump Buoy 8A	1												
LL# 1483 DE Bay Entrance Junction LB DF	0												
LL# 1485 DE Bay Approach LWB CH	0											1	7
LL# 1495 Hen and Chickens Shoal LB 3HC	0											1	20
LL# 1505 DE Bay Entrance Channel LGB 5	0					1	7	1	1				
LL# 190 Hen and Chickens Shoal LGB 1HC	0												
LL# 220 Great Gull Bank LB 4	0												

Table 2. Continued.

Acoustic tag		A115		A114		A116		A112		A117		A118	
Fork length (mm)		967		913		970		768		523		566	
Life stage		subadult		subadult		subadult		subadult		subadult		subadult	
Date tagged		9/24/09		9/24/09		9/24/09		9/24/09		10/1/09		10/1/09	
Period of detection		9/24-10/20/09		9/24-11/4/09		9/24-10/14/09		9/24-11/14/09		10/1/09-1/1/10		10/1-12/19/09	
Location[1]	km^2	No. Days	No. Detects	No. Days	No. Detects	No. Days	No. Detects	No. Days	No. Detects	No. Days	No. Detects	No. Days	No. Detects
LL# 4120 Upper DE River CB 66	199												
LL# 3920 Upper DE River CLB 36	186												
LL# 3775 Upper DE River CLB 18	176												
LL# 3605 DE River LB 50	163												
LL# 3565 Horseshoe Bend LB 39	154												
LL# 3405 Elbow LBB 44	148									3	28		
LL# 3395 Mantua Creek Anchorage Buoy B	147												
LL# 3380 Mifflin Range LB 1F	144									3	21		
LL# 3315 Tinicum Island Range LB 5T	141									4	122		
LL# 3270 Tinicum Island Range LB 2T	135									3	71	2	349
LL# 3255 Chester Range LB 6C	134	1	4	1	3					3	35	4	97
LL# 3215 Chester Range LGB 1C	130									15	133	5	69
LL# 3240 Chester Range Buoy 2C	130												
LL# 3210 Marcus Hook Range LB 9M	129	19	457	11	194	3	75	11	169	21	612	16	447
LL# 3180 Marcus Hook Anchorage Buoy B	127									20	3648	5	119
LL# 3160 Marcus Hook Range LB 6M	125	20	477	21	891	5	106	11	163	21	312	24	503
LL# 3130 Marcus Hook Range LBB 2M	123	4	123	20	1697	3	110	1	57	27	1102	24	1970
LL# 3105 Bellevue Range Buoy 4B	120	1	2	9	62	3	15			2	39	6	20
LL# 3045 Bellevue Range LB 2B	118												
LL# 3065 Cherry Is. Flats E Channel B 4	118	2	20	4	12	4	120	1	10	2	35	7	153
LL# 3030 Cherry Island Range Red 4C	116	3	69	1	3	4	80	1	1	4	54	4	58
LL# 2995 Cherry Is. Range Buoy 3C	112	2	18	1	1	2	6	1	32	3	40	4	47
LL# 2960 New Castle Flats Buoy 29	108									4	26	3	11
LL# 2945 Deepwater Point Range LB 4D	105	1	5	1	25	1	3	1	4	1	7	3	32
LL# 2820 Bulkhead Shoal Channel B 10	99	1	2					1	31	3	20		
LL# 2835 New Castle Range Buoy 7N	99					1	12	2	20	3	49	3	81
LL# 2725 New Castle Range Buoy 2N	93			2	23	1	7	1	11	5	54	6	83
LL# 2630 Artificial Is Anchorage Buoy B	89	1	1					1	2	1	3	10	107
LL# 2515 Baker Range Buoy 3B	83	1	1			1	10	4	103	7	39	14	107
LL# 2470 Liston Range LB 8L	77									8	187	5	75
LL# 2455 Liston Range Buoy 4L	70			1	5	1	27	3	60	6	77	5	32
LL# 2235 Blake Channel Buoy 1	41												
LL# 1700 Maurice River Entrance LB 1	30												
LL# 2230 Joe Flogger Shoal Jct Buoy J	29												
LL# 2220 Channel Crossing Buoy 1	28												
LL# 2195 Tanker Anchorage LB D	27					1	12						
LL# 2200 Tanker Anchorage Buoy E	25												
LL# 1570 DE Bay Main Channel LBB 16	23							2	23				
LL# 2190 Tanker Anchorage Buoy C	21							2	8				
LL# 1565 DE Bay Main Channel LB 14	19	1	4										
LL# 2185 Tanker Anchorage LB B	19												
LL# 2210 Tanker Anchorage Buoy G	18			1	2								
Shark Array 2B	18					1	3						
LL# 1550 DE Bay Main Channel LBB 12	17	1	25										

Table 2. Continued.

Acoustic tag		A115		A114		A116		A112		A117		A118	
Fork length (mm)		967		913		970		768		523		566	
Life stage		subadult		subadult		subadult		subadult		subadult		subadult	
Date tagged		9/24/09		9/24/09		9/24/09		9/24/09		10/1/09		10/1/09	
Period of detection		9/24-10/20/09		9/24-11/4/09		9/24-10/14/09		9/24-11/14/09		10/1/09-1/1/10		10/1-12/19/09	
Location[1]	km[2]	No. Days	No. Detects	No. Days	No. Detects	No. Days	No. Detects	No. Days	No. Detects	No. Days	No. Detects	No. Days	No. Detects
Shark Array 3B	16					1	2						
LL# 1540 DE Bay Main Channel LB 10	13							1	82				
LL# 95 Hereford Inlet LWB H	13							1	2				
Shark Array 4B	13					1	2	1	4				
LL# 2180 Tanker Anchorage Appr LB A	11			1	11								
LL# 1660 Cape May W Ent Approach LB 5	8												
LL# 1665 Cape May Canal W Ent App LB 8	7												
LL# 1650 Cape May W Ent Approach LB 2	6												
Shark Array 7B	5												
LL# 160 McCrie Shoal LGB 2MS	4												
LL# 1515 DE Bay Entrance Channel LB 8	1												
LL# 1525 South Shoal Lump Buoy 8A	1												
LL# 1483 DE Bay Entrance Junction LB DF	0			1	18								
LL# 1485 DE Bay Approach LWB CH	0												
LL# 1495 Hen and Chickens Shoal LB 3HC	0	2	67					1	2				
LL# 1505 DE Bay Entrance Channel LGB 5	0	1	7			1	20						
LL# 190 Hen and Chickens Shoal LGB 1HC	0			1	7			1	1				
LL# 220 Great Gull Bank LB 4	0			1	4								
LL# 240 Ocean City Inlet LBB 2	0							1	2				
LL# 4360 Indian River Inlet LGB 1	0					3	15	1	11				
LL# 4365 Indian River Inlet LGB 2	0					2	22						

Table 2. Continued.

Acoustic tag		A119		A120		A121		A125		A122		A123	
Fork length (mm)		738		278		289		315		284		304	
Life stage		subadult		YOY		YOY		YOY		YOY		YOY	
Date tagged		10/6/09		10/29/09		11/4/09		11/24/09		11/24/09		11/24/09	
Period of detection		10/7-11/28/09		10/29-12/27/09		11/5/09-1/14/10		11/24/09-1/19/10		11/24/09-2/4/10		11/24/09-2/4/10	
Location[1]	km^2	No. Days	No. Detects	No. Days	No. Detects	No. Days	No. Detects	No. Days	No. Detects	No. Days	No. Detects	No. Days	No. Detects
LL# 4120 Upper DE River CB 66	199											5	120
LL# 3920 Upper DE River CLB 36	186									8	93	4	202
LL# 3775 Upper DE River CLB 18	176							3	41			2	10
LL# 3605 DE River LB 50	163							1	1			1	3
LL# 3565 Horseshoe Bend LB 39	154											2	27
LL# 3405 Elbow LBB 44	148							2	10	2	6	5	34
LL# 3395 Mantua Creek Anchorage Buoy B	147									1	2	4	35
LL# 3380 Mifflin Range LB 1F	144											4	36
LL# 3315 Tinicum Island Range LB 5T	141					3	25	2	2	1	1	3	48
LL# 3270 Tinicum Island Range LB 2T	135					2	2	4	10			3	98
LL# 3255 Chester Range LB 6C	134							2	6			3	13
LL# 3215 Chester Range LGB 1C	130					3	21			1	1	14	187
LL# 3240 Chester Range Buoy 2C	130			1	4								
LL# 3210 Marcus Hook Range LB 9M	129	1	17	2	3	2	2			1	2	22	362
LL# 3180 Marcus Hook Anchorage Buoy B	127			11	200	5	84	4	9	2	8	24	635
LL# 3160 Marcus Hook Range LB 6M	125	2	13	3	34	2	6	2	20			14	238
LL# 3130 Marcus Hook Range LBB 2M	123	1	13	6	272							5	64
LL# 3105 Bellevue Range Buoy 4B	120	2	20									2	126
LL# 3045 Bellevue Range LB 2B	118												
LL# 3065 Cherry Is. Flats E Channel B 4	118	1	1									1	1
LL# 3030 Cherry Island Range Red 4C	116	7	343			3	3	2	13			1	2
LL# 2995 Cherry Is. Range Buoy 3C	112	7	278			1	1					1	1
LL# 2960 New Castle Flats Buoy 29	108												
LL# 2945 Deepwater Point Range LB 4D	105	6	185			2	2						
LL# 2820 Bulkhead Shoal Channel B 10	99	1	29										
LL# 2835 New Castle Range Buoy 7N	99	1	6										
LL# 2725 New Castle Range Buoy 2N	93	3	152										
LL# 2630 Artificial Is Anchorage Buoy B	89	4	52										
LL# 2515 Baker Range Buoy 3B	83	16	108										
LL# 2470 Liston Range LB 8L	77	2	19										
LL# 2455 Liston Range Buoy 4L	70	5	57										
LL# 2235 Blake Channel Buoy 1	41												
LL# 1700 Maurice River Entrance LB 1	30												
LL# 2230 Joe Flogger Shoal Jct Buoy J	29												
LL# 2220 Channel Crossing Buoy 1	28												
LL# 2195 Tanker Anchorage LB D	27												
LL# 2200 Tanker Anchorage Buoy E	25												
LL# 1570 DE Bay Main Channel LBB 16	23												
LL# 2190 Tanker Anchorage Buoy C	21												
LL# 1565 DE Bay Main Channel LB 14	19												
LL# 2185 Tanker Anchorage LB B	19												
LL# 2210 Tanker Anchorage Buoy G	18												
Shark Array 2B	18												
LL# 1550 DE Bay Main Channel LBB 12	17												

Table 2. Continued.

Acoustic tag		A119		A120		A121		A125		A122		A123	
Fork length (mm)		738		278		289		315		284		304	
Life stage		subadult		YOY		YOY		YOY		YOY		YOY	
Date tagged		10/6/09		10/29/09		11/4/09		11/24/09		11/24/09		11/24/09	
Period of detection		10/7-11/28/09		10/29-12/27/09		11/5/09-1/14/10		11/24/09-1/19/10		11/24/09-2/4/10		11/24/09-2/4/10	
Location[1]	km^2	No. Days	No. Detects	No. Days	No. Detects	No. Days	No. Detects	No. Days	No. Detects	No. Days	No. Detects	No. Days	No. Detects
Shark Array 3B	16												
LL# 1540 DE Bay Main Channel LB 10	13												
LL# 95 Hereford Inlet LWB H	13												
Shark Array 4B	13												
LL# 2180 Tanker Anchorage Appr LB A	11												
LL# 1660 Cape May W Ent Approach LB 5	8												
LL# 1665 Cape May Canal W Ent App LB 8	7												
LL# 1650 Cape May W Ent Approach LB 2	6												
Shark Array 7B	5												
LL# 160 McCrie Shoal LGB 2MS	4												
LL# 1515 DE Bay Entrance Channel LB 8	1												
LL# 1525 South Shoal Lump Buoy 8A	1												
LL# 1483 DE Bay Entrance Junction LB DF	0												
LL# 1485 DE Bay Approach LWB CH	0												
LL# 1495 Hen and Chickens Shoal LB 3HC	0												
LL# 1505 DE Bay Entrance Channel LGB 5	0												
LL# 190 Hen and Chickens Shoal LGB 1HC	0												
LL# 220 Great Gull Bank LB 4	0												
LL# 240 Ocean City Inlet LBB 2	0												
LL# 4360 Indian River Inlet LGB 1	0												
LL# 4365 Indian River Inlet LGB 2	0												

Table 2. Continued.

Acoustic tag Fork length (mm) Life stage Date tagged Period of detection		A124 315 YOY 11/24/09 11/24/09-1/14/10		**Total Subadults**		**Total Young of the Year**	
Location[1]	km^2	No. Days	No. Detects	**No. Days**	**No. Detects**	**No. Detects**	**No. Days**
LL# 4120 Upper DE River CB 66	199			**0**	**0**	**5**	**120**
LL# 3920 Upper DE River CLB 36	186			**0**	**0**	**12**	**295**
LL# 3775 Upper DE River CLB 18	176			**0**	**0**	**5**	**51**
LL# 3605 DE River LB 50	163			**0**	**0**	**2**	**4**
LL# 3565 Horseshoe Bend LB 39	154			**0**	**0**	**2**	**27**
LL# 3405 Elbow LBB 44	148			**5**	**57**	**9**	**50**
LL# 3395 Mantua Creek Anchorage Buoy B	147			**0**	**0**	**5**	**37**
LL# 3380 Mifflin Range LB 1F	144			**13**	**255**	**4**	**36**
LL# 3315 Tinicum Island Range LB 5T	141			**45**	**1602**	**9**	**76**
LL# 3270 Tinicum Island Range LB 2T	135			**8**	**479**	**9**	**110**
LL# 3255 Chester Range LB 6C	134	3	47	**63**	**850**	**8**	**66**
LL# 3215 Chester Range LGB 1C	130	18	121	**68**	**5689**	**36**	**330**
LL# 3240 Chester Range Buoy 2C	130			**0**	**0**	**1**	**4**
LL# 3210 Marcus Hook Range LB 9M	129	24	646	**260**	**5122**	**51**	**1015**
LL# 3180 Marcus Hook Anchorage Buoy B	127	22	916	**35**	**3988**	**68**	**1852**
LL# 3160 Marcus Hook Range LB 6M	125	13	151	**378**	**9149**	**34**	**449**
LL# 3130 Marcus Hook Range LBB 2M	123	4	43	**326**	**16244**	**15**	**379**
LL# 3105 Bellevue Range Buoy 4B	120			**162**	**1368**	**2**	**126**
LL# 3045 Bellevue Range LB 2B	118			**27**	**2936**	**0**	**0**
LL# 3065 Cherry Is. Flats E Channel B 4	118			**166**	**4647**	**1**	**1**
LL# 3030 Cherry Island Range Red 4C	116			**181**	**5051**	**6**	**18**
LL# 2995 Cherry Is. Range Buoy 3C	112			**119**	**1607**	**2**	**2**
LL# 2960 New Castle Flats Buoy 29	108			**21**	**283**	**0**	**0**
LL# 2945 Deepwater Point Range LB 4D	105			**45**	**645**	**2**	**2**
LL# 2820 Bulkhead Shoal Channel B 10	99			**13**	**184**	**0**	**0**
LL# 2835 New Castle Range Buoy 7N	99			**29**	**433**	**0**	**0**
LL# 2725 New Castle Range Buoy 2N	93			**53**	**827**	**0**	**0**
LL# 2630 Artificial Is Anchorage Buoy B	89			**44**	**866**	**0**	**0**
LL# 2515 Baker Range Buoy 3B	83			**82**	**951**	**0**	**0**
LL# 2470 Liston Range LB 8L	77			**32**	**435**	**0**	**0**
LL# 2455 Liston Range Buoy 4L	70			**48**	**665**	**0**	**0**
LL# 2235 Blake Channel Buoy 1	41			**8**	**46**	**0**	**0**
LL# 1700 Maurice River Entrance LB 1	30			**2**	**4**	**0**	**0**
LL# 2230 Joe Flogger Shoal Jct Buoy J	29			**1**	**2**	**0**	**0**
LL# 2220 Channel Crossing Buoy 1	28			**2**	**6**	**0**	**0**
LL# 2195 Tanker Anchorage LB D	27			**8**	**71**	**0**	**0**
LL# 2200 Tanker Anchorage Buoy E	25			**2**	**5**	**0**	**0**
LL# 1570 DE Bay Main Channel LBB 16	23			**3**	**24**	**0**	**0**
LL# 2190 Tanker Anchorage Buoy C	21			**8**	**51**	**0**	**0**
LL# 1565 DE Bay Main Channel LB 14	19			**1**	**4**	**0**	**0**
LL# 2185 Tanker Anchorage LB B	19			**1**	**3**	**0**	**0**
LL# 2210 Tanker Anchorage Buoy G	18			**2**	**3**	**0**	**0**
Shark Array 2B	18			**1**	**3**	**0**	**0**
LL# 1550 DE Bay Main Channel LBB 12	17			**1**	**25**	**0**	**0**

Table 2. Continued.

Acoustic tag Fork length (mm) Life stage Date tagged Period of detection		A124 315 YOY 11/24/09 11/24/09-1/14/10		**Total Subadults**		**Total Young of the Year**	
Location[1]	km^2	No. Days	No. Detects	**No. Days**	**No. Detects**	**No. Detects**	**No. Days**
Shark Array 3B	16			**1**	**2**	**0**	**0**
LL# 1540 DE Bay Main Channel LB 10	13			**1**	**82**	**0**	**0**
LL# 95 Hereford Inlet LWB H	13			**1**	**2**	**0**	**0**
Shark Array 4B	13			**3**	**7**	**0**	**0**
LL# 2180 Tanker Anchorage Appr LB A	11			**1**	**11**	**0**	**0**
LL# 1660 Cape May W Ent Approach LB 5	8			**2**	**2**	**0**	**0**
LL# 1665 Cape May Canal W Ent App LB 8	7			**1**	**2**	**0**	**0**
LL# 1650 Cape May W Ent Approach LB 2	6			**2**	**22**	**0**	**0**
Shark Array 7B	5			**4**	**20**	**0**	**0**
LL# 160 McCrie Shoal LGB 2MS	4			**1**	**6**	**0**	**0**
LL# 1515 DE Bay Entrance Channel LB 8	1			**2**	**12**	**0**	**0**
LL# 1525 South Shoal Lump Buoy 8A	1			**1**	**1**	**0**	**0**
LL# 1483 DE Bay Entrance Junction LB DF	0			**1**	**18**	**0**	**0**
LL# 1485 DE Bay Approach LWB CH	0			**1**	**7**	**0**	**0**
LL# 1495 Hen and Chickens Shoal LB 3HC	0			**4**	**89**	**0**	**0**
LL# 1505 DE Bay Entrance Channel LGB 5	0			**7**	**57**	**0**	**0**
LL# 190 Hen and Chickens Shoal LGB 1HC	0			**2**	**8**	**0**	**0**
LL# 220 Great Gull Bank LB 4	0			**1**	**4**	**0**	**0**
LL# 240 Ocean City Inlet LBB 2	0			**2**	**5**	**0**	**0**
LL# 4360 Indian River Inlet LGB 1	0			**7**	**52**	**0**	**0**
LL# 4365 Indian River Inlet LGB 2	0			**4**	**50**	**0**	**0**

Table 3. Shortnose sturgeon collected in the tidal Delaware River, June 2008-October 2009.

Date	Location	Gear[1]	Depth (m)	Total length (mm)	Fork length (mm)	Weight (g)	Water temp. (ºC)	Dissolved oxygen (mg/L)	Specific conductance (µS/cm)	Salinity (‰)	Acoustic Tag	Acoustic Tag Type
6/3/2008	Perriwig Channel	C	8.5	542	471	760	22.7	---	102	0.1	A126	V13-P-1H
11/4/2008	Upper Cherry Isl. Flats	A	7.2	635	532	1000	12.8	8.4	2881	1.6	A127	V13-P-1H
6/3/2009	Duck Island Range	C	9.0	547	496	1130	19.5	8.8	137	0.1	A128	V13-P-1H
7/14/2009	Upper Cherry Isl. Flats	C	7.3	650	557	1360	24.5	6.6	232	0.1	A129	V-16-1L
7/15/2009	Upper Cherry Isl. Flats	C	6.6	651	572	1860	24.7	7.2	236	0.1	A130	V13-1H
7/28/2009	Upper Cherry Isl. Flats	C	7.9	630	542	1760	25.8	5.8	410	0.2	A131	V9-2L
8/18/2009	Marcus Hook anchorage	C	13.9	688	591	2480	26.4	7.4	208	0.1	---	---
9/1/2009	Marcus Hook anchorage	C	13.9	657	578	1740	24.8	6.8	221	0.1	---	---
9/1/2009	Marcus Hook anchorage	C	13.9	720	627	2360	24.8	6.8	221	0.1	---	---
9/1/2009	Marcus Hook anchorage	C	13.7	796	702	3480	24.8	6.8	221	0.1	---	---
10/6/2009	Marcus Hook anchorage	B+B	14.6	438	381	410	18.9	6.7	331	0.2	---	---
10/12/2009	Marcus Hook anchorage	C	12.8	707	640	2460	17.9	7.3	357	0.2	---	---
10/21/2009	Upper Cherry Isl. Flats	C	7.6	696	589	1900	13.9	8.2	1517	0.8	---	---
10/21/2009	Upper Cherry Isl. Flats	C	7.6	745	648	2700	13.9	8.2	1517	0.8	---	---

[1]Gear
A = 100- x 1.8-m, 33 m panels of 2.5-, 5.1- and 7.6 cm mesh
B = 66- x 1.8-m, 33 m panels of 5.1 and 7.6 cm mesh
C = 100- x 1.8-m, 12.7 cm mesh

Table 4. Occurrence of acoustically tagged shortnose sturgeon at telemetry receivers in the Delaware Estuary.

Acoustic tag Fork length (mm) Life stage Date tagged Period of detection		A126 471 juvenile 6/3/08 6/3-12/2/08		A127 532 probable juvenile 11/4/08 11/4/08-5/20/09		A128 496 juvenile 6/3/09 6/4-12/30/09		A129 557 probable juvenile 7/14/09 8/25-10/28/09		A130 572 recently matured 7/15/09 7/15/09-2/4/10		A131 542 probable juvenile 7/28/09 7/28-11/1/09		**Total**	
Location[1]	km[2]	No. Days	No. Detects	No. Days	No. Detects	No. Days	No. Detects	No. Days	No. Detects	No. Days	No. Detects	No. Days	No. Detects	**No. Days**	**No. Detects**
LL# 4330 Upper DE River 103	211	3	801	1	52							10	591	**14**	**1444**
LL# 4275 Upper DE River CB 92	207	7	345	3	362					3	93	4	89	**17**	**889**
LL# 4170 Upper DE River Channel LB 76	201					1	103	3	40			1	7	**5**	**150**
LL# 4120 Upper DE River CB 66	199	44	5556	3	95	1	30	5	68	62	10632	2	17	**117**	**16398**
LL# 4070 Upper DE River Channel LB 58	195			2	148	1	33	13	284			5	35	**21**	**500**
LL# 3990 Upper DE River Channel LB 48	190			2	160	1	35	39	616			2	15	**44**	**826**
LL# 3920 Upper DE River CLB 36	186	28	1741	3	47	2	154	30	1555	28	687	2	7	**93**	**4191**
LL# 3775 Upper DE River CLB 18	176	24	1577	2	18	2	53	8	48	13	125	1	4	**50**	**1825**
LL# 3680 Upper DE River Channel LB 8	170			2	23	1	22							**3**	**45**
LL# 3645 Delaware River Channel LB 55	166			2	5	2	60	1	2					**5**	**67**
LL# 3605 DE River LB 50	163	3	23	2	43			4	69	1	3			**10**	**138**
LL# 3565 Horseshoe Bend LB 39	154			2	29	1	172	4	8	2	7			**9**	**216**
LL# 3405 Elbow LBB 44	148			2	7	1	14	1	7	6	165	4	12	**14**	**205**
LL# 3395 Mantua Creek Anchorage Buoy B	147									3	55			**3**	**55**
LL# 3380 Mifflin Range LB 1F	144			2	74	2	152	2	6	3	69			**9**	**301**
LL# 3315 Tinicum Island Range LB 5T	141			1	7	2	139	4	124	8	86	3	42	**18**	**398**
LL# 3300 Tinicum Island Spit Buoy 4T	136			2	14	2	76	1	1					**5**	**91**
LL# 3270 Tinicum Island Range LB 2T	135									3	30			**3**	**30**
LL# 3255 Chester Range LB 6C	134			1	28	2	134	4	5	5	60	4	40	**16**	**267**
LL# 3215 Chester Range LGB 1C	130							7	84	3	16			**10**	**100**
LL# 3210 Marcus Hook Range LB 9M	129			3	194			10	157	7	69			**20**	**420**
LL# 3180 Marcus Hook Anchorage Buoy B	127					16	265	12	208	3	27			**31**	**500**
LL# 3160 Marcus Hook Range LB 6M	125			20	781	80	6528	48	1109	9	173	3	19	**160**	**8610**
LL# 3130 Marcus Hook Range LBB 2M	123			32	3182	116	5548	69	1685	15	304	2	8	**234**	**10727**
LL# 3105 Bellevue Range Buoy 4B	120			36	710	72	564	57	858	21	196	2	2	**188**	**2330**
LL# 3065 Cherry Is. Flats E Channel B 4	118			8	216	119	6635	55	2065	49	862			**231**	**9778**
LL# 3030 Cherry Island Range Red 4C	116			43	2457	143	13734	38	811	77	3015	2	17	**303**	**20034**
LL# 2995 Cherry Is. Range Buoy 3C	112							16	199	77	1952	2	10	**95**	**2161**
LL# 2965 Cherry Island Range LBB 1C	110			2	73	15	529			2	19			**19**	**621**
LL# 2960 New Castle Flats Buoy 29	108					4	95	3	50	1	1			**8**	**146**

Table 4. Continued.

Acoustic tag Fork length (mm) Life stage Date tagged Period of detection		A126 471 juvenile 6/3/08 6/3-12/2/08		A127 532 probable juvenile 11/4/08 11/4/08-5/20/09		A128 496 juvenile 6/3/09 6/4-12/30/09		A129 557 probable juvenile 7/14/09 8/25-10/28/09		A130 572 recently matured 7/15/09 7/15/09-2/4/10		A131 542 probable juvenile 7/28/09 7/28-11/1/09		**Total**	
Location[1]	km[2]	No. Days	No. Detects	No. Days	No. Detects	No. Days	No. Detects	No. Days	No. Detects	No. Days	No. Detects	No. Days	No. Detects	**No. Days**	**No. Detects**
LL# 2945 Deepwater Point Range LB 4D	105			52	3329	5	232			9	187			**66**	**3748**
LL# 2820 Bulkhead Shoal Channel B 10	99			2	152	1	29			2	57			**5**	**238**
LL# 2835 New Castle Range Buoy 7N	99			31	3230	3	85							**34**	**3315**
LL# 2725 New Castle Range Buoy 2N	93			20	1484	5	121							**25**	**1605**
LL# 2630 Artificial Is Anchorage Buoy B	89					3	21							**3**	**21**
LL# 2515 Baker Range Buoy 3B	83			21	3011	12	130							**33**	**3141**
LL# 2470 Liston Range LB 8L	77					6	92							**6**	**92**

[1]Location - aid to navigation name and light list (LL) number from USCG, 2007
[2]River km based on DRBC, 1969

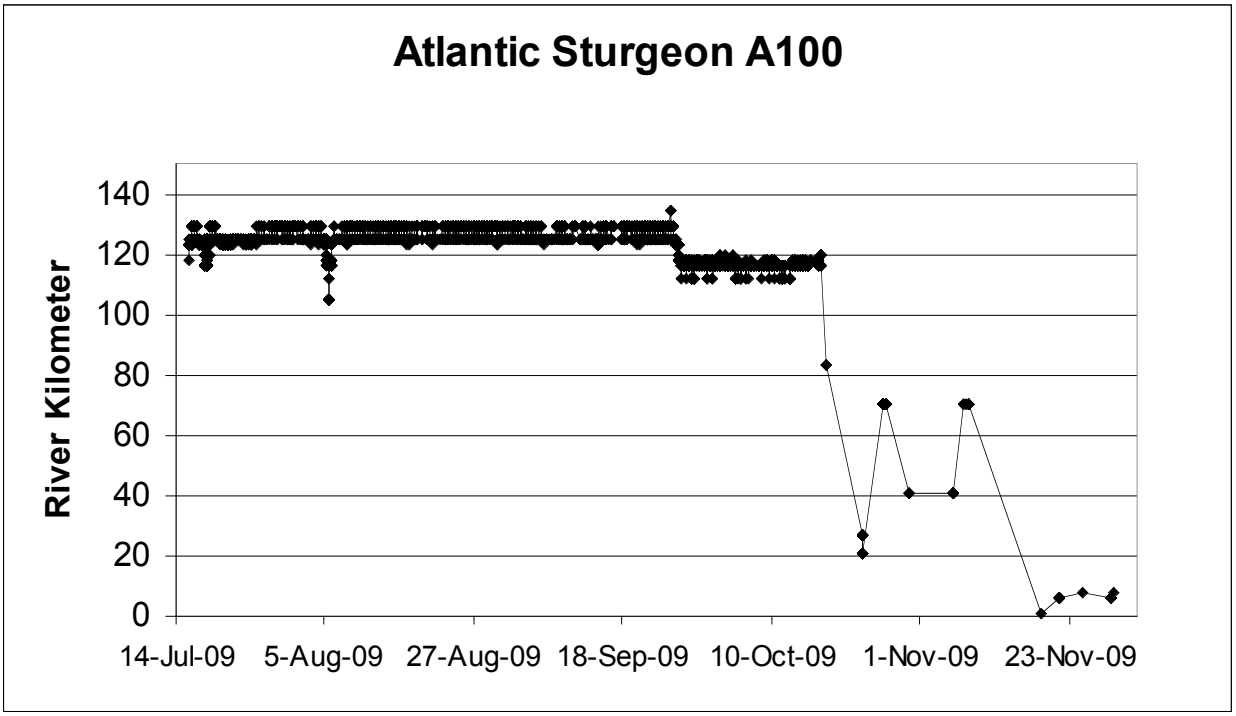

Figure A-1. Movements of Atlantic sturgeon tag A100 in the Delaware Estuary.

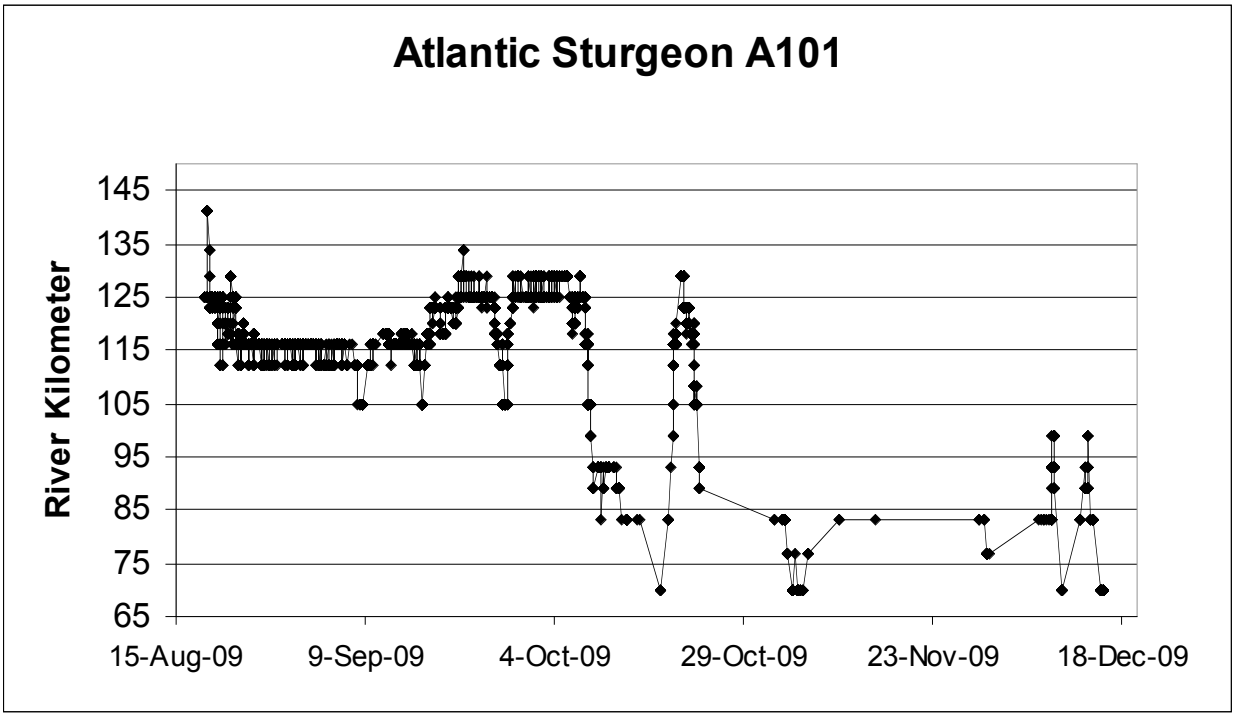

Figure A-2. Movements of Atlantic sturgeon tag A101 in the Delaware Estuary.

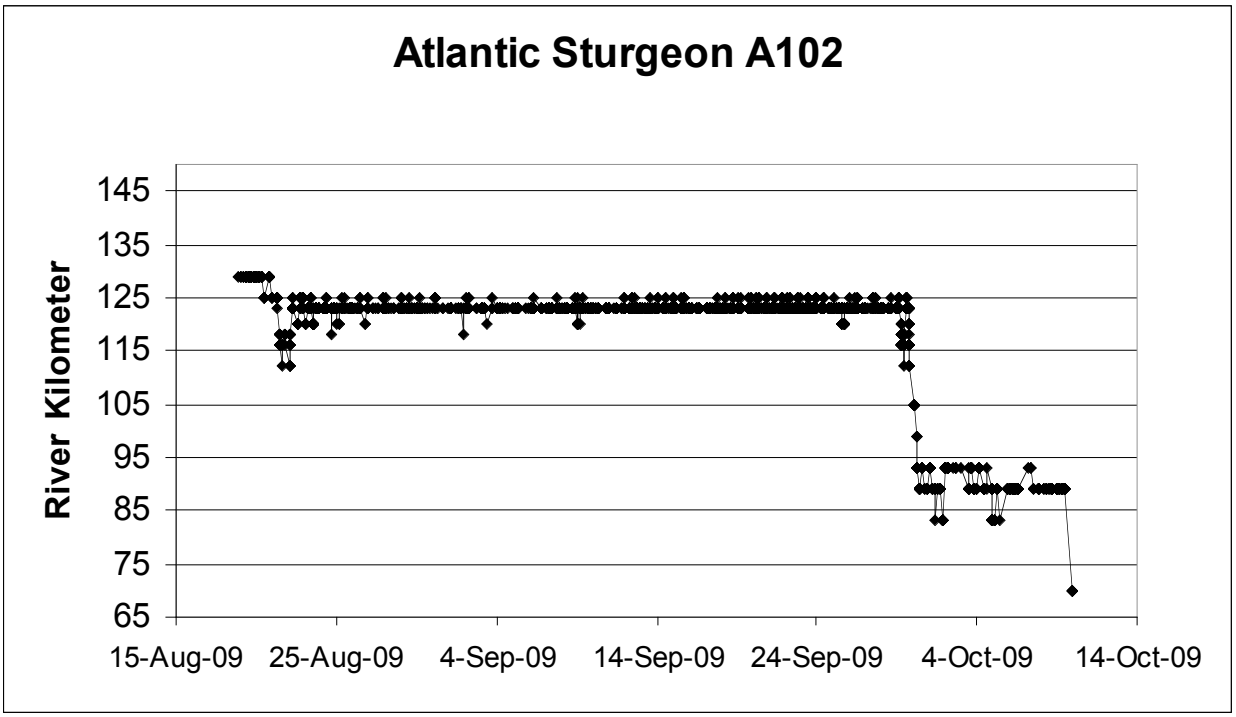

Figure A-3. Movements of Atlantic sturgeon tag A102 in the Delaware Estuary.

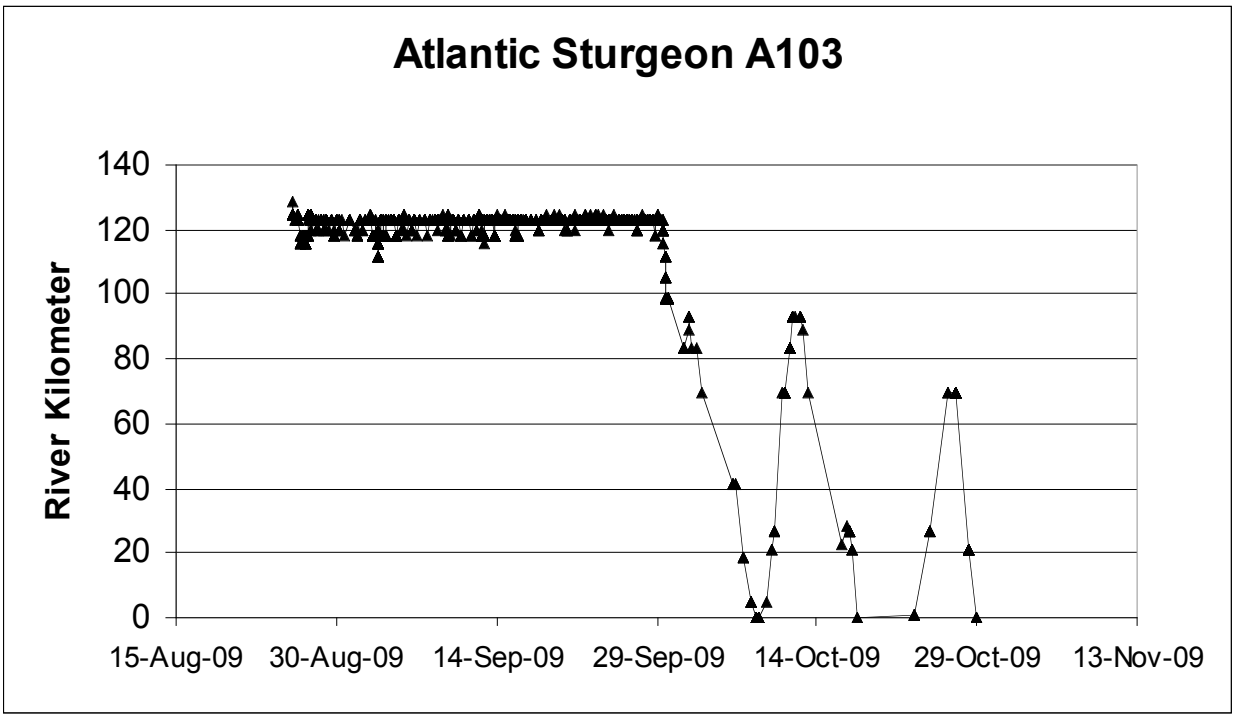

Figure A-4. Movements of Atlantic sturgeon tag A103 in the Delaware Estuary.

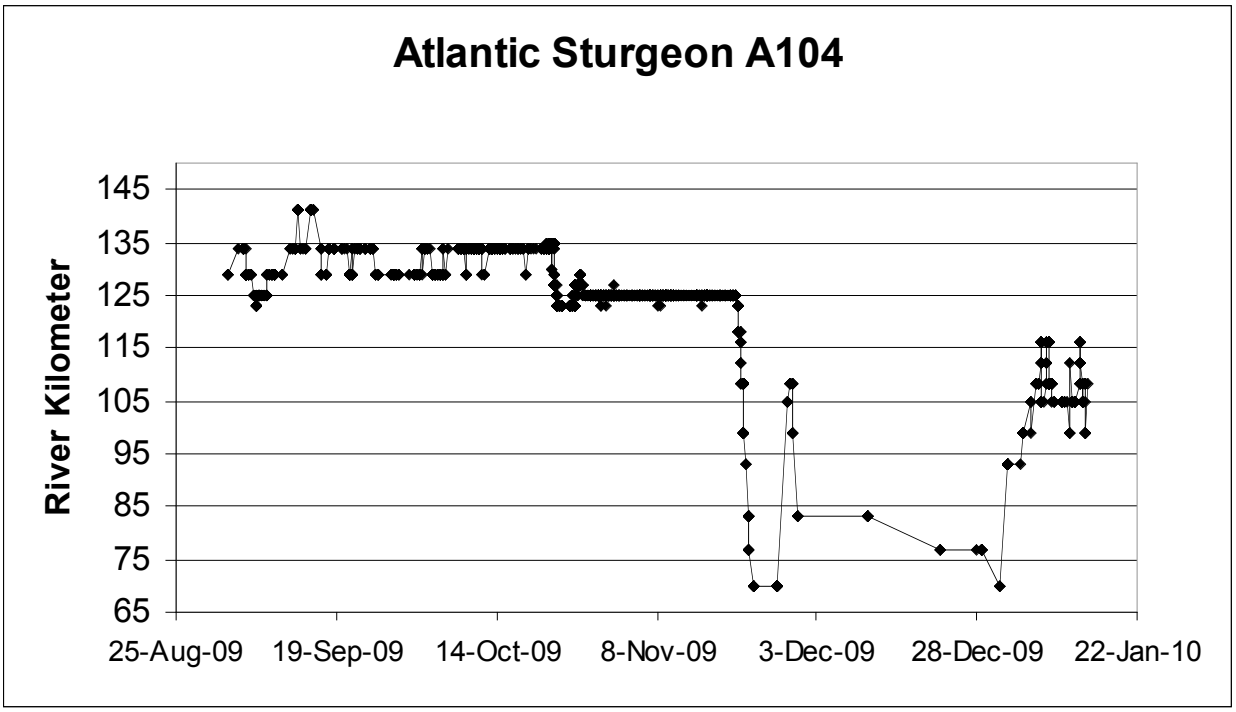

Figure A-5. Movements of Atlantic sturgeon tag A104 in the Delaware Estuary.

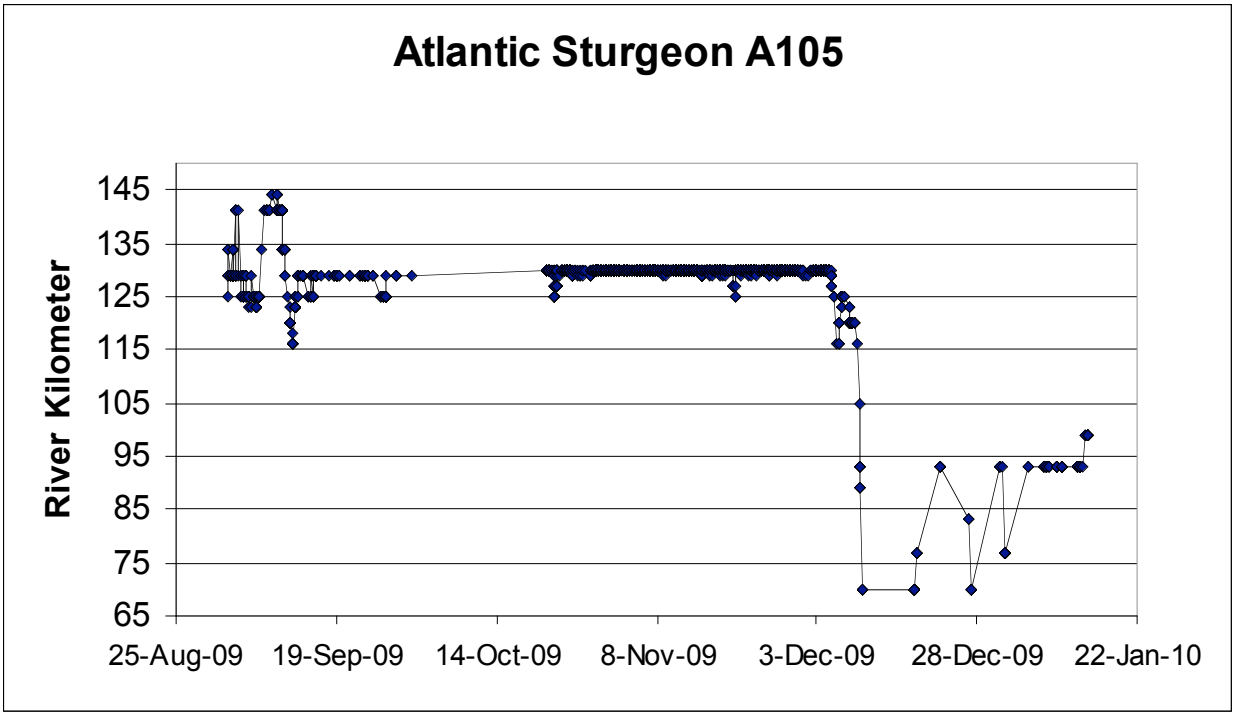

Figure A-6. Movements of Atlantic sturgeon tag A105 in the Delaware Estuary.

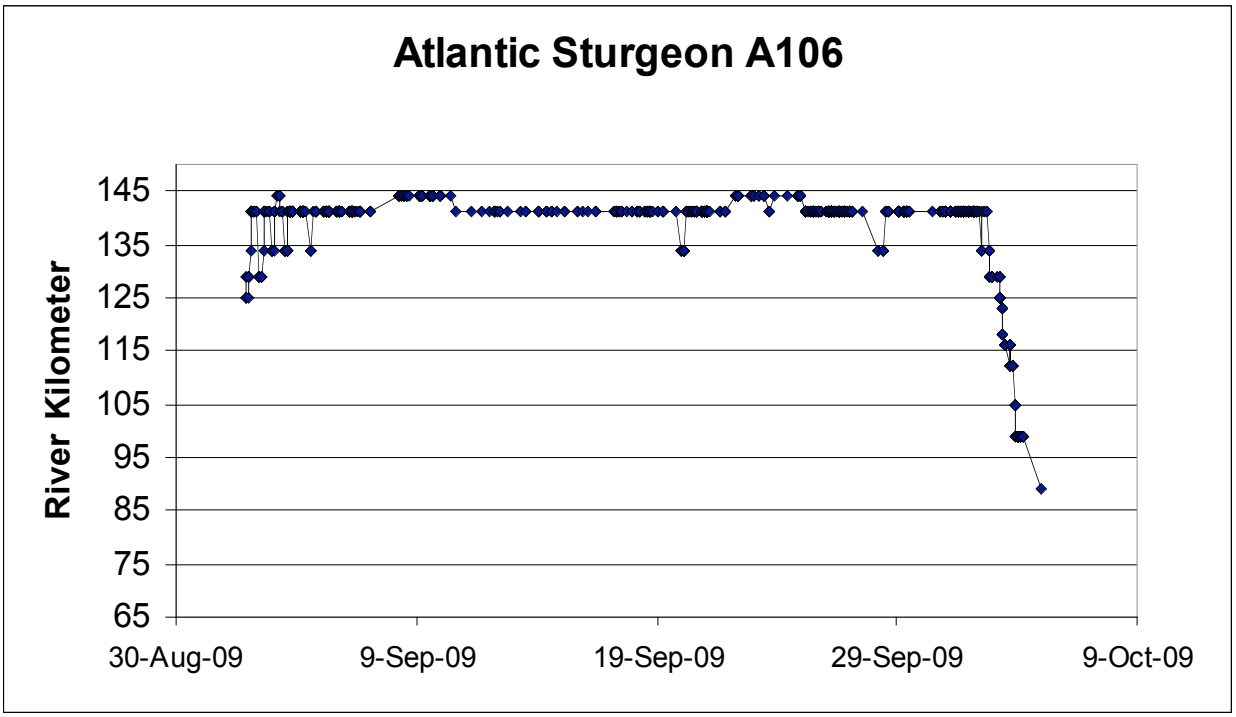

Figure A-7. Movements of Atlantic sturgeon tag A106 in the Delaware Estuary.

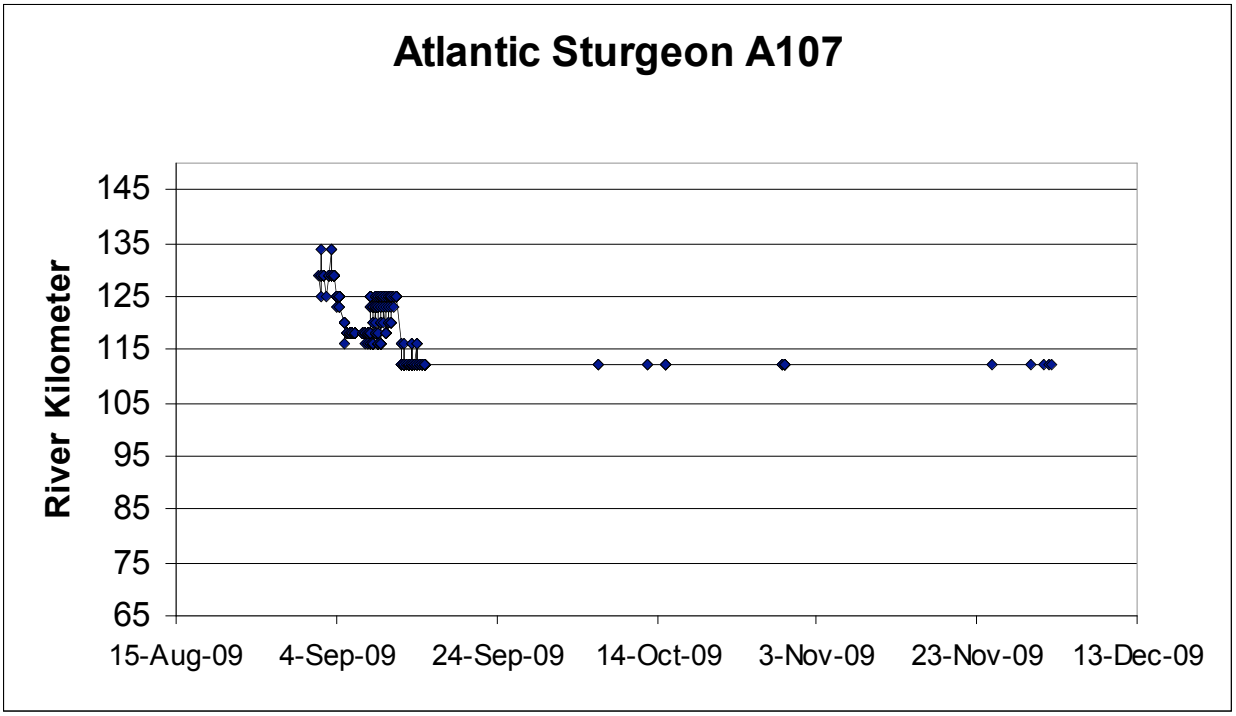

Figure A-8. Movements of Atlantic sturgeon tag A107 in the Delaware Estuary.

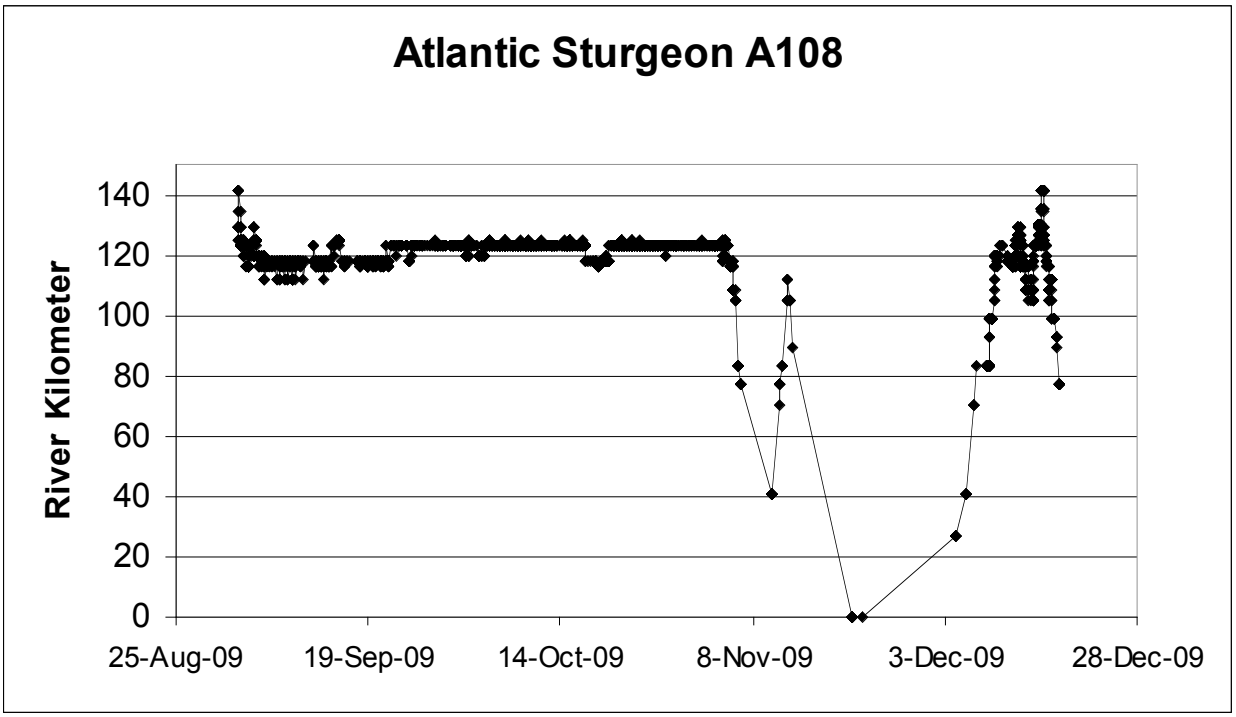

Figure A-9. Movements of Atlantic sturgeon tag A108 in the Delaware Estuary.

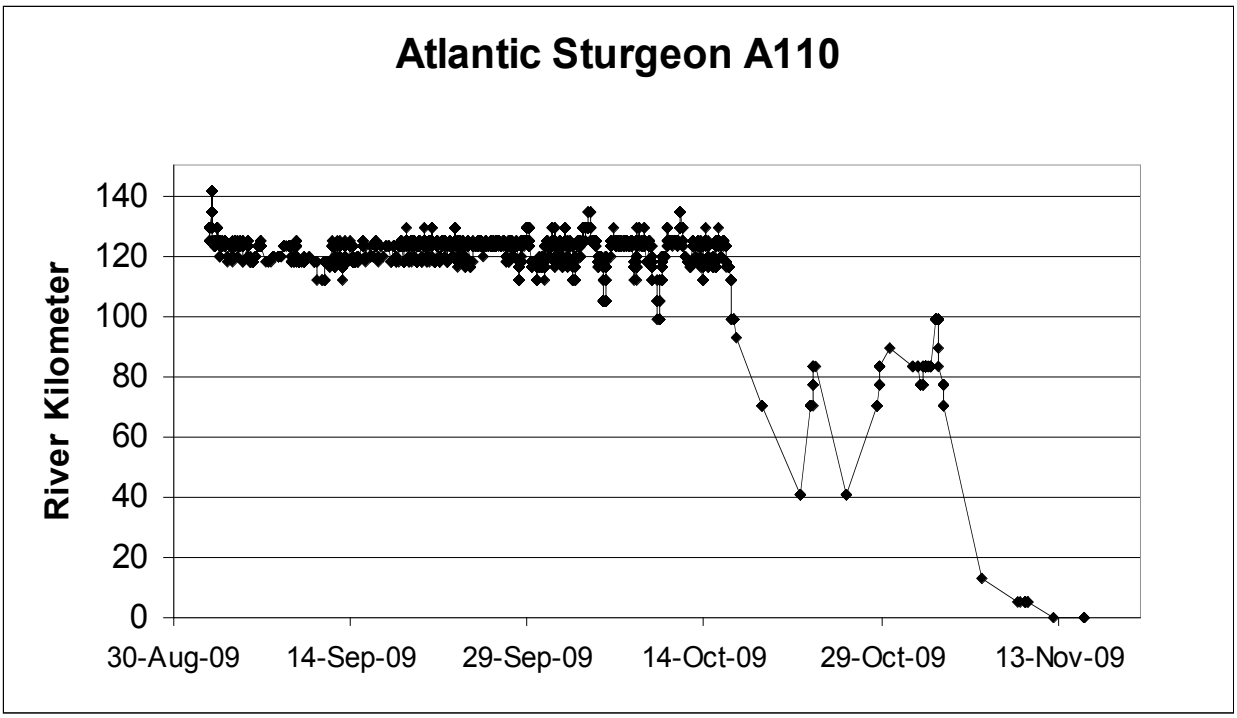

Figure A-10. Movements of Atlantic sturgeon tag A110 in the Delaware Estuary.

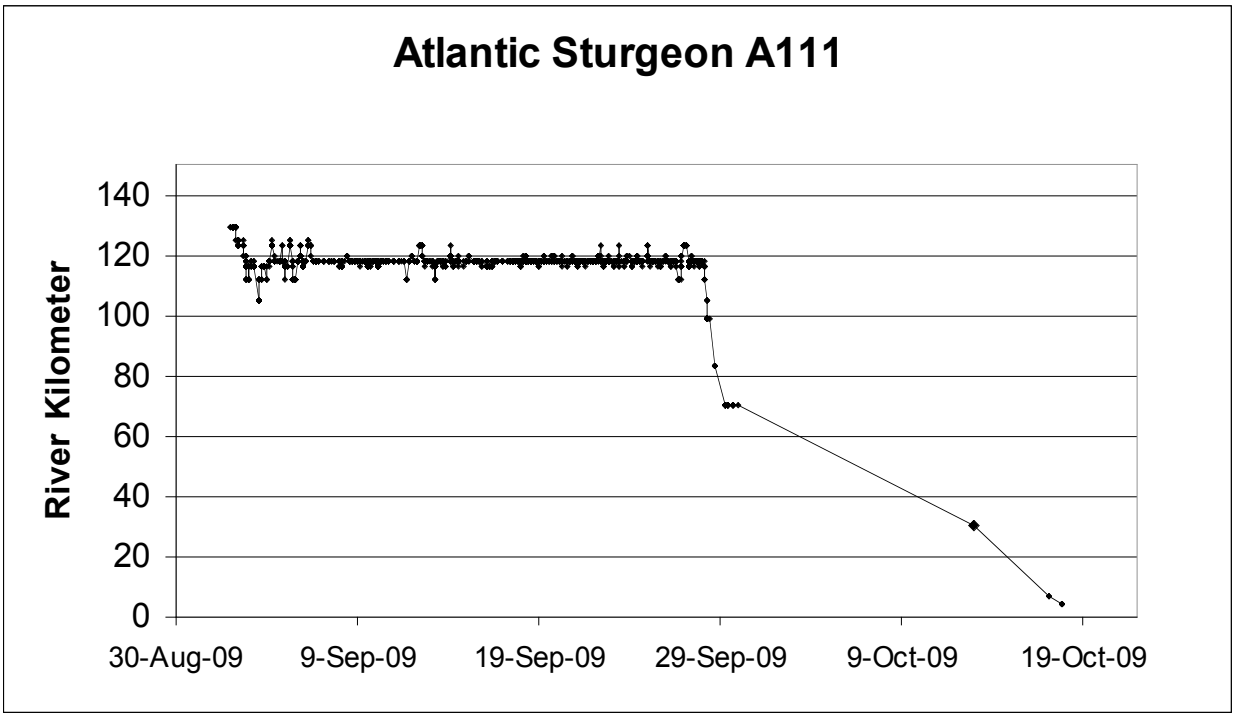

Figure A-11. Movements of Atlantic sturgeon tag A111 in the Delaware Estuary**.**

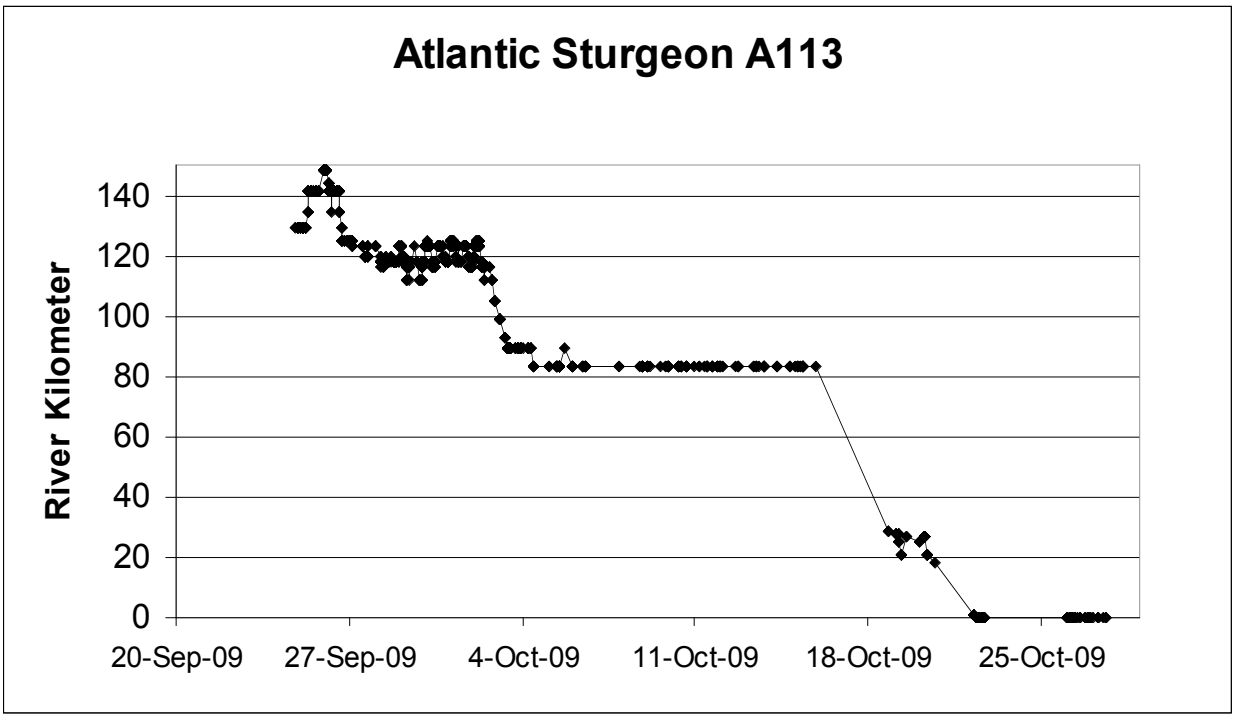

Figure A-12. Movements of Atlantic sturgeon tag A113 in the Delaware Estuary.

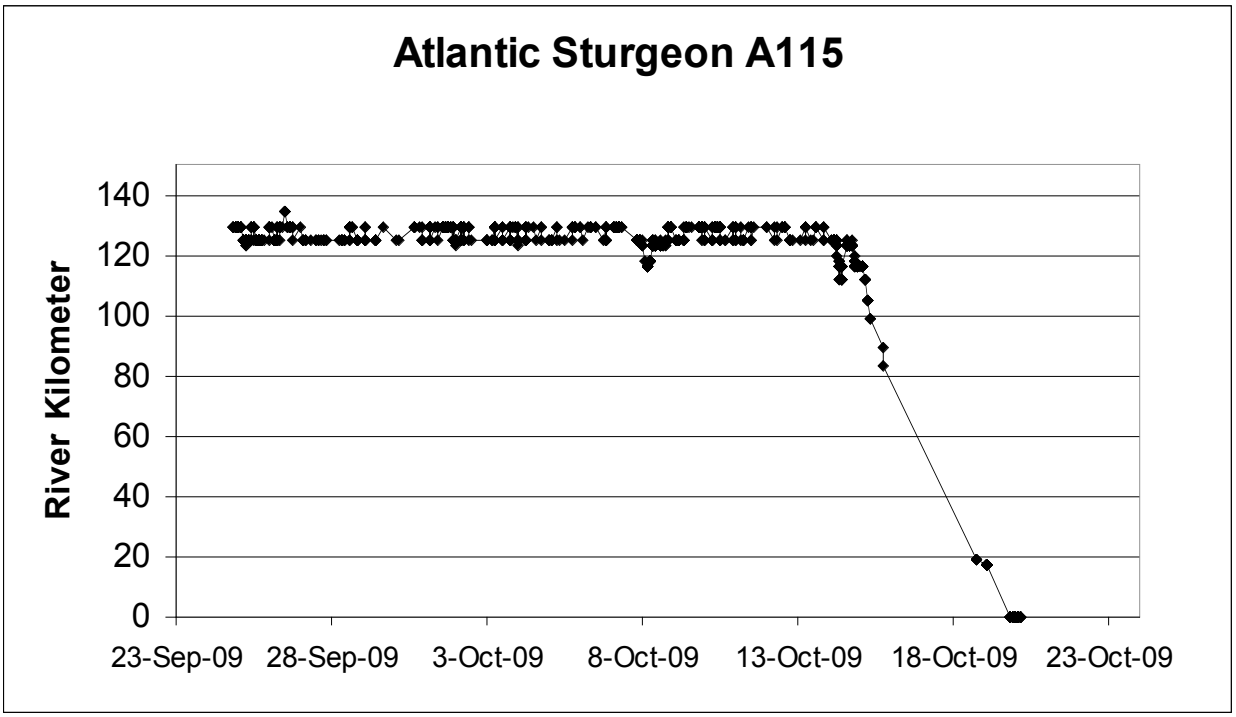

Figure A-13. Movements of Atlantic sturgeon tag A115 in the Delaware Estuary.

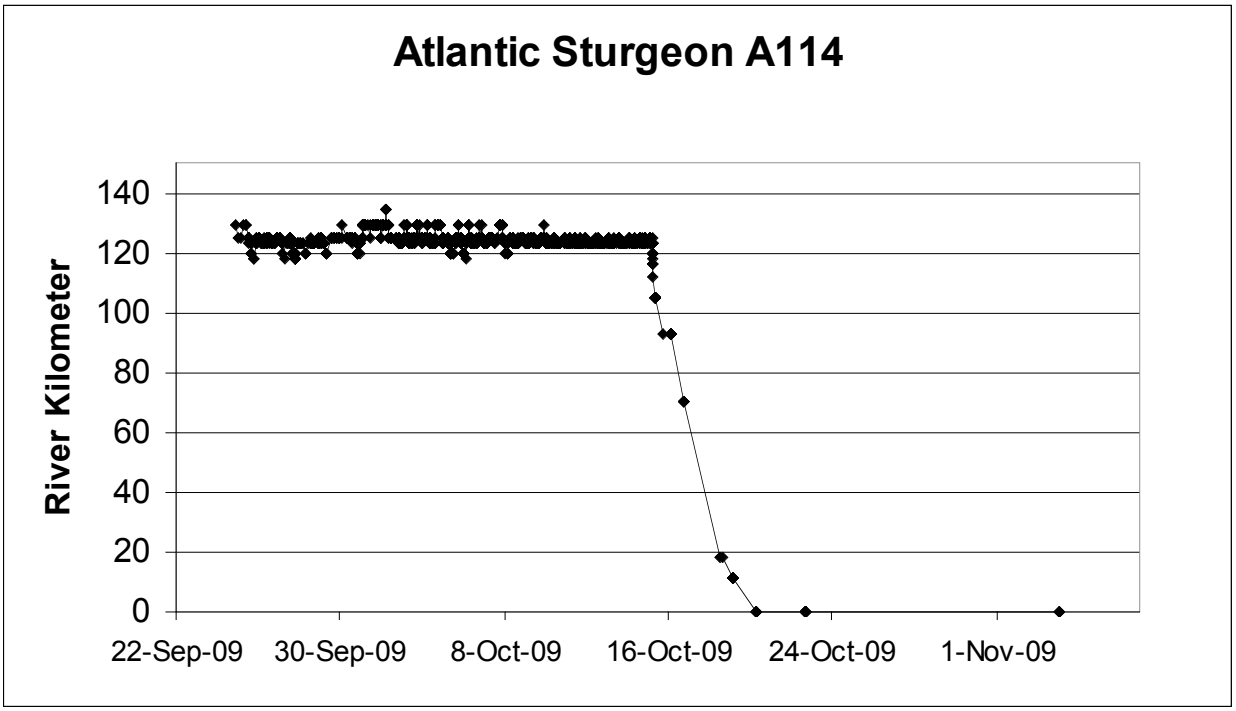

Figure A-14. Movements of Atlantic sturgeon tag A114 in the Delaware Estuary.

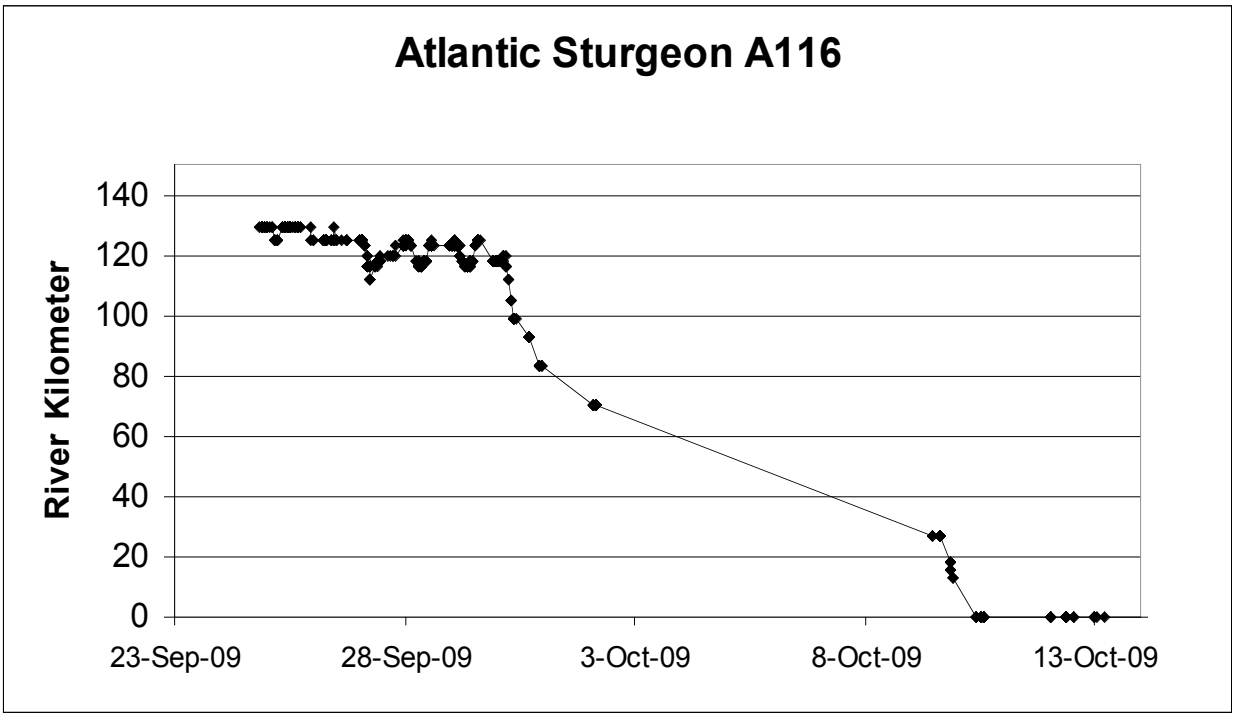

Figure A-15. Movements of Atlantic sturgeon tag A116 in the Delaware Estuary.

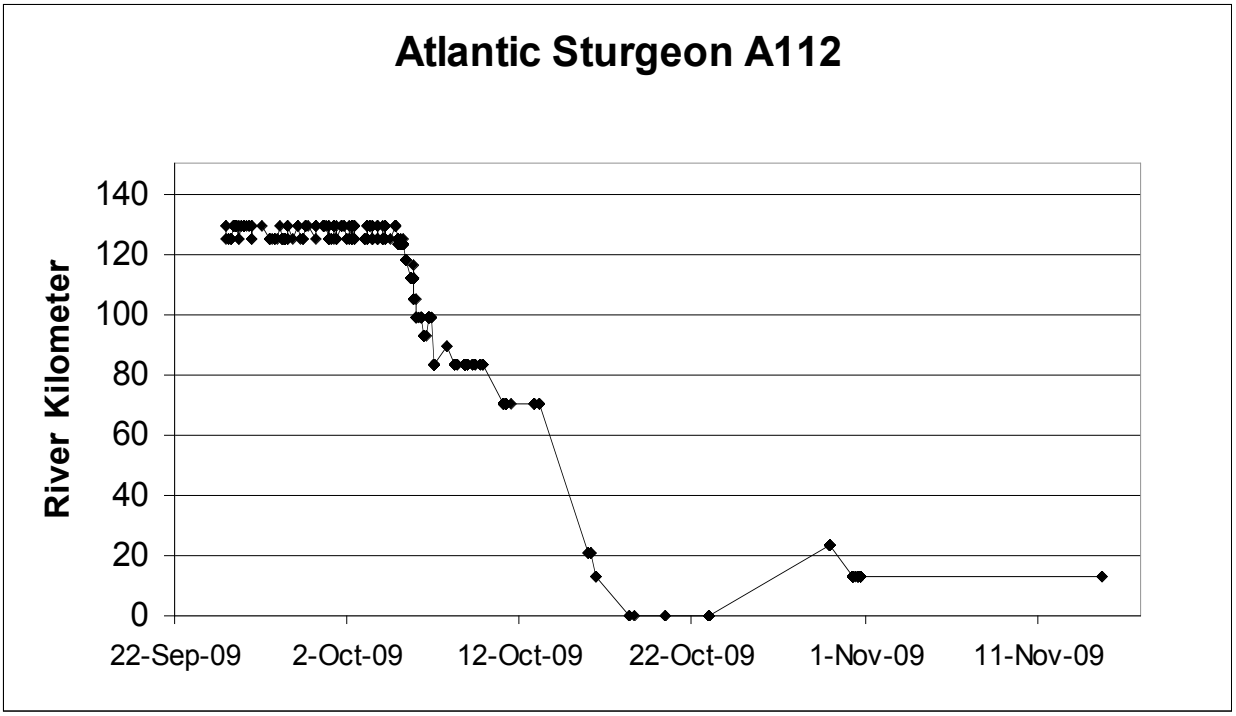

Figure A-16. Movements of Atlantic sturgeon tag A112 in the Delaware Estuary.

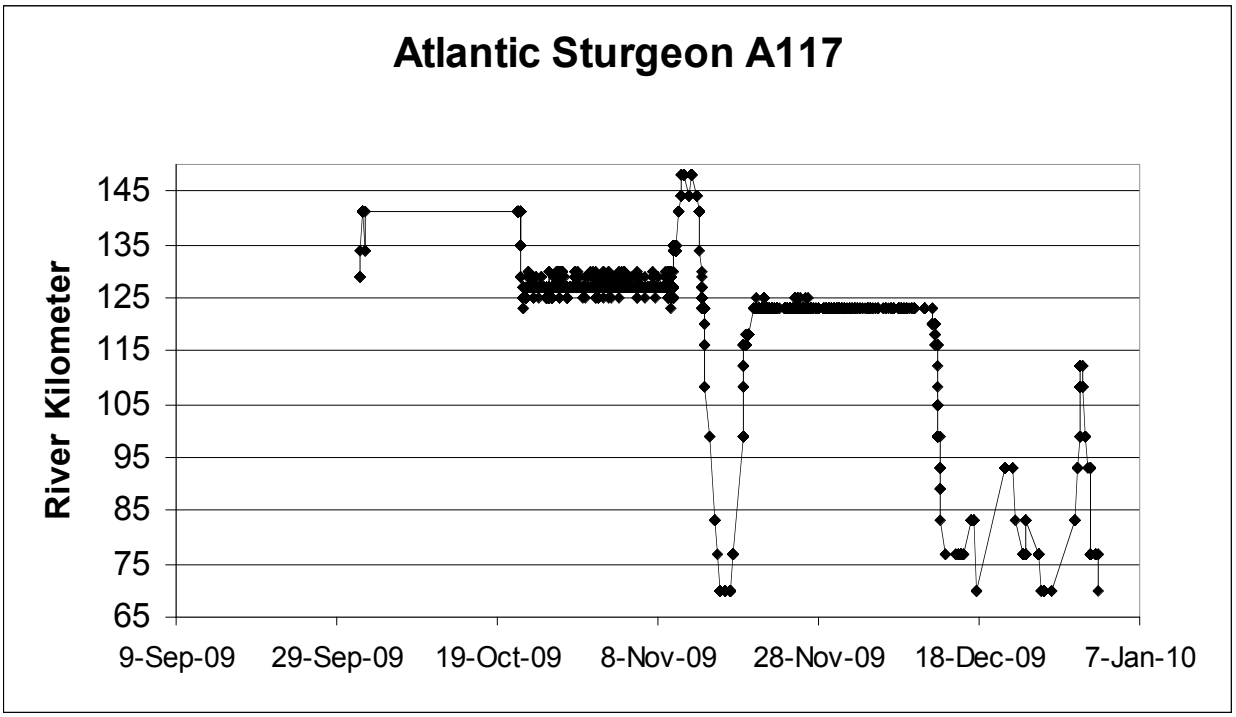

Figure A-17. Movements of Atlantic sturgeon tag A117 in the Delaware Estuary.

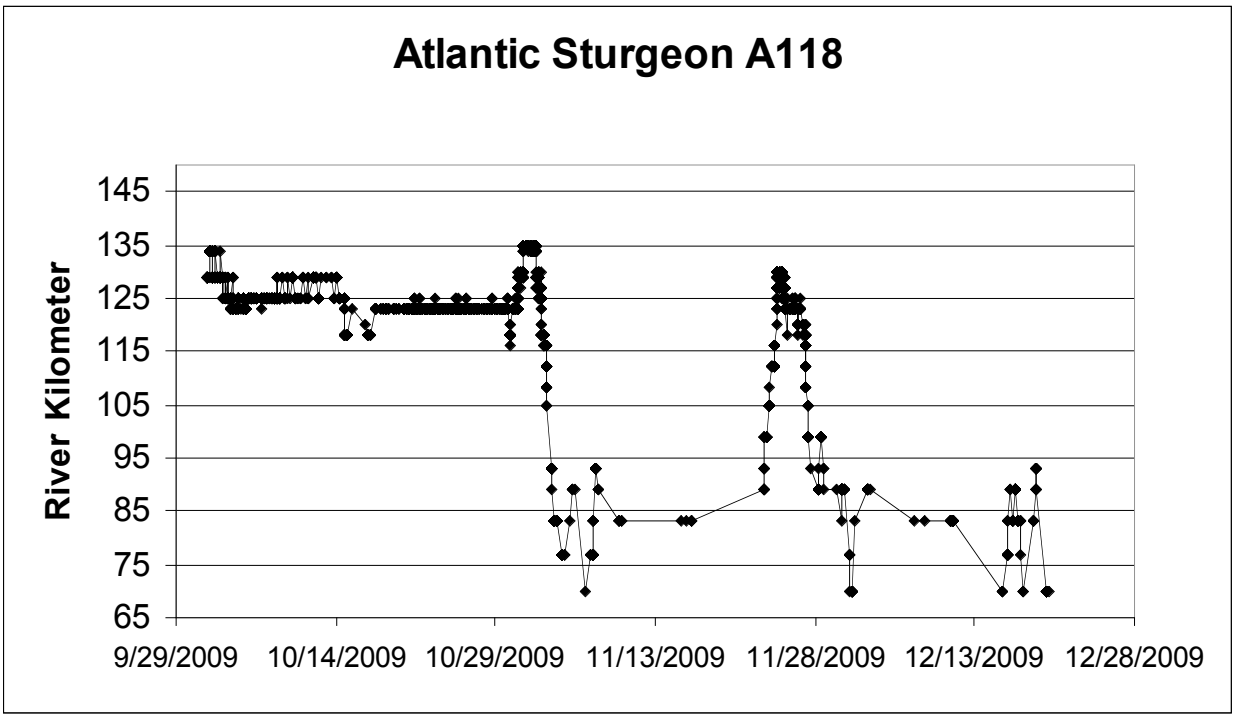

Figure A-18. Movements of Atlantic sturgeon tag A118 in the Delaware Estuary.

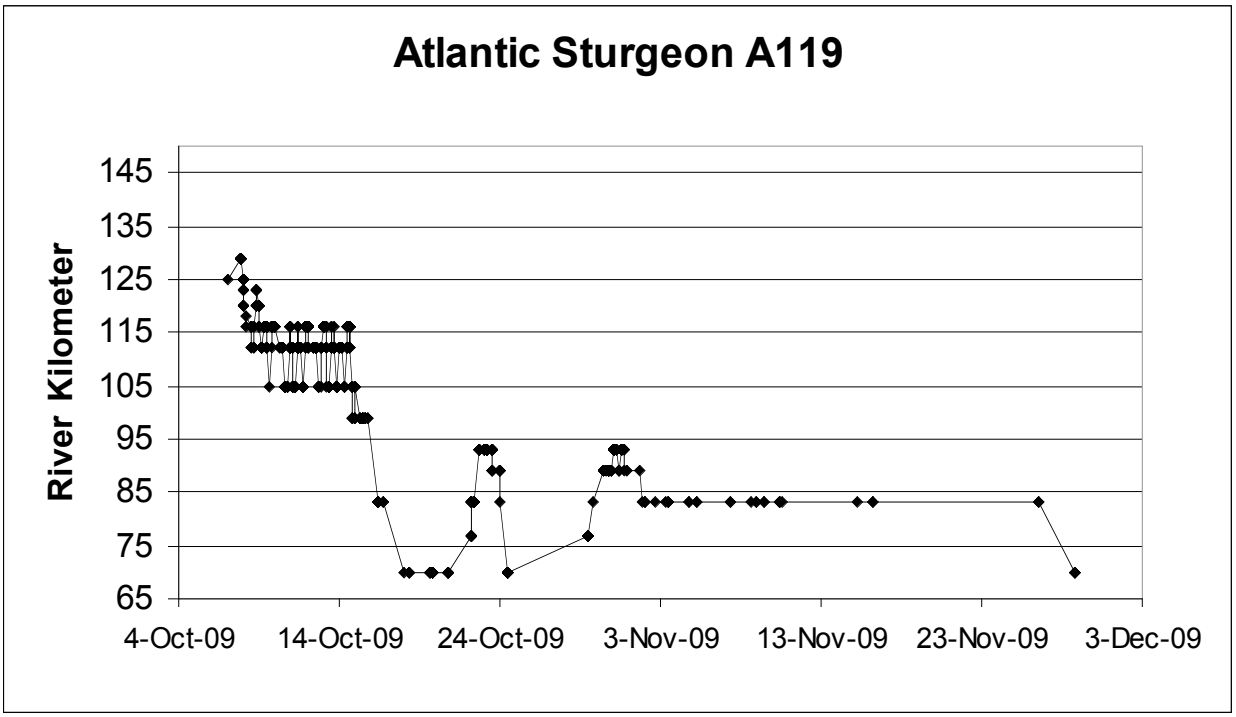

Figure A-19. Movements of Atlantic sturgeon tag A119 in the Delaware Estuary.

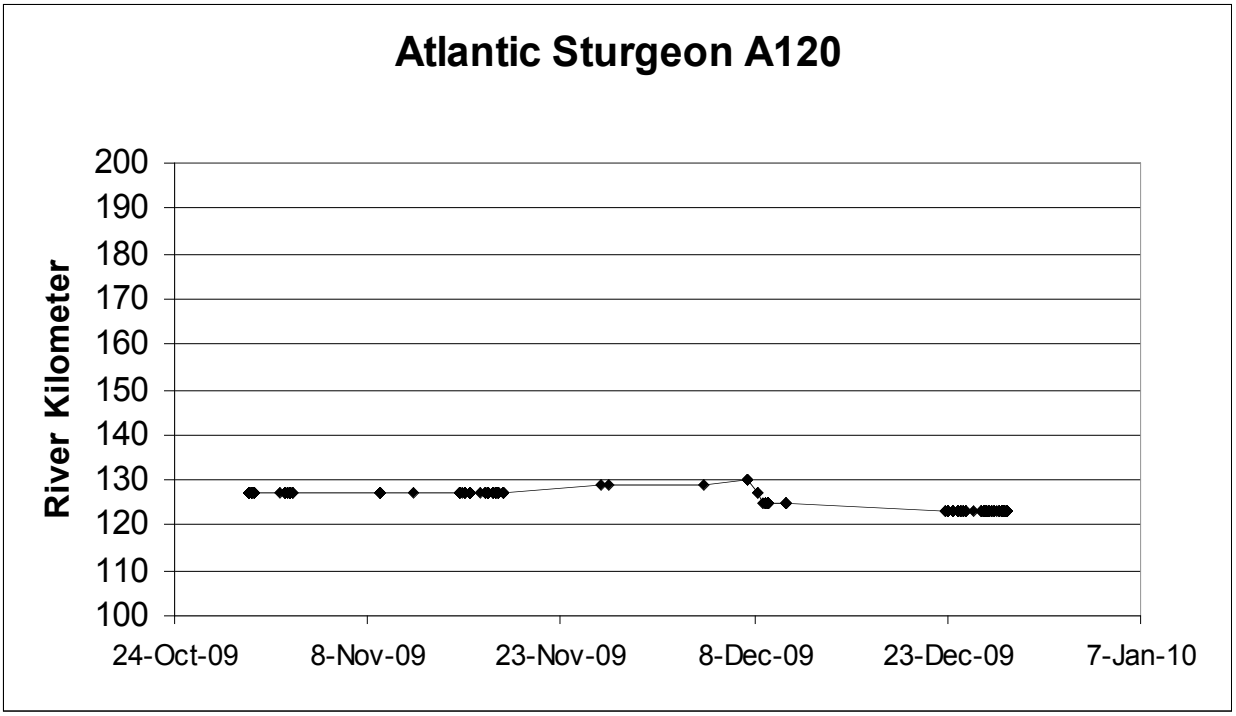

Figure A-20. Movements of Atlantic sturgeon tag A120 in the Delaware Estuary.

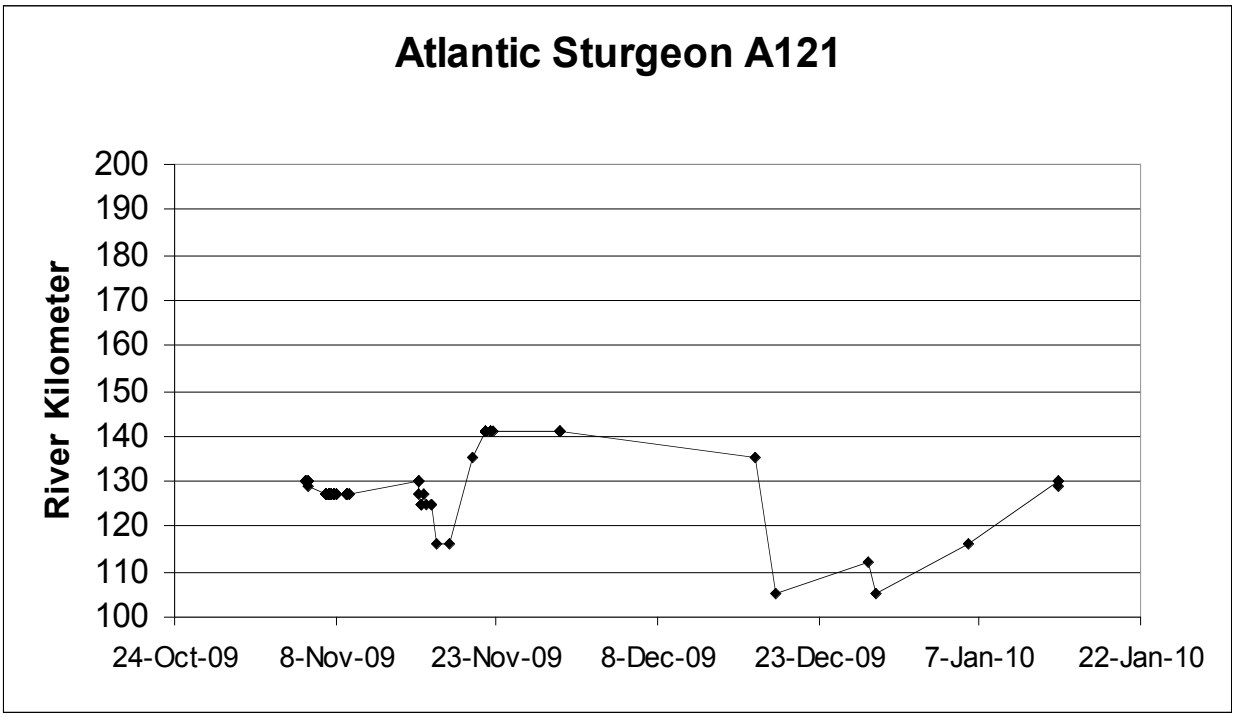

Figure A-21. Movements of Atlantic sturgeon tag A121 in the Delaware Estuary.

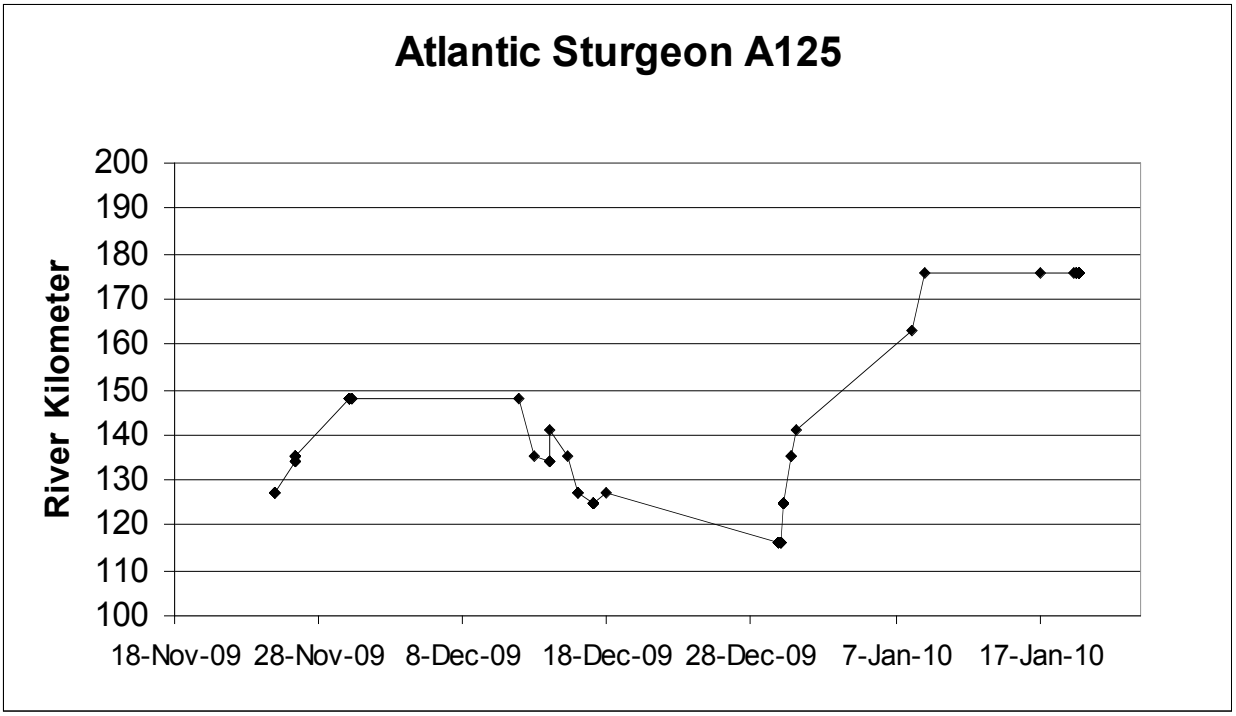

Figure A-22. Movements of Atlantic sturgeon tag A125 in the Delaware Estuary.

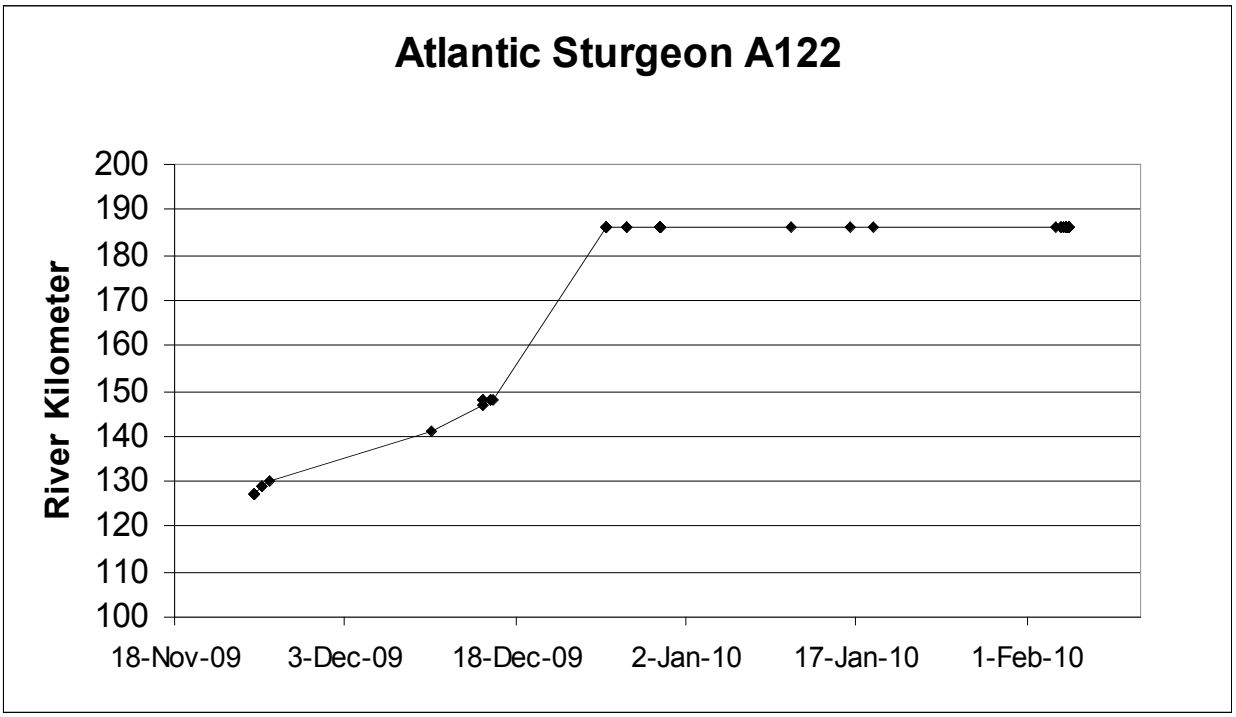

Figure A-23. Movements of Atlantic sturgeon tag A122 in the Delaware Estuary.

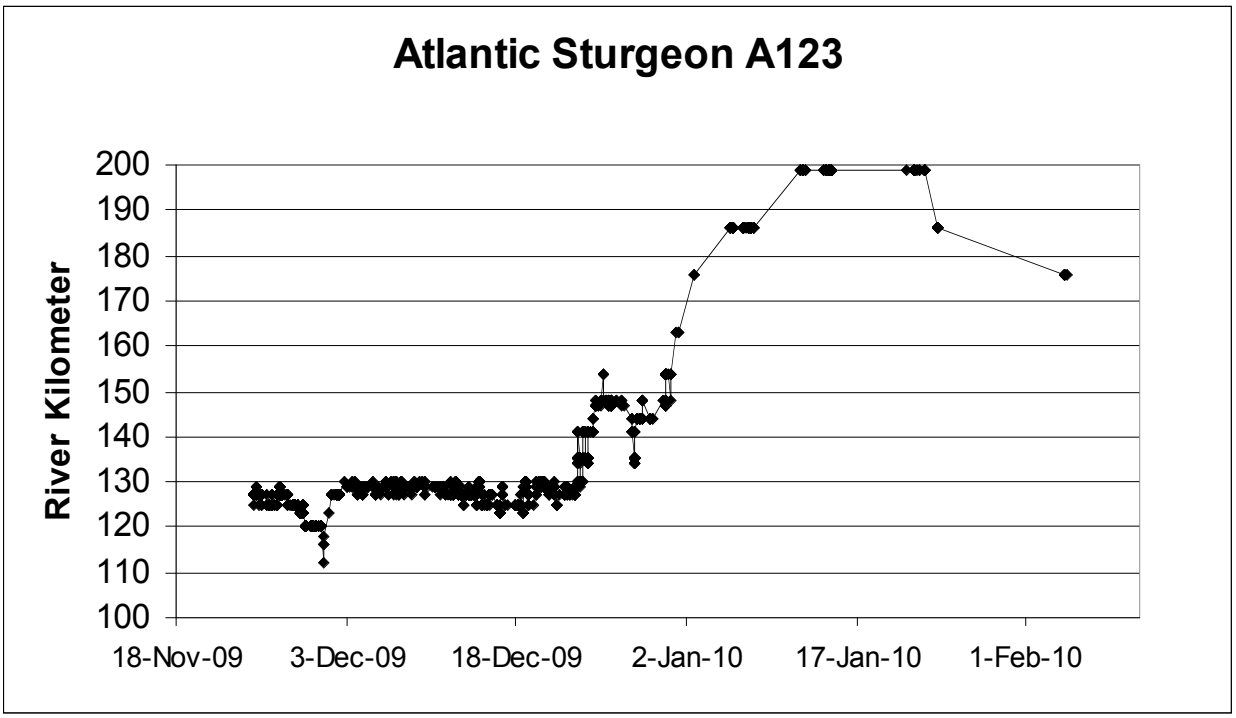

Figure A-24. Movements of Atlantic sturgeon tag A123 in the Delaware Estuary.

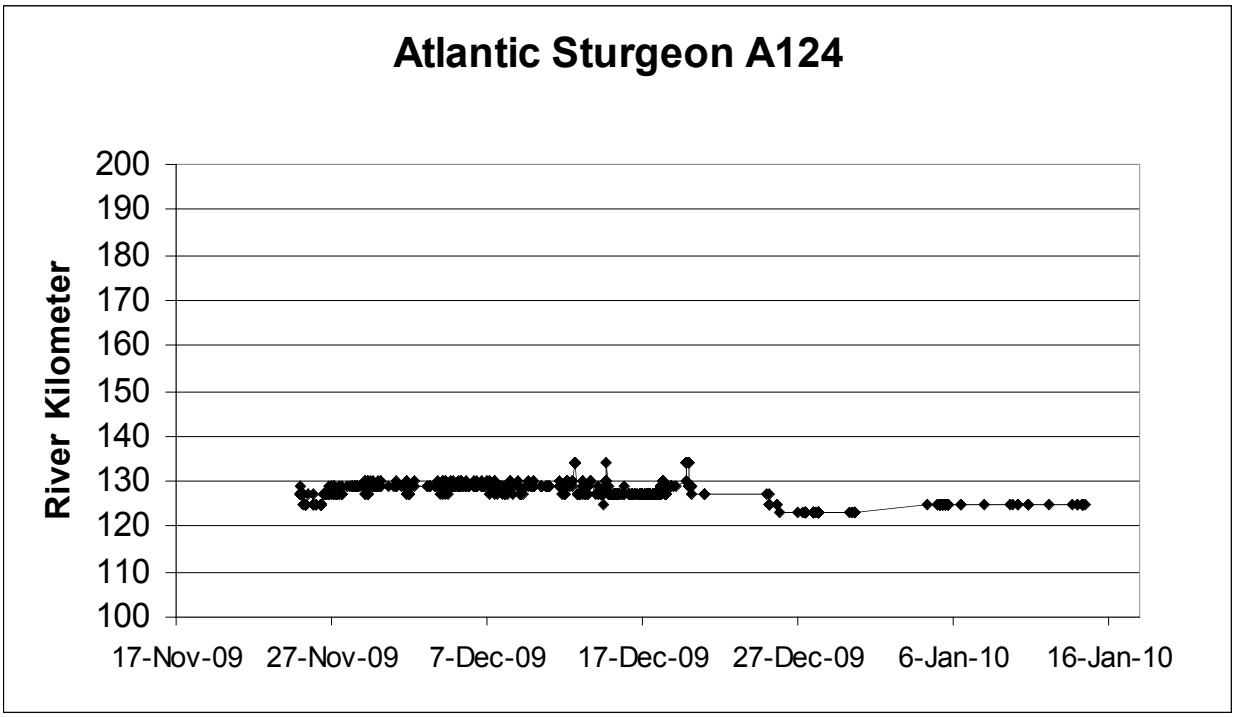

Figure A-25. Movements of Atlantic sturgeon tag A124 in the Delaware Estuary.

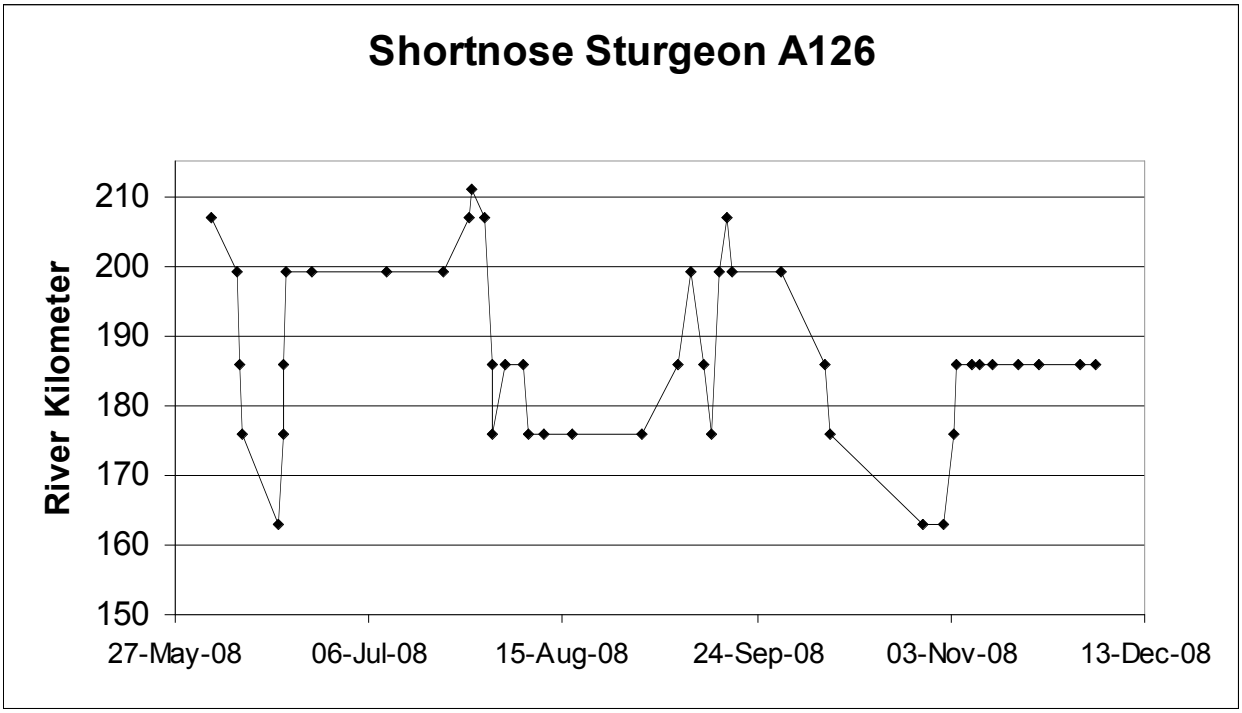

Figure B-1. Movements of shortnose sturgeon tag A126 in the Delaware Estuary.

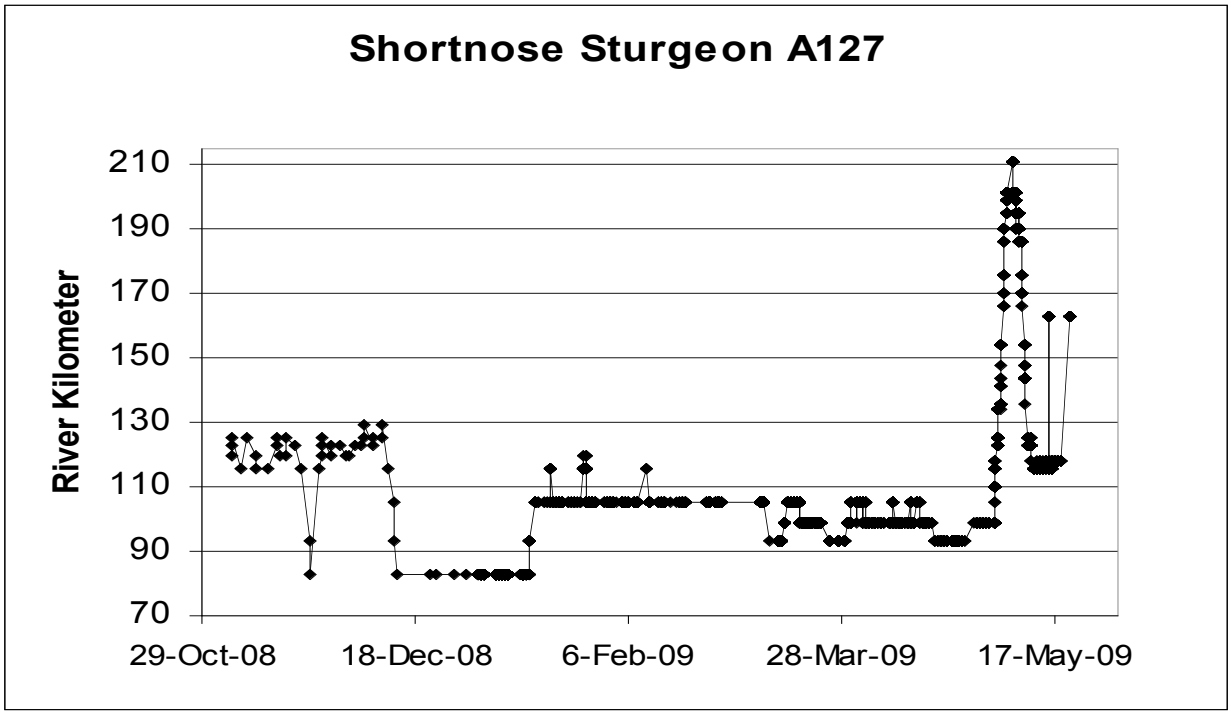

Figure B-2. Movements of shortnose sturgeon tag A127 in the Delaware Estuary.

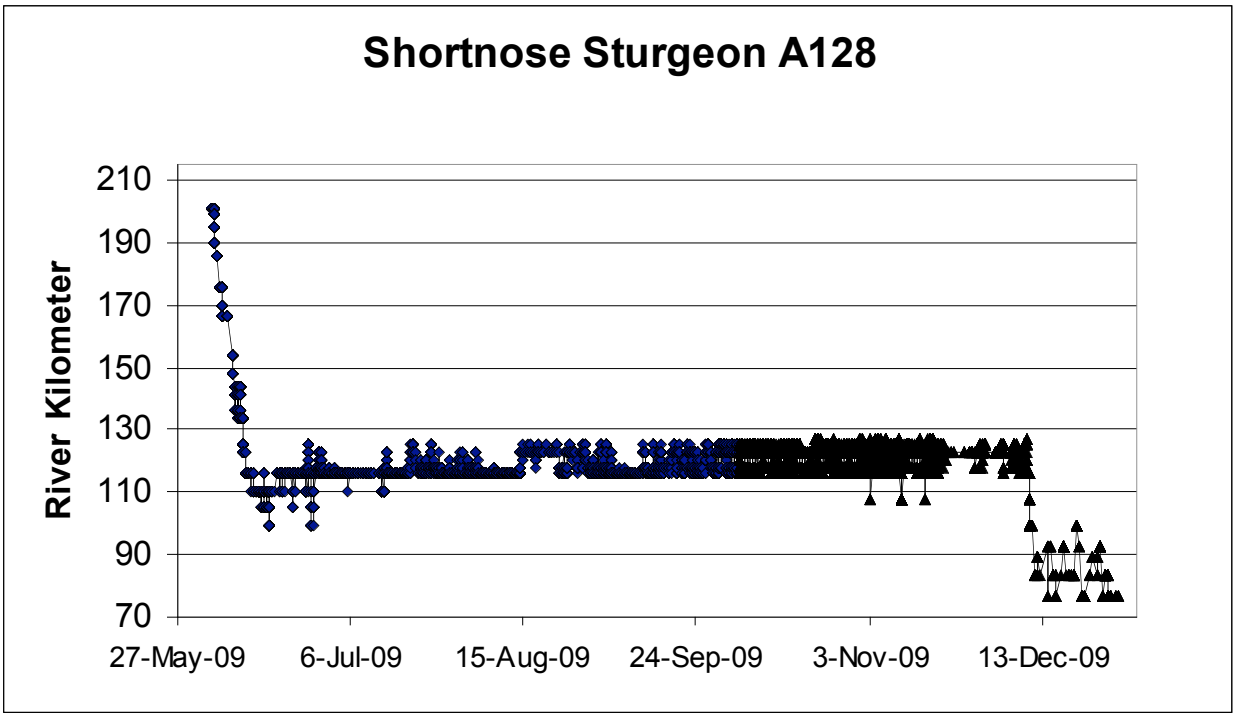

Figure B-3. Movements of shortnose sturgeon tag A128 in the Delaware Estuary.

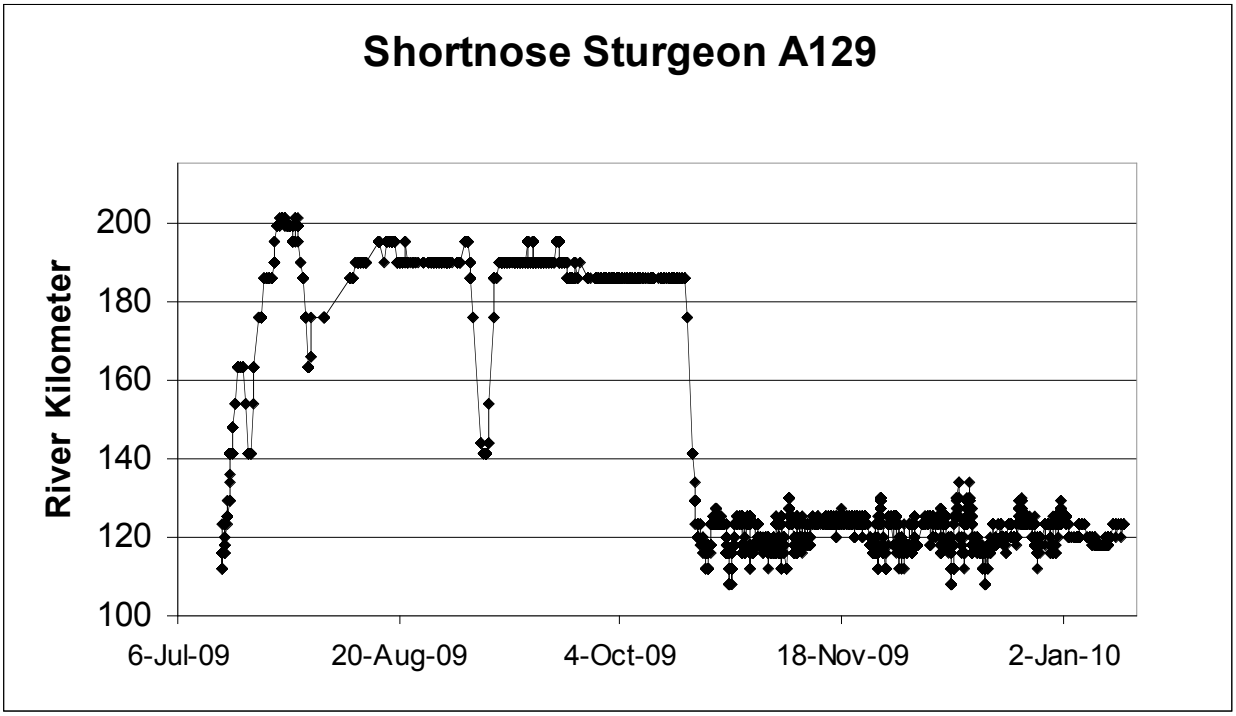

Figure B-4. Movements of shortnose sturgeon tag A129 in the Delaware Estuary.

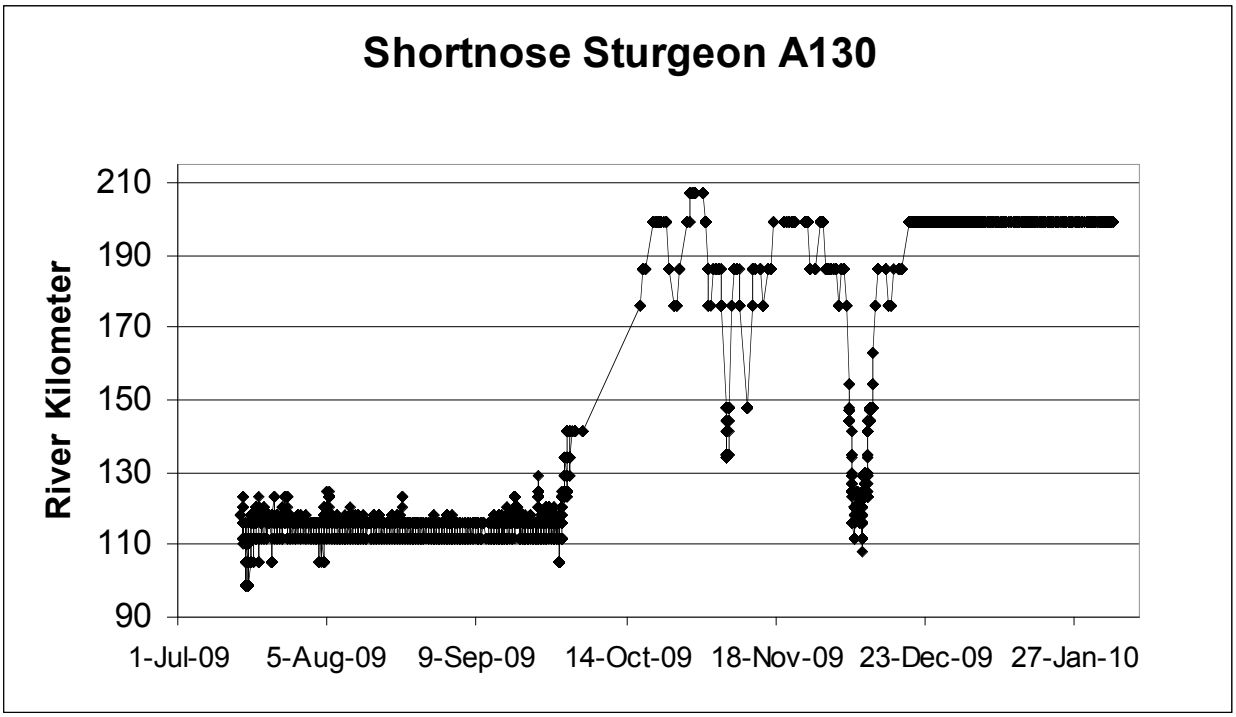

Figure B-5. Movements of shortnose sturgeon tag A130 in the Delaware Estuary.

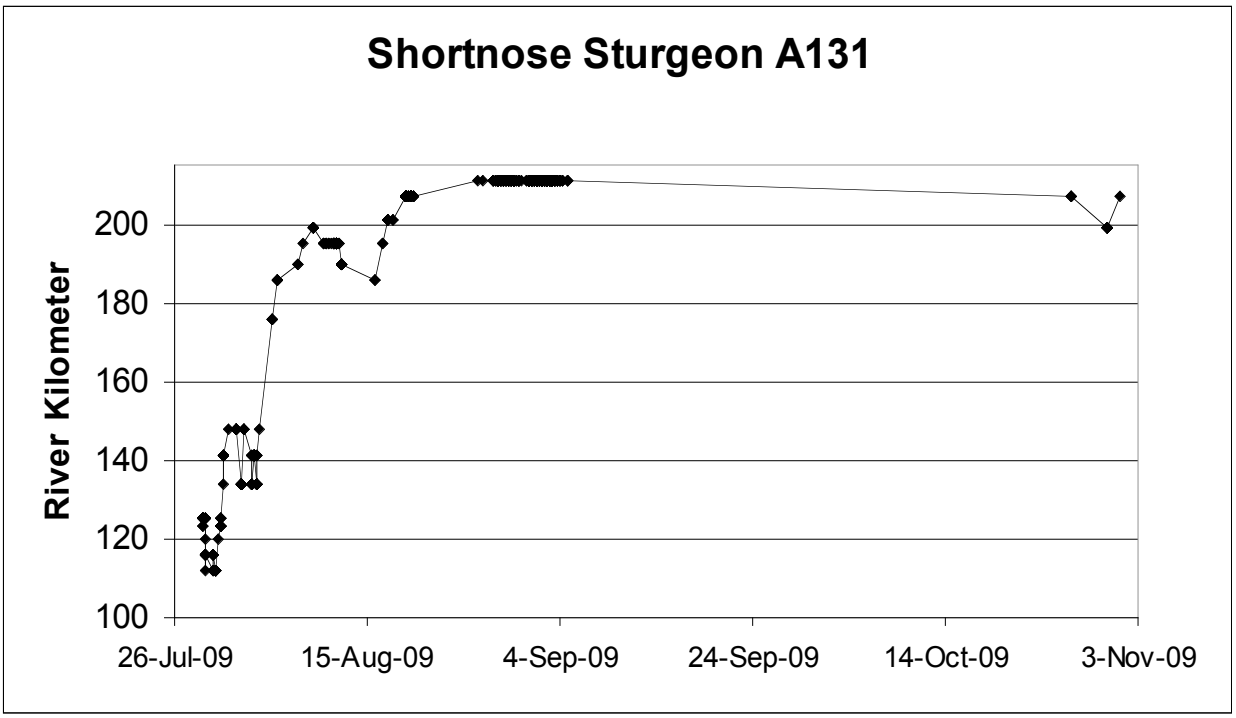

Figure B-6. Movements of shortnose sturgeon tag A131 in the Delaware Estuary.

CHAPTER 2 APPENDIX

Table 1. GPS coordinates for all 18 sites.

SITE	LATITUDE	LONGITUDE
Maurice River Cove	39º 08.16"	75º 00.24"
Egg Island	39º 12.70"	75º 11.50"
Nantuxent	39º 16.40"	75º 14.70"
Bennies	39º 15.10"	75º 18.10"
Sea Breeze	39º 18.78"	75º 19.80"
Ship John Bed	39º 18.50"	75º 22.10"
Arnolds	39º 22.98"	75º 27.00"
Hope Creek	39º 26.64"	75º 31.20"
Liston Point	39º 25.68"	75º 31.62"
Smyrna River	39º 22.56"	75º 28.08"
Ship John Channel	39º 17.82"	75º 22.56"
Over the Bar	39º 15.50"	75º 22.48"
Ridge	39º 12.18"	75º 21.48"
Lower Side Delaware	39º 08.16"	75º 22.80"
Elbow of Crossledge	39º 10.81"	75º 16.32"
Reedy Point	39º 30.78"	75º 33.30"
Cherry Island	39º 43.20"	75º 30.42"
Eddystone	39º 50.82"	75º 20.28"

Table 2. Collection dates and water parameters.

DATE	SAMPLING	SITE	T	DO	S
1/22/09	1	Maurice River Cove	-0.1	0.12	22
1/22/09	1	Egg Island	-0.2	1.26	20
1/22/09	1	Nantuxent P	-0.4	5.40	15
1/22/09	1	Bennies	0.2	4.37	17
1/22/09	1	Sea Breeze	-0.1	4.48	15
1/22/09	1	Ship John Bed	0/4	4.19	14
1/22/09	1	Arnolds	0.7	5.29	11
1/22/09	1	Hope Creek	1.0	4.33	6
1/22/09	1	Liston Point	0.9	4.51	8
1/22/09	1	Smyrna River	0.9	5.69	10
1/22/09	1	Ship John Channel	0.8	4.46	11
1/22/09	1	Over the Bar	1.1	5.61	12
1/22/09	1	Ridge	1.0	5.13	15
1/22/09	1	Lower Side DE	1.6	5.21	20
1/22/09	1	Elbow of Crossledge	0.7	6.51	17
3/18/09	2	Maurice River Cove	8.2	3.20	24
3/18/09	2	Egg Island	5.9	5.30	21
3/18/09	2	Nantuxent P	6.7	4.61	19
3/18/09	2	Bennies	5.9	5.14	16
3/18/09	2	Sea Breeze	6.3	4.89	15
3/18/09	2	Ship John Bed	6.4	4.98	14
3/18/09	2	Arnolds	6.8	5.23	11
3/18/09	2	Hope Creek	7.6	5.14	9
3/18/09	2	Liston Point	6.6	5.04	6
3/18/09	2	Smyrna River	7.4	5.45	9
3/18/09	2	Ship John Channel	6.4	5.82	11
3/18/09	2	Over the Bar	7.0	5.88	12
3/18/09	2	Ridge	6.8	5.92	19
3/18/09	2	Lower Side DE	7.8	4.99	23
3/18/09	2	Elbow of Crossledge	6.8	6.17	18
4/21/09	3	Maurice River Cove	12.7	10.94	24
4/21/09	3	Egg Island	12.4	10.81	23
4/21/09	3	Nantuxent P	12.5	11.33	19
4/21/09	3	Bennies	11.4	12.75	16
4/21/09	3	Sea Breeze	12.2	12.06	15
4/21/09	3	Ship John Bed	11.7	11.62	15
4/21/09	3	Arnolds	11.7	12.39	13
4/21/09	3	Hope Creek	11.9	11.27	11
4/21/09	3	Liston Point	11.5	11.40	10
4/21/09	3	Smyrna River			
4/21/09	3	Ship John Channel	11.3	12.30	16
4/21/09	3	Over the Bar	11.9	11.82	16
4/21/09	3	Ridge	12.1	12.04	19
4/21/09	3	Lower Side DE	12.5	12.70	21
4/21/09	3	Elbow of Crossledge			

Table 2 continued.

DATE	SAMPLING	SITE	T	DO	S
5/5/09	4	Maurice River Cove	15.4	10.84	24
5/5/09	4	Egg Island	15.4	9.47	22
5/5/09	4	Nantuxent P	16.2	9.44	19
5/5/09	4	Bennies	15.9	8.76	17
5/5/09	4	Sea Breeze	16.0	8.78	15
5/5/09	4	Ship John Bed	16.2	9.18	13
5/5/09	4	Arnolds	16.4	8.48	10
5/5/09	4	Hope Creek	16.6	8.72	7
5/5/09	4	Liston Point	17.2	8.32	7
5/5/09	4	Smyrna River	16.3	9.30	11
5/5/09	4	Ship John Channel	15.3	9.49	14
5/5/09	4	Over the Bar	15.3	9.09	18
5/5/09	4	Ridge	15.0	10.35	21
5/5/09	4	Lower Side DE	14.9	10.32	26
5/5/09	4	Elbow of Crossledge	14.1	9.55	26
6/10/09	5	Maurice River Cove	23.7	9.34	25
6/10/09	5	Egg Island	22.1	12.18	23
6/10/09	5	Nantuxent P	22.5	5.92	19
6/10/09	5	Bennies	22.2	8.86	19
6/10/09	5	Sea Breeze	22.7	5.95	16
6/10/09	5	Ship John Bed	22.7	6.81	15
6/10/09	5	Arnolds	24.1	9.20	11
6/10/09	5	Hope Creek	24.5	8.51	8
6/10/09	5	Liston Point	24.6	8.44	8
6/10/09	5	Smyrna River	24.6	7.93	11
6/10/09	5	Ship John Channel	24.2	7.78	14
6/10/09	5	Over the Bar	24.9	8.35	18
6/10/09	5	Ridge	24.3	9.93	22
6/10/09	5	Lower Side DE	26.7	8.72	24
6/10/09	5	Elbow of Crossledge	22.6	6.39	25
7/23/09	6	Maurice River Cove	25.2	6.32	25
7/23/09	6	Egg Island	25.4	4.40	21
7/23/09	6	Nantuxent P	25.4	4.04	19
7/23/09	6	Bennies	25.3	4.05	20
7/23/09	6	Sea Breeze	25.3	3.73	19
7/23/09	6	Ship John Bed	25.4	3.40	18
7/23/09	6	Arnolds	25.5	3.27	14
7/23/09	6	Hope Creek	25.9	3.85	11
7/23/09	6	Liston Point	26.3	3.33	11
7/23/09	6	Smyrna River	25.7	3.16	15
7/23/09	6	Ship John Channel	25.5	3.30	18
7/23/09	6	Over the Bar	25.3	3.27	20
7/23/09	6	Ridge	25.5	4.30	25
7/23/09	6	Lower Side DE	25.8	2.53	27
7/23/09	6	Elbow of Crossledge	24.6	2.76	27

Table 2 continued.

DATE	SAMPLING	SITE	T	DO	S
8/12/09	7	Maurice River Cove	26.7	4.02	26
8/12/09	7	Egg Island	26.7	2.33	22
8/12/09	7	Nantuxent P	27.6	2.74	18
8/12/09	7	Bennies	28.8	2.43	12
8/12/09	7	Sea Breeze	28.7	2.55	14
8/12/09	7	Ship John Bed	28.7	1.26	11
8/12/09	7	Arnolds	29.4	2.31	8
8/12/09	7	Hope Creek	28.8	3.12	5
8/12/09	7	Liston Point	28.3	2.50	4
8/12/09	7	Smyrna River	28.3	1.43	5
8/12/09	7	Ship John Channel	28.1	3.43	10
8/12/09	7	Over the Bar	28.1	3.12	11
8/12/09	7	Ridge	27.4	3.05	15
8/12/09	7	Lower Side DE	27.5	1.20	19
8/12/09	7	Elbow of Crossledge	26.2	2.26	24
9/23/09	8	Maurice River Cove	23.8	0.86	24
9/23/09	8	Egg Island	21.6	0.84	24
9/23/09	8	Nantuxent P	21.0	1.10	22
9/23/09	8	Bennies	21.8	1.11	19
9/23/09	8	Sea Breeze	22.1	1.35	15
9/23/09	8	Ship John Bed	21.8	1.61	18
9/23/09	8	Arnolds	22.6	1.01	14
9/23/09	8	Hope Creek	24.0	1.06	11
9/23/09	8	Liston Point	22.5	1.00	10
9/23/09	8	Smyrna River	23.0	1.14	13
9/23/09	8	Ship John Channel	24.4	1.30	15
9/23/09	8	Over the Bar	22.5	1.62	20
9/23/09	8	Ridge	22.9	1.33	24
9/23/09	8	Lower Side DE	22.8	1.53	28
9/23/09	8	Elbow of Crossledge	23.8	0.93	31
10/21/09	9	Maurice River Cove	11.2	8.34	27
10/21/09	9	Egg Island	12.5	7.97	28
10/21/09	9	Nantuxent P	11.1	7.30	27
10/21/09	9	Bennies	14.1	9.83	28
10/21/09	9	Sea Breeze	14.0	9.80	25
10/21/09	9	Ship John Bed	13.8	9.53	25
10/21/09	9	Arnolds	13.4	9.61	21
10/21/09	9	Hope Creek	14.9	9.39	17
10/21/09	9	Liston Point	14.6	9.48	25
10/21/09	9	Smyrna River	13.7	9.36	20
10/21/09	9	Ship John Channel	13.8	9.46	23
10/21/09	9	Over the Bar	14.2	8.47	25
10/21/09	9	Ridge	13.3	7.92	29
10/21/09	9	Lower Side DE	13.4	7.80	30
10/21/09	9	Elbow of Crossledge	14.4	7.80	35

Table 2 continued.

DATE	SAMPLING	SITE	T	DO	S
12/1/09	10	Maurice River Cove	9.9	10.14	30
12/1/09	10	Egg Island	9.4	9.83	29
12/1/09	10	Nantuxent P	9.0	9.37	24
12/1/09	10	Bennies	9.8	9.73	26
12/1/09	10	Sea Breeze	9.6	9.71	23
12/1/09	10	Ship John Bed	9.9	9.64	23
12/1/09	10	Arnolds	10.0	8.92	19
12/1/09	10	Hope Creek	10.2	9.32	18
12/1/09	10	Liston Point	10.4	8.99	18
12/1/09	10	Smyrna River	10.4	9.38	21
12/1/09	10	Ship John Channel	10.3	10.02	22
12/1/09	10	Over the Bar	10.3	10.03	24
12/1/09	10	Ridge	10.2	9.81	26
12/1/09	10	Lower Side DE	9.6	9.96	27
12/1/09	10	Elbow of Crossledge	10.6	10.50	32

(A)

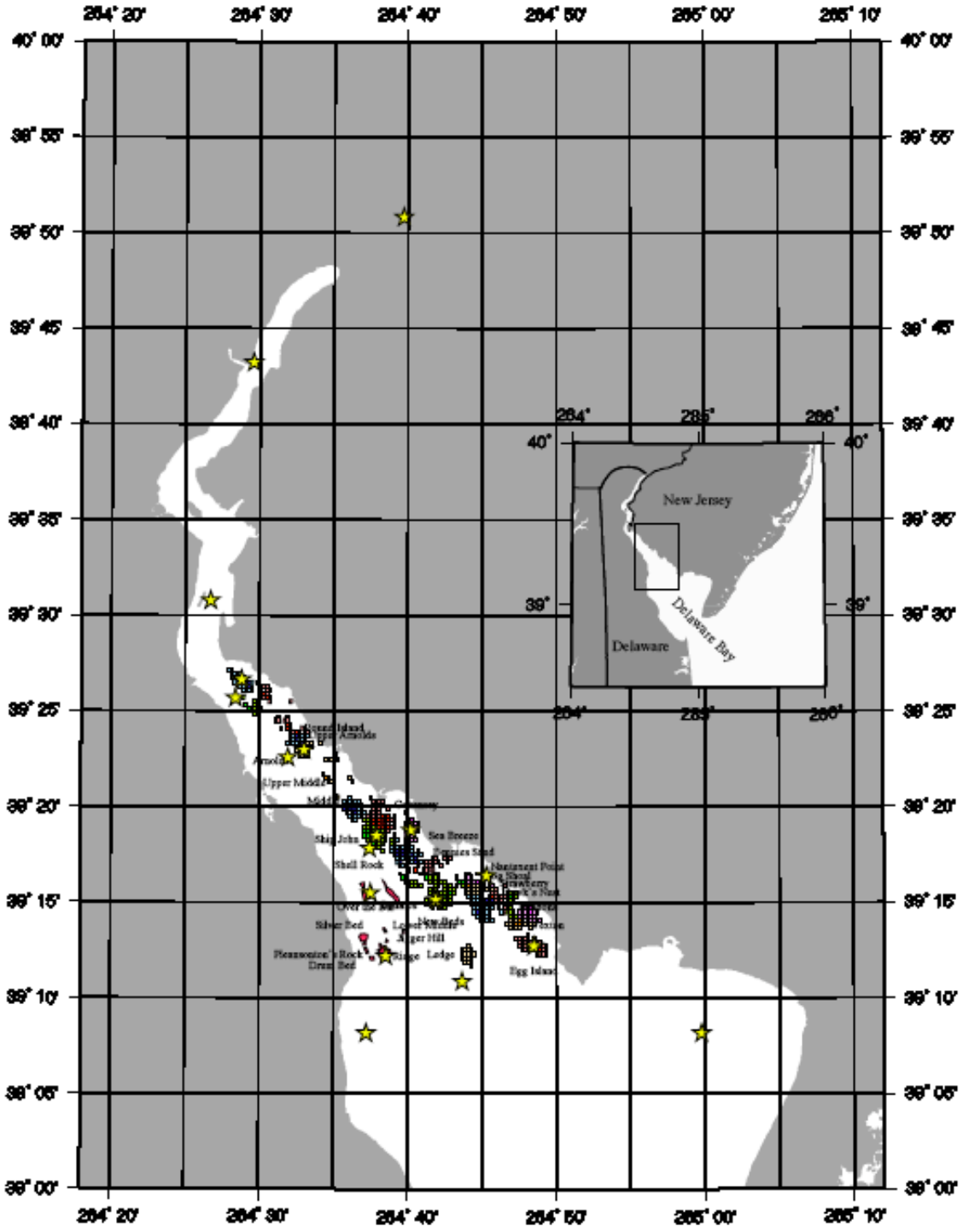

Figure 1. Map of the Delaware Bay and River. (A) Overview of all 18 sites indicated by yellow stars.

(B)

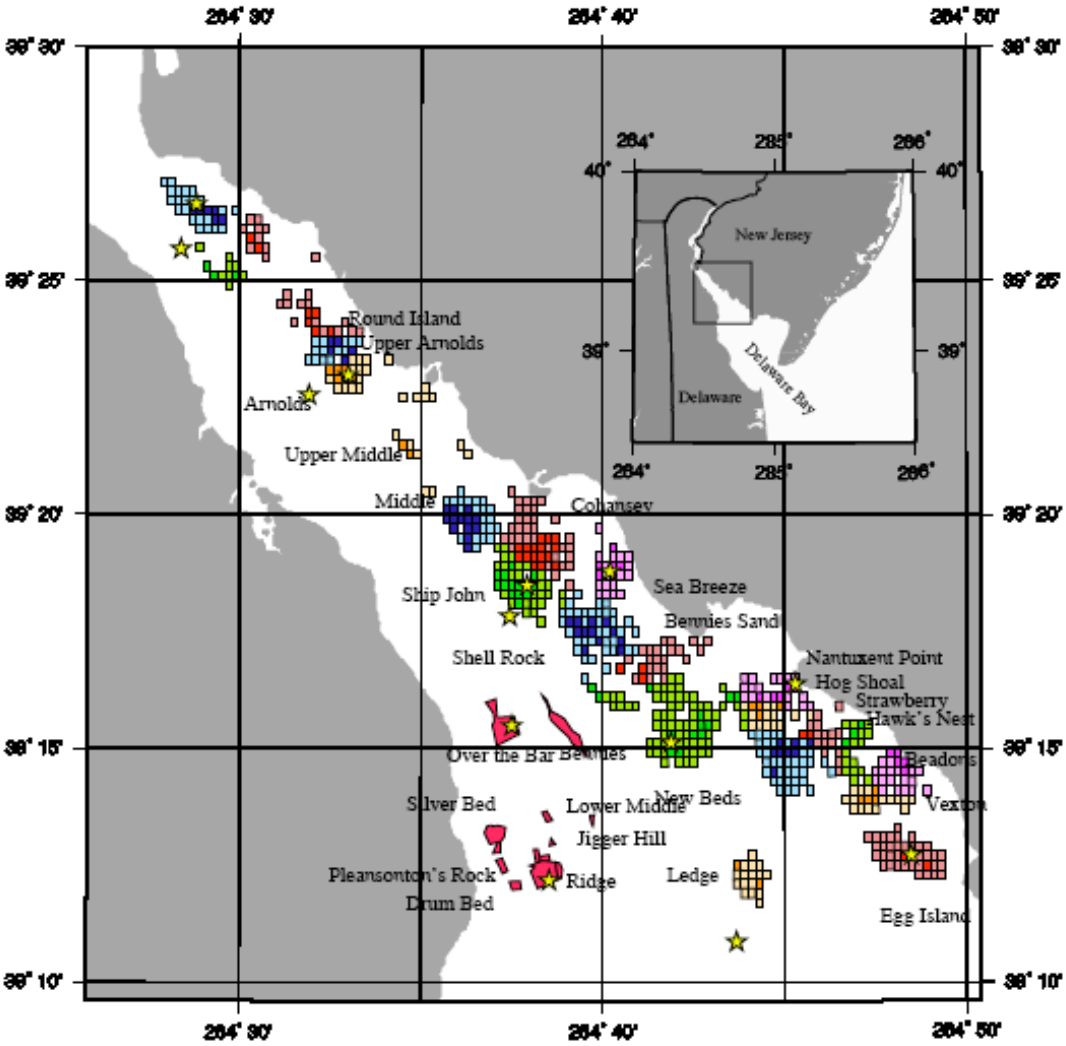

Figure 1. Map of the Delaware Bay and River. (B) Close up of sites over oyster beds.